Evaluation of Overlay/Underlay Waveform via SD-SMSE Framework for Enhancing Spectrum Efficiency

A dissertation submitted in partial fulfillment
of the requirements for the degree of
Doctor of Philosophy

by

Vasu D. Chakravarthy
M.S.E., Wright State University, 1998
B.S.E.E., University of Illinois, Chicago, 1988

2008
Wright State University

Wright State University
SCHOOL OF GRADUATE STUDIES

July 31, 2008

I HEREBY RECOMMEND THAT THE DISSERTATION PREPARED UNDER MY SUPERVISION BY Vasu D. Chakravarthy ENTITLED Evaluation of Overlay/Underlay Waveform via SD-SMSE Framework for Enhancing Spectrum Efficiency BE ACCEPTED IN PARTIAL FULFILLMENT OF THE REQUIREMENTS FOR THE DEGREE OF Doctor of Philosophy.

Arnab K. Shaw, Ph.D.
Dissertation Director

Zhiqiang Wu, Ph.D.
Dissertation Co-Director

Ramana V. Grandhi, Ph.D.
Director, Ph.D. in Engineering Program

Joseph F. Thomas, Jr., Ph.D.
Dean, School of Graduate Studies

Committee on
Final Examination

Arnab K. Shaw, Ph.D.

Zhiqiang Wu, Ph.D.

Fred Garber, Ph.D.

Michael A. Temple, Ph.D.

Michael L. Bryant, Ph.D.

ABSTRACT

Chakravarthy, Vasu. Ph.D., Engineering Ph.D. Program, College of Engineering and Computer Science, Wright State University, 2008.
Title: Evaluation of Overlay/Underlay Waveform via SD-SMSE Framework for Enhancing Spectrum Efficiency.

Recent studies have suggested that spectrum congestion is mainly due to the inefficient use of spectrum rather than its unavailability. Dynamic Spectrum Access (DSA) and Cognitive Radio (CR) are two terminologies which are used in the context of improved spectrum efficiency and usage. The DSA concept has been around for quite some time while the advent of CR has created a paradigm shift in wireless communications and instigated a change in FCC policy towards spectrum regulations. DSA can be broadly categorized as using a 1)Dynamic Exclusive Use Model, 2) Spectrum Commons or Open sharing model or 3) Hierarchical Access model. The hierarchical access model envisions primary licensed bands, to be opened up for secondary users, while inducing a minimum acceptable interference to primary users. Spectrum overlay and spectrum underlay technologies fall within the hierarchical model, and allow primary and secondary users to coexist while improving spectrum efficiency. Spectrum overlay in conjunction with the present CR model considers only the *unused* (white) spectral regions while in spectrum underlay the *underused* (gray) spectral regions are utilized. The underlay approach is similar to ultra wide band (UWB) and spread spectrum (SS) techniques utilize much wider spectrum and operate below the noise floor of primary users.

Software defined radio (SDR) is considered a key CR enabling technology. Spectrally modulated, spectrally encoded (SMSE) multi-carrier signals such as Orthogonal Frequency Domain Multiplexing (OFDM) and Multi-carrier Code Division Multiple Access(MCCDMA) are hailed as candidate CR waveforms. The SMSE structure supports and is well-suited for SDR based CR applications. This work began by developing a general soft decision (SD) CR framework, based on a previously developed SMSE framework that

combines benefits of both the overlay and underlay techniques to improve spectrum efficiency and maximizing the channel capacity. The resultant SD-SMSE framework provides a user with considerable flexibility to choose overlay, underlay or hybrid overlay/underlay waveform depending on the scenario, situation or need. Overlay/Underlay SD-SMSE framework flexibility is demonstrated by applying it to a family of SMSE modulated signals such as OFDM, MCCDMA, Carrier Interferometry (CI) MCCDMA and Transform Domain Communication System (TDCS). Based on simulation results, a performance analysis of Overlay, Underlay and hybrid Overlay/Underlay waveforms is presented. Finally, the benefits of combining overlay/underlay techniques to improve spectrum efficiency and maximize channel capacity is addressed.

Contents

List of Figures

List of Tables

Acknowledgement

I would like to thank all my committee members (Dr. Arnab Shaw, Dr. Zhiqiang Wu, Dr. Fred Garber, Dr. Michael Temple and Dr. Michael Bryant) for their invaluable support and advice during the work on this thesis. In particular, I would like to thank Dr. Michael Temple for his positive outlook and feedback over the many years spent on this research. Special thanks to Dr. Zhiqiang Wu who has been an integral part of this thesis work, for spending countless hours in shaping this research and for playing a key role in bringing the best out of me.

I would like to extend my sincere thanks to my AFRL colleagues and fellowmen, Jill Johnson, Cliff Bullmaster, James Stephens and Anthony White, for their continual support and endurance, to Dr. Steve Schneider, Emil Martinsek, Dr. Murali Rangaswamy, Dr. Leo Kempel, Maj. Roberts and Maj. Nunez for their encouragement and moral support. I feel extremely fortunate for having had the opportunity to interact intellectually with all of you who have been instrumental in molding me into the researcher I am today.

A special thanks to my fellow students Shirley, Meng and Ruolin and the friendly staff at the Electrical Engineering department at Wright State University for all the assistance they have provided me in achieving this goal.

I would like to thank Asha Manohar who has been my friend, philosopher and a spiritual guide. To my parents, I can never thank you enough for imparting the importance of perseverance without which I would not be on this pedestal today. I am indeed honored to be one of your children. I would like to thank my brothers and sisters who have always cheered and encouraged me along the way in both good and not so good times. I would especially like to thank my four little wonderful boys, who have been a source of unconditional love, joy, encouragement and for giving me that extra spurt of energy to reach the finish line. You have always put a smile on my face when I needed it. Finally, words cannot describe the role played by my dear wife Latha who has endured the strife along with me, always by my side. I would like to share this trophy with you.

Dedication

कायेन वाचा मनसेन्द्रियैर्वा
बुद्ध्याऽऽत्मना वा प्रकृतेः स्वभावात्।
करोमि यद्यत् सकलं परस्मै
नारायणायेति समर्पयामि॥ ११ ॥

kāyena vācā manasendriyairvā
buddhyātmanā vā prakṛteḥ svabhāvāt।
karomi yadyat sakalaṃ parasmai
nārāyaṇāyeti samarpayāmi॥

Meaning: Whatever I do through my body, speech, mind, sense organs, reason, will or natural inclination, I offer it all to the Ultimate Being. This oft-recited Sanskrit verse signifies an ardent attitude of a spiritual seeker for whom all life is or must be pervaded by intense desire to reach the acme of spiritual accomplishment. Material achievement is consummated by acquiring something from without; while spiritual accomplishment is marked by selfless giving of one's whole being, together with all of its activities, to the ultimate spiritual being that sustains the universe and stretches far beyond [16].

Introduction

1.1 Motivation

”Spectrum is the lifeblood of Radio Frequency (RF) Communications” [17]. With an ever increasing demand for higher data rates, coupled with an increase in new applications and the number of users, spectrum crowding and congestion continue to increase. Spectrum congestion is a concern and problem to both military and commercial users. At first glance, as depicted in Fig. 1.1 which shows the Federal Communication Commission’s (FCC) fully allocated spectrum chart, it seems like there is a spectrum scarcity [18] . Recent studies have suggested that spectrum congestion is mainly due to the inefficient use of the spectrum rather than its scarcity [19].

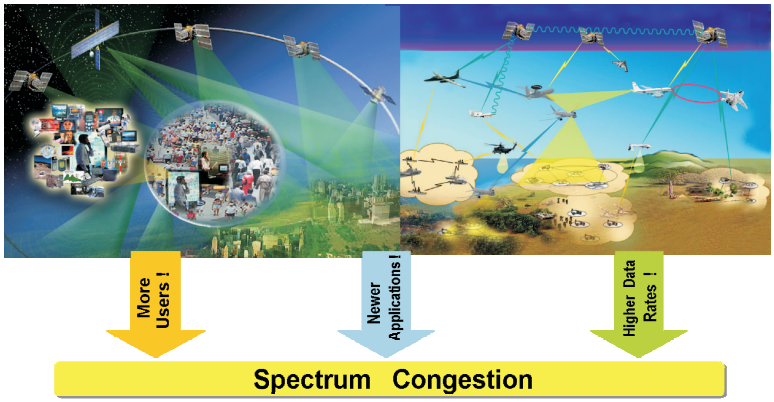

Figure 1.1: Illustration of spectrum congestion factors

A number of studies by different institutions, government agencies and academia such

as Shared Spectrum, Defense Advanced Research Project Agency (DARPA), FCC, U.C. Berkeley to name a few, have performed number of measurements to study spectrum utilization in and outside USA. One such study performed under DARPA's NeXt Generation (XG) communication program suggested that on average, only two percent of the spectrum is actually in use in the United States at any given time [1]. Another study by the FCC revealed that about five to ten percent is being used at any given time. These measurements revealed that in many bands spectrum access is more of a problem than spectrum scarcity.

The problem of spectrum inefficiency stems from the fact that we are trying to adapt the 21st century technology coupled with the increase in number of users and demand for more spectrum, to the policies and regulations formulated in 1934, wherein different frequency bands are assigned to different users or service providers, and licenses are required to operate within those bands.

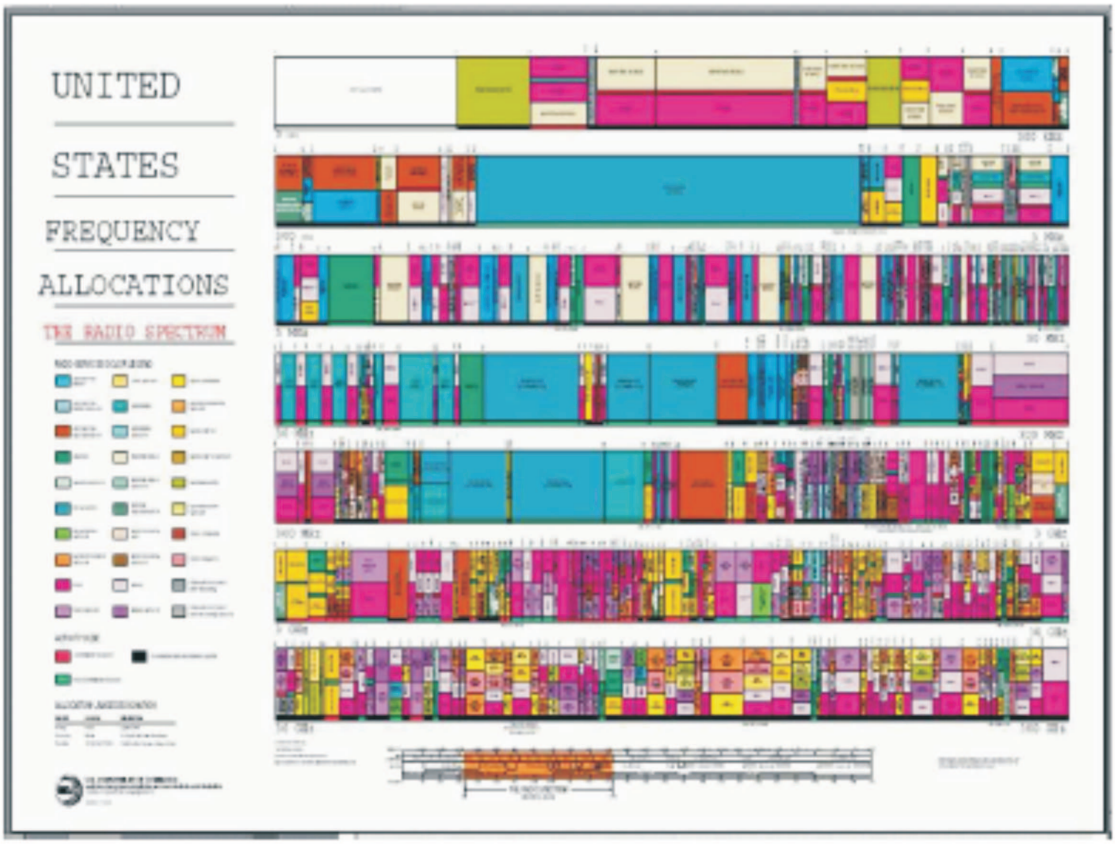

Figure 1.2: FCC's spectrum utilization chart

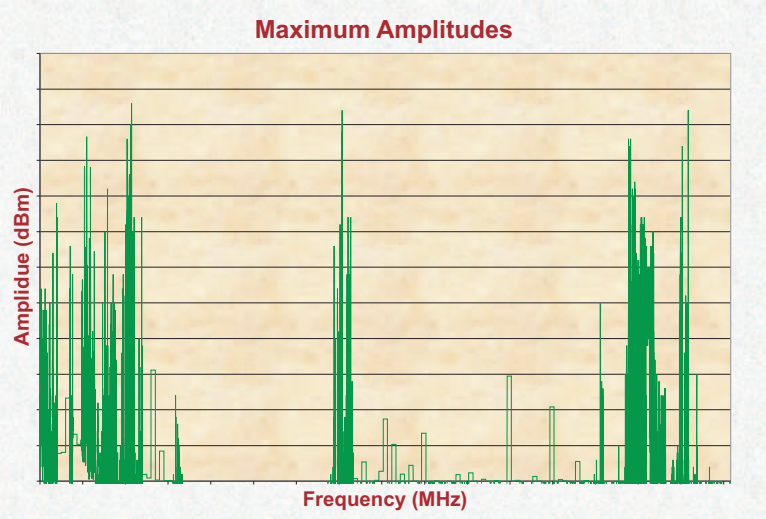

Figure 1.3: Spectrum utilization study by DARPA's Next Generation (XG) program [1]

To exploit the unused spectrum more efficiently in dynamically changing environments, it is desirable to have a secondary communication system capable of utilizing the unused spectrum, by adapting to the rapidly changing environmental conditions while ensuring minimal, or at least manageable interference to existing primary users. Such a technology is termed the Cognitive Radio (CR) [3]. In 2003 the FCC issued a Notice of Proposed Rule Making (NPRM)[19] calling for inputs on how CR could be realized, and in 2005 the FCC adopted rule changes to include CR in the Television (TV) bands [20].

1.1.1 Dynamic Spectrum Access

Two terminologies namely Dynamic Spectrum Access (DSA) and Cognitive Radio (CR) have been used by the research community in the context of improving spectrum efficiency. As illustrated in Fig. 1.4, DSA can be categorized into three groups namely 1) Dynamic exclusive use model, 2) Open Sharing Model and 3) Hierarchical Access Model [2]. Dynamic exclusive model basically follows the present policy and regulations. Spectrum property rights and dynamic spectrum allocation are two methods introduced within this model to add flexibility for spectrum efficiency. In the first method, primary user (licensees) are

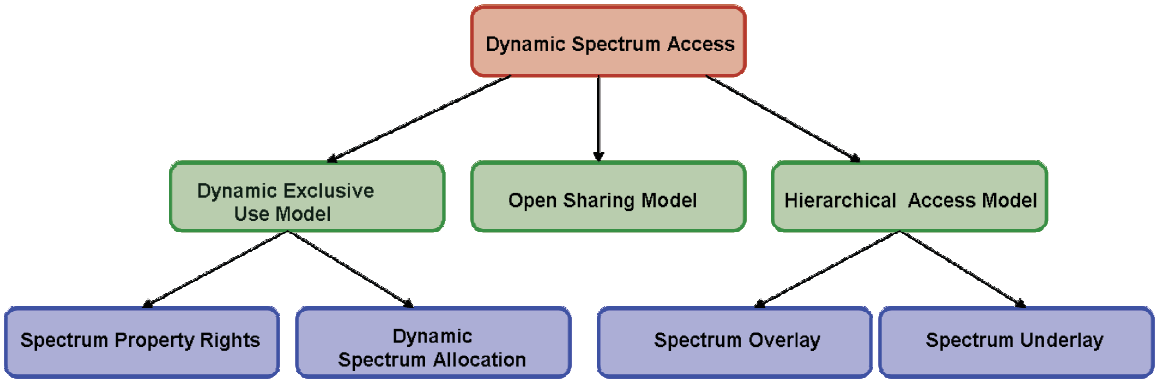

Figure 1.4: Dynamic Spectrum Access scenarios [2]

allowed to sell/trade spectrum and can choose technology of their choice. The second method, dynamic spectrum allocation introduced by the European DRiVE project, aims to improve spectrum efficiency via dynamic spectrum assignment utilizing the spatial and temporal statistics of different users. Open sharing model also known as spectrum commons employs sharing among peers as the basis to manage a spectrum region. This model basically gains support from the success of wireless services operating in unlicensed industrial, scientific and medical (ISM) band. Finally, in the hierarchical access model interaction between primary and secondary users are considered for achieving spectrum efficiency. The basic idea here is to open the licensed spectrum to secondary users while maintaining minimum acceptable interference to the primary users. Spectrum overlay and Spectrum underlay are two spectrum sharing approaches which have been under consideration. Spectrum overlay allows the unlicensed secondary users to utilize the unused spectrum simultaneously with the primary user on a non-interference basis. This overlay approach was first adapted by [3] and further researched by the DARPA's Next Generation (XG) program under the term opportunistic spectrum access [21]. Similarly, spectrum underlay allows the unlicensed secondary user to simultaneously operate in primary user bands but with a severe power constraint on the transmit power of the secondary user. Out of all these three spectrum access models, the hierarchical access model is perhaps the most compatible one with current FCC policies and legacy wireless systems.

Out of all the three DSA methods discussed, Cognitive Radio (CR) seems to be most compatible with the hierarchical access method. Even though the present definition of CR only considers overlay approach, research trend suggests that a combination of overlay/underlay can be employed to maximize the spectral efficiency utilizing both white and gray portion of the spectrum [2, 22, 23]. Therefore, CR can be further categorized as overlay-CR and underlay-CR.

1.2 Overview of Cognitive Radio

Over the last few decades, radio engineering, and in particular wireless communication has made significant advances enabled by Moore's law of computational evolution. Advances in Digital Signal Processor (DSP) and General Purpose Processer (GPP) were key enablers in implementing modulation, demodulation and signaling protocols, revolutionizing technologies from analog to digital to software functions [17]. The 90's introduced the concept of Software Defined Radio (SDR) [24, 25]. These radios typically have a RF front-end with a software-controlled tuner. Digitized baseband signal processing is performed by a reconfigurable device such as field-programmable gate array or DSP processor [13]. Department of Defense (DOD) programs such as Speakeasy I and Speakeasy II demonstrated the feasibility of SDR [26]. Later in 2000, Mitola in his dissertation work extended the concept of SDR and coined the term *Cognitive radio* [3, 27].

The introduction of CR technology has created a paradigm shift in wireless communications. It has instigated research interest not only among radio engineering community but also among other disciplines such as networking, mathematics (game theory), Economics, Marketing, Business law to name a few. With the involvement all the these heterogeneous disciplines many different interpretation and definitions of the term *Cognitive Radio* can be found in the literature.

Ever since Mitola coined the word *Cognitive Radio*[3] many definitions have emerged

depending on the usage and viewpoint.Perhaps the most complete and extensive definition of CR found in literature are given by Mitola and Haykin. Mitola [3] defines CR as *"Systems consisting of wireless Personal Communication System (PCS) and other wired networks which are computationally intelligent about radio resources and related computer-to-computer communications to detect user communication needs as a function of use context, and to provide radio resources and wireless services most appropriate to those needs. It is a vision of intelligent wireless "black-box" with which the user travels. Wherever the user goes, cognitive device will adapt to new environment allowing the user to be always connected"*.

Mitola envisions an ideal CR as one which integrates CR techniques with advanced software defined radio, computer vision, high performance speech understanding, global positioning system (GPS), sophisticated adaptive networking, adaptive physical layer radio waveform and a wide range of machine learning process in creating an ideal CR or personal digital assistant (PDA) [21]. Some of the functionality of the ideal CR are:

- CRs see what you see, discovering radio frequency uses, needs, and preferences.
- CRs hear what you hear, augmenting your personal skills.
- CRs learn to differentiate speakers to reduce confusion..

Haykin defines it as *"An intelligent wireless communication system that is aware of its surrounding environment (i.e. outside world), and uses the methodology of understanding by building to learn from the environment and adapt its internal states to statistical variations in the incoming RF stimuli by making corresponding changes in certain parameters (e.g. transmit power, carrier frequency, and modulation strategy) in real time, with two primary objectives in mind: highly reliable communications whenever and wherever needed and efficient utilization of the spectrum"* [28].

FCC has opted for a more concise definition by just focusing on the physical layer adaptation. FCC defines CR as *" A radio that can change its transmitter parameters based*

on interaction with the environment in which it operates" [20].

Meanwhile, National Telecommunications and Information Adminstration (NTIA) the other spectrum regulatory body in the US focuses on the applications of cognitive radio and defines CR as *A radio or system that senses its operational electromagnetic and can dynamically and autonomously adjust its radio operating parameters to modify system operations, such as maximize throughput, mitigate interference, facilitate inter-operability, and access secondary markets,"*[15].

Similarly, there are other definitions of cognitive radio from institutions such as IEEE USA, IEEE 1900 Software Defined Radio Forum Cognitive Radio Working Group (SDFR CRWG) and Virginia Tech Cognitive Radio Working Group (VT CRWG) to name a few. Even though all these definitions by these various groups and institutions appear to create more confusion than harmony, a closer look at the fundamental functionalities of these definitions as summarized in Table 1.1 actually reveals some commonalities amongst these definitions. The common underlying assumption in all these definitions is that they have some level of cognition and autonomous operation. Also, the common capabilities found in all the definitions are, observation, adaptability and intelligence [15].

So far, various definitions of cognitive radio from number of different perspectives have been presented. A group of cognitive radios communicating and interacting with each other exchanging information can be termed as Cognitive Radio Networks (CRN) [17, 29]. CRN clearly delineates from cognitive radios in terms of the controlling goals. In a CRN, goals are derived based on end-to-end network performance objectives, whereas in CR the goals are localized only to the radio's user. These end-to-end goals are derived at run-time from operators, users, applications and resource requirements in addition to any design-time goals. The difference in the scope of the goal from local to end-to-end enables the cognitive radio networks to operate more easily across all layers of the protocol stack [17, 30]. Next, some of the basic building blocks and terminologies associated with cognitive radio will be discussed.

Table 1.1: Cognitive Radio Definition Matrix [15]

Definer	Adapts (Intelligenly)	Autonomous	Can Sense Environment	Transmitter	Receiver	'Aware' Environment	Goal Driven	Learn the Environment	'Aware' Capabilities	Negotiate Waveforms	No interference
FCC	•	•	•	•							
Haykin	•	•	•	•	•	•	•	•			
IEEE 1900.1	•	•	•	•	•						
IEEE USA	•	•	•	•	•	•					•
ITU-R	•	•	•	•	•	•					
Mitola	•	•	•	•	•	•	•	•	•	•	
NTIA	•	•	•	•	•	•	•				
SDRF CRWG	•	•	•	•	•		•				
SDRF SIG	•	•	•	•	•	•	•	•	•		
VT CRWG	•	•	•	•	•	•	•	•	•		

1.2.1 Types of Radios

Since the FCC definition is primarily focusing on the physical layer adaptation of the spectrum, there is common belief that CR is just another fancy name for adaptive radios [30]. In general, radios can be classified as 1) Aware radios, 2) Adaptive radios and 3) Cognitive radios [21].

Aware Radio

Radios which are capable of sensing all or part of their environment are considered as radios with spectrum awareness or simply aware radio. A voice radio inherently has sensing capabilities in both audio and RF frequencies. When these sensors are used for the purpose of collecting environmental information, it becomes an aware radio. RF spectrum sensing information is utilized in channel, interference or signal estimation.

Adaptive Radio

Radio with ability to sense the RF environment as well as autonomously change its operating parameters are termed as adaptive radios. Frequency, instantaneous bandwidth, modulation, error correction code, equalizers are examples of operating parameters which can be utilized in adaptation. For example, a frequency hopping spread spectrum system (FHSS) is not considered adaptive since the hopping patterns are predetermined. However, if the FHSS is capable of changing its hop pattern to reduce collision, then it can be considered as an adaptive radio.

Cognitive Radio

A radio which is aware, has ability to adapt and also is capable of learning is considered as cognitive radio. The first examples of CRs were modeled in the DARPA's XG program. These radios sense the spectrum environment, identify an unoccupied or unused spectrum, and rendezvous multiple radios in the unused spectrum band and move to another band if a legacy user re-enters that band. The adaptive capability of these radios improves as they learn more about the environment.

1.2.2 Cognition in Cognitive Radio

The term cognition is usually associated with human thought process and reasoning abilities. It is defined as a mental processing to analyze a given situation utilizing aspects such as, awareness perception, reasoning and judgement. Cognition in cognitive radio sense is defined as, monitoring and structuring the knowledge of self, other users, and the environment to provide information services. It is also defined as learning from experience to tailor services to user requirements, scenarios and environments [3, 17].

Similar to cognitive radios, there does not seem to be a commonly accepted definition of cognition cycle. As a reference to cognition cycle in relation to cognitive radios, Mitola's

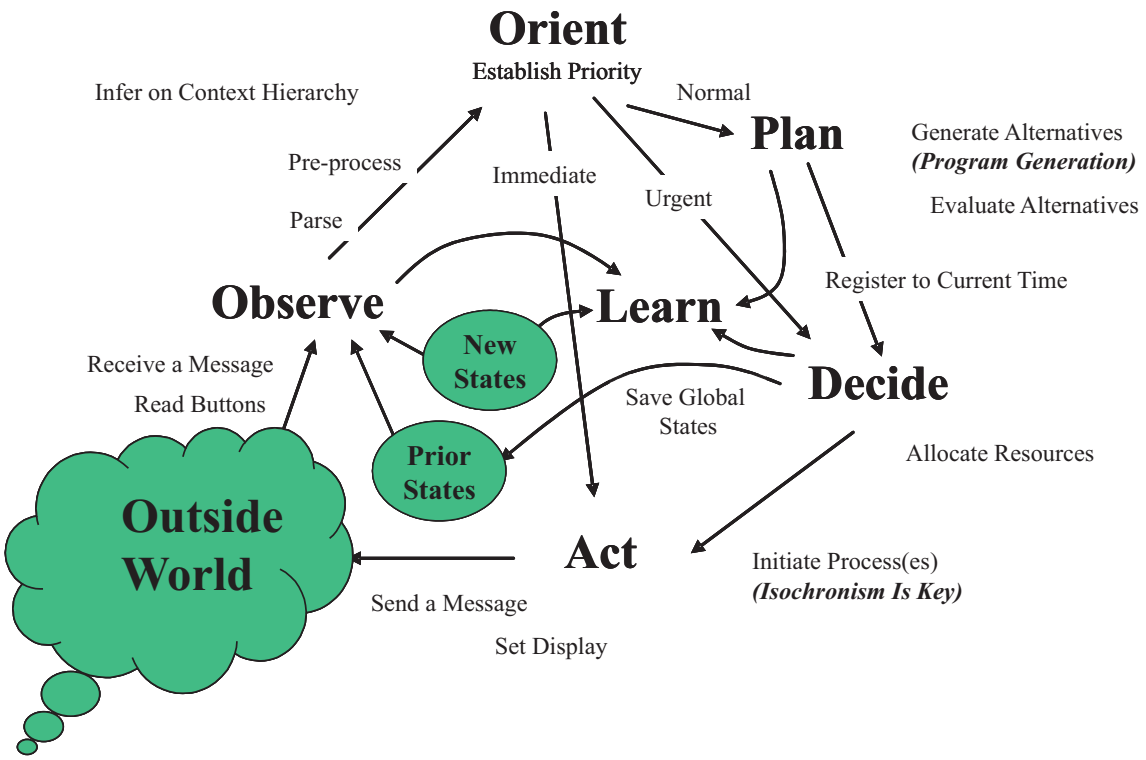

Figure 1.5: Cognition Cycle as defined by Mitola [3]

version of cognition cycle provides a good example [3]. Mitola's cognition cycle in Fig. 1.5 stems from the OODA loop concept. The OODA loop is a concept that originated from the military strategist Col. John Boyd of the United States Air Force. Its main outline consists of four overlapping and interacting processes: Observe, Orient, Decide and Act.

In the cognition cycle of Fig. 1.5, a radio gathers information regarding its operating scenario by observation *(Observe)*. The information is then analyzed *(Orient)* to determine its importance. Based on this evaluation, a radio sorts through it's various options *(Plan)* and chooses the best option *(Decide)* suitable for that situation and radio scenario. Finally, assuming a waveform change is necessary, the radio adapts, implementing the alternative solution *(Act)* by adjusting its resources and applying appropriate signaling.

There are a number of different cognition cycle in the literature depending on one's need and interpretation of a cognitive radio. A cognition cycle can be as elaborate as the one in Fig. 1.5 or as simple as the one shown in Fig. 1.6.

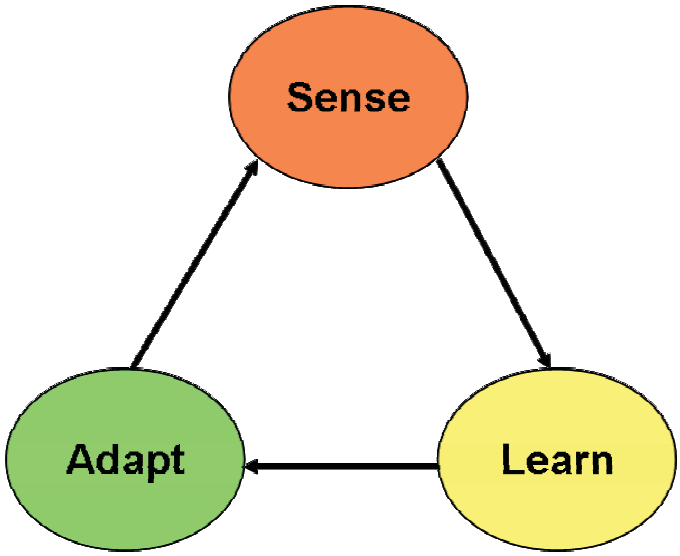

Figure 1.6: A simpler version of the cognition cycle

Figure 1.6 shows the key components in a cognitive radio or cognitive radio network. The sensing function can include environmental changes, spectrum holes and primary/secondary users and their positions. Learning functions includes protocols, physical/network layer parameters, interference levels and system or channel capacity. Learning tools includes algorithms (genetic, game theory, pattern recognition, etc.), external inputs and past experiences. Finally, adaptation can take place at any single layer or by using a cross-layered approach.

Fig. 1.7 illustrates different types of diversity techniques presently under consideration for cognitive radio application. In general, diversity paves way for orthogonality and orthogonality is essential in minimizing multi-user interference. The combination of these diversity techniques spanning across different layers of a communication system is also termed as Cross-Layer design of Cognitive Network.

1.2.3 Spectrum Sensing

Spectrum sensing is one of the most important functions in the realization of Cognitive Radios. In general, spectrum sensing is associated with measuring the spectral content using

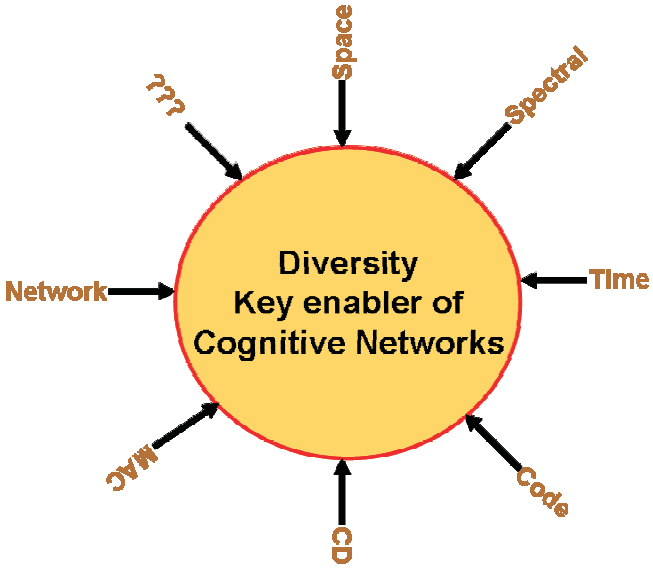

Figure 1.7: Diversity: A Key Enabler of Cognitive Radio Networks

a number of spectrum estimation methods. In a CR sense, spectrum sensing not only has to deal with identifying spectrum holes but also requires awareness about their operating environment in a multi-dimensional space such as frequency, time, space and code [17]. Other unique signal features such as modulation, waveform bandwidth, baud rate, carrier frequency and geolocation are also important not only in distinguishing primary/secondary users but also in designing a waveform which can minimize interference and maximize spectral efficiency. There are a number of challenges in implementing spectrum sensing techniques in CR scenario. To begin with there are Radio Frequency (RF) front-end design requirements, the need for a wide band antenna with a narrow band frequency resolution, Analog-to-Digital Converter with high sampling rate and dynamic range, and high performance signal processing algorithms. Other challenges and considerations in design and implementation of sensing algorithms are, identifying the hidden node, detection of agile and spread spectrum primary signals, sensing window or time, implementation complexity, presence of multiple secondary users, coherence time, multipath, competition, robustness

and power consumption [17].

Even though spectrum sensing in a CR sense is still in its infancy stages, number of approaches which are utilized in the signal detection methods have been extended in detection, identification and classification of primary and secondary signals. Match Filtering, Waveform-Based sensing, Cyclostationary featured based sensing, Energy or Power spectrum based sensing are some of the methods proposed in the literature. Matched filtering is an optimum detection method when primary user signal features are known [12, 31, 32, 33, 34, 35, 36, 37]. Energy detection is simple and can be implemented efficiently by using an FFT algorithm. However, there are some drawbacks for energy detection: 1) the decision threshold is subject to changing signal to noise ratios. 2) it can not distinguish interference from a user signal. 3) it is not effective for signals whose signal power has been spread over a wide bandwidth. Feature based detection methods have been extensively utilized in military application to detect the presence of weak signals [38]. Cyclostationary feature detection is a promising option especially in the situation where energy detection is not so effective. However, it requires a large computational capacity [11]. A detailed discussion of cyclostationary based signal detection is presented in Appendix 8.1.

So far, the discussion has been limited to physical layer detection related to cognitive radio or single user, but in a practical scenario it is expected that a network or cognitive radio will operate in the presence of network of primary users. Cooperative and collaborative sensing approaches have been proposed in addressing a number of issues raised in spectrum sensing discussion such as noise uncertainty, fading, shadowing and hidden node problems, to name a few. Centralized and distributed sensing are two cooperative methods discussed in literature [39, 40].

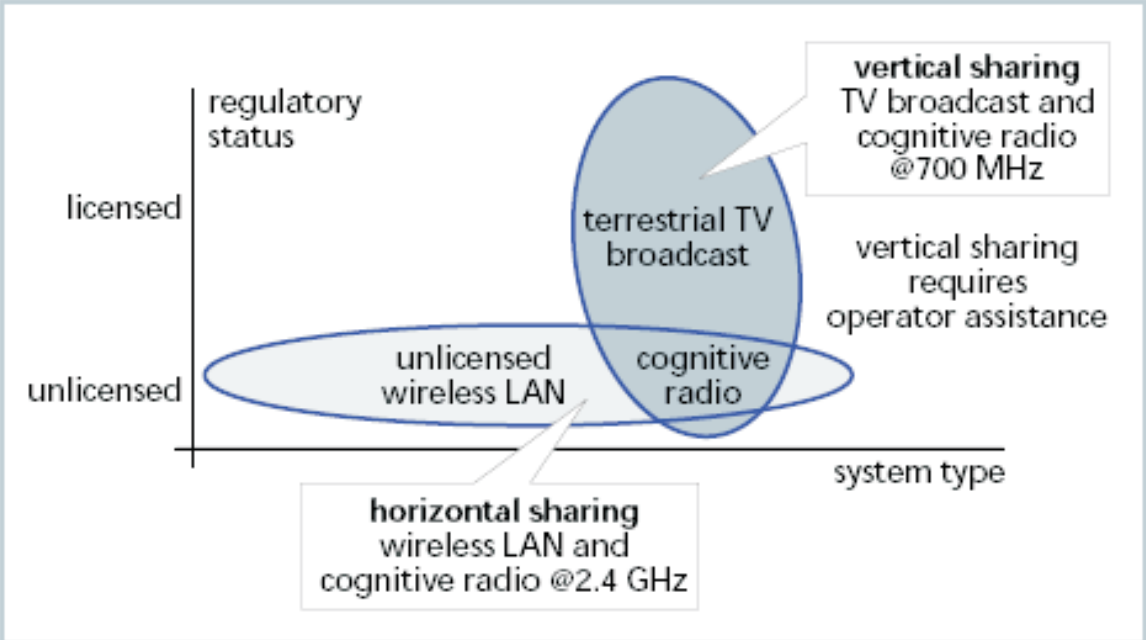

Figure 1.8: Illustration of horizontal and vertical sharing [4]

1.2.4 Spectrum Sharing

Spectrum sharing or learning how to share can be viewed as a two dimensional problem consisting of vertical and horizontal sharing [41]. Vertical sharing is defined as sharing resources with users of multiple systems with different levels of regulatory status. Horizontal sharing is between users of systems with equal regulatory status. Fig. 1.8 shows spectrum sharing between TV broadcast (primary users) and CR systems (secondary users) an example of vertical sharing. Sharing with other cognitive radio systems or secondary user "systems" such as 802.11 and 802.16 is an example of horizontal sharing. For both vertical or horizontal sharing, a CR system must not only be capable of identifying spectrum holes, it should be also able to design an appropriate waveform which will cause minimal interference.

CR waveforms can be classified as two types: underlay and overlay waveforms [4, 42]. Underlay waveforms are those which operate on top of other systems. Fig. 1.9 depicts Ultra Wide Band (UWB) as an underlay waveform approved by the FCC. Overlay waveforms are those which are designed to operate only in the spectrum holes. Fig. 1.10 illustrates an

overlay scenario consisting of primary and secondary systems.

Spectrum sharing or spectral co-existence is not entirely a new concept, multi-users in a homogeneous system can share the spectrum using a number of Multiple Access (MA) techniques such as Code Division Multiple Access (CDMA), Time Division Multiple Access (TDMA), Frequency Division Multiple Access (FDMA) and Carrier Sense Multiple Access (CSMA) [43]. Studies up until now have been focused on spectrum sharing issues related to legacy cellular system, users in the unlicensed band using different 802.xx standards and more recently a lot of attention has been given to UWB communication and its ability to coexist with other systems [44, 45, 46, 47]. In the case of cellular systems and unlicensed band users, spectral coexistence occurs in a limited sense using spatial and temporal diversity along with power control etiquettes. UWB systems have shown promise for short range applications. UWB causing interference for other systems as the number of UWB users increase remains a concern.

1.2.5 Physical Layer Adaptation

The parameters influencing cognitive radio physical layer waveform design includes power, frequency, modulation, symbol rate, pulse shaping and coding. The main objective and challenge of CR physical layer is designing a waveform which will be overlayed across multiple primary users bands while at the same time minimizing mutual interference to both primary and cognitive radio secondary users. Multi-Carrier modulations have been recognized as a potential candidate for the physical layer waveform design [28, 37, 48, 49]. In [48] the OFDM modulation scheme was chosen to implement its proposed spectrum spooling method to enhance spectrum efficiency. The goal of spectrum spooling is to enhance spectral efficiency of mobile radio systems by overlaying secondary mobile radio systems on existing primary users. The work in [37, 49] also considered OFDM based Multi-carrier modulation as an ideal candidate for overlay cognitive radio systems. The Fast Fourier Transform (FFT) used in OFDM are very effective in channel sensing in iden-

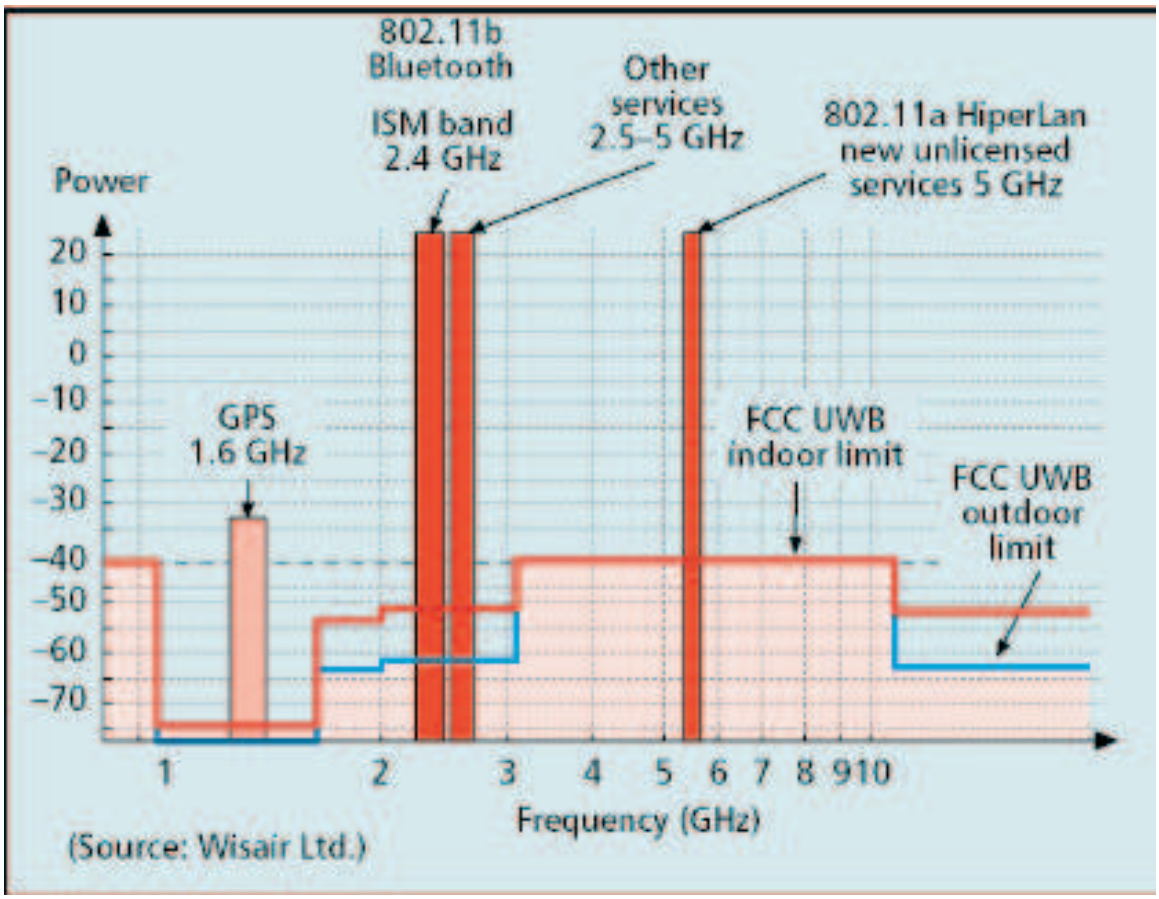

Figure 1.9: Illustrates CR-Underlay spectrum sharing concept.

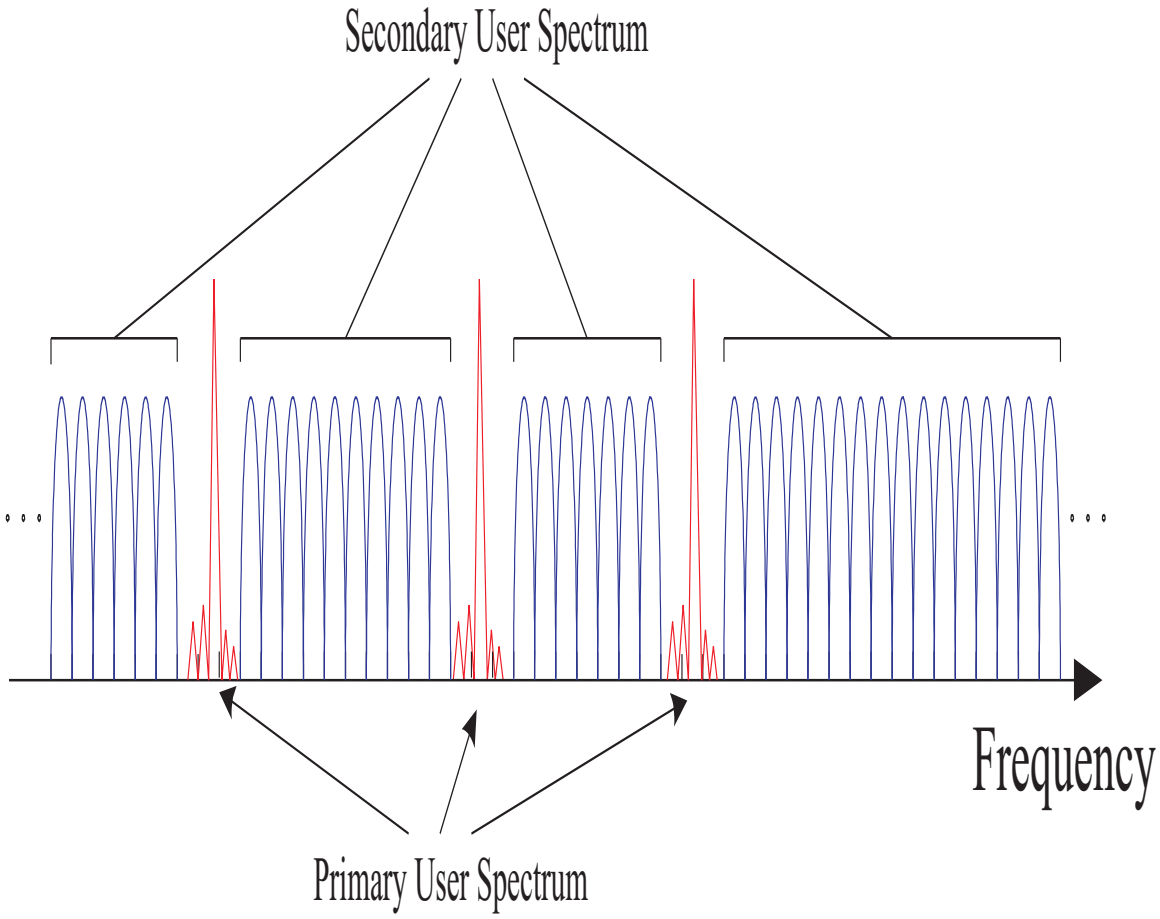

Figure 1.10: Illustrates CR-overlay spectrum sharing [5].

tifying spectrum holes, however they are also known for their spectral leakage problem. To mitigate this spectral leakage problem a multi-carrier filter bank approach was proposed [37].

A variant of the OFDM scheme in which arbitrarily selected subcarriers are disabled or de-activated to avoid interference to primary user bands is termed as discontiguous or non-contiguous orthogonal frequency division multiplexing (NC-OFDM) [50, 51]. Researchers have proposed and implemented a hardware prototype demonstrating the NC-OFDM concept. Work in [50] adopted the NC-OFDM and build a hardware prototype in implementing the IEEE 802.22 format which envisions improvement to the spectrum efficiency by utilizing the vacant TV bands. Work in [51] proposed a field programmable gate array (FPGA) based SDR transceiver capable of generating arbitrary NC-OFDM type waveforms.

In NC-OFDM, the sub carriers which are used by the primary user will be de-activated. Therefore, there are zero-valued inputs for the IFFT of the transmitter and zero valued outputs for the FFT of the receiver. When zero-valued inputs/outputs are greater than non-zero inputs/outputs, the standard FFT/IFFT used in OFDM application in no longer efficient [52]. The authors in [52, 53, 54] have all proposed computationally efficient methods in implementing NC-OFDM architecture.

The above research efforts have thus far identified multi-carrier waveforms in particular OFDM based waveforms as a strong CR candidate. The next series of papers [5, 55, 56] have considered other physical layer parameters such as power, modulation and coding in optimization of CR physical layer. Dynamic spectrum access utilizing CR concept will no doubt improve spectrum efficiency but it will increase the overhead information of the CR users reducing their effective throughput. To minimize the CR overhead, an adaptive sub-carrier block size algorithm proportional to the incumbent spectral occupancy has been proposed [5]. CR users in a dynamically time varying environment will experience performance degradation due to propagation loss because of fading. Assuming constraints on available subcarrier and power, a CR protocol which will employ adaptive modulation,

coding and power control algorithms before increasing the power or subcarrier block size has been proposed [55, 56].

Even though most of the initial research has focused and suggested OFDM based multi-carrier modulation as a suitable candidate for CR applications, OFDM by itself is not utilized in practical application due to its performance degradation in frequency selective fading [10]. Further more, a pure OFDM is more suitable for only broadcast type scenarios such as cellular down links or digital audio broadcast applications[56]. To mitigate these problems and to satisfy high data rate requirements as well as to improve spectrum efficiency and at the same time avoid interference to primary and other secondary users, other multi-carrier modulations such as MC-CDMA [57], CI/MC-CDMA [58, 59] and TDCS [7] have also been proposed as a possible CR candidate waveform [60, 61, 62, 63, 64, 65].

Software defined radio (SDR) is another promising DSA enabling technology where the radio transceivers perform baseband processing in software. SDR has the ability to quickly reconfigure its operating parameters, which is a fundamental requirement in the CR scenarios. The synergistic union of these two DSA technologies is termed *"CR-based SDR"*. That is, the SDR provides the software controlled communication vehicle (core technology for air interface and waveform generation), the control and application of which is based on CR principles guided by spectral monitoring to achieve efficient spectrum usage [66]. Driven by SDR principles, a general analytic framework was developed to encompass a myriad of multi-carrier signals. The framework is applicable to a broad class of waveforms that are called *Spectrally Modulated, Spectrally Encoded* (SMSE) signals [66, 67, 68]. Using this SMSE framework and depending on a CR user needs, various multi-carrier waveforms can be generated, including: OFDM, MC-CDMA, CI/MC-CDMA or TDCS.

1.2.6 Cognitive Radio Standards

There are a number of standards related to DSA. DSA's main objective is to improve spectrum efficiency by accommodating spectrum coexistence. Majority of the IEEE 802 standards (802.11h, 802.15 and 802.16) have been extended to include dynamic spectrum access capabilities [69]. Cognition is not particularly necessary to implement co-existence in improving spectrum efficiency, but cognitive techniques can be helpful in facilitating coexistence. In this section two well-known cognitive radio standards namely SCC41 and IEEE 802.22 will be examined.

Standards Coordinating Committee

The Standards Coordinating Committee 41 (SCC41 or P1900) standards evolved from the Dynamic Spectrum Access Networks (DySPAN) Standards Coordinating Committee (SCC) projects. Instead of just recommending a specific physical (PHY) or media access control (MAC) layer, SCC41 focuses on developing architectural concepts and specifications for network management between heterogeneous wireless networks [69]. The SCC41 is sub-divided into six working groups as follows:

IEEE P1900.1 This group works on terminologies and concepts for the next generation radio systems and spectrum management initiations.

IEEE P1900.2 The main focus is on recommended practice for interference and coexistence analysis.

IEEE P1900.3 This groups function is to lay out techniques for testing and analysis to be used in evaluating new radio systems. It also identifies radio system design features to simplify the evaluation process.

IEEE P1900.4 The objective of this standard is to define basic building blocks such as network resource managers and device resource manager, enabling coordinated network-device distributed decision making which will aid in the optimum use of radio resources.

IEEE P1900.5 and IEEE P1900.6 SSS41 has recently proposed two new working groups to address policy language and RF sensing. The objective of these two working groups is to develop the policy language framework using ontology-based language and also to the address spectrum sensing function to be managed by each CR terminal [69].

IEEE 802.22

In 2004, the FCC formalized a Notice of Proposed Rule Making (NPRM) that announced the use of unlicensed wireless operation in the analog television (TV) bands [70]. In response to this notice, the IEEE 802 standards committee created the IEEE 802.22 working group (WG) on wireless regional area networks (WRANs) with a CR-based air interface for use by license-exempt devices on a non-interfering basis in the very high frequency (VHF) and ultra high frequency (UHF) bands. Since its inception, significant progress has been made towards the PHY, MAC and cognitive domain definitions of the standard.

1.3 Scope and Assumptions

1.3.1 Scope

Of all the dynamic spectrum access methods discussed, this research effort is limited to the hierarchical spectrum access methodology. In particular, the focus here is on the physical layer design of CR-Overlay, CR-Underlay and hybrid overlay/underlay waveforms.

1.3.2 Assumptions

A number of assumptions have been made throughout the document in order to constrain the research effort and to focus on physical layer waveform design and analysis. Some of the major assumptions are:

- Perfect Synchronization was assumed between primary and secondary users when performing co-existence analysis. Synchronization between secondary transmitter and receiver was also assumed.
- Since the spectrum sensing function requires identifying spectrum holes, primary and other secondary users, and also setting up an interference threshold, a spectrum utilizations map was assumed to be known.
- In the performance evaluation of CR-Overlay and CR-Underlay waveforms over a frequency selective fading channel, it was assumed that the primary user interference to secondary user was not experiencing fading effects.
- The secondary user receiver can perfectly estimate the channel fading coefficients required for the maximum diversity combiner.

1.4 Dissertation Contributions

Driven by SDR principles, a general analytic framework was developed to encompass a myriad of multi-carrier signals. The framework is applicable to a broad class of signals that are called *Spectrally Modulated, Spectrally Encoded* (SMSE) signals [66, 67, 68]. Depending on CR user needs, various multi-carrier waveforms can be generated, e.g., OFDM, MC-CDMA, CI/MC-CDMA or TDCS, using this SMSE framework. Given the original SMSE framework employed hard decision frequency allocation, its applicability is limited to overlay-CR signals. To extend its applicability and maximize spectrum efficiency by

utilizing both *unused* and *underused* regions, a soft decision SMSE (SD-SMSE) framework was subsequently developed to realize overlay-CR, underlay-CR and hybrid overlay/underlay CR signals [8].

- Presented a novel multi-functional SDR based SD-SMSE framework which can be utilized to generate overlay-CR, underlay-CR, and hybrid overlay/underlay CR waveforms.
- Extended the analytic SMSE expression to SD-SMSE by taking into account both *unused* and *underused* spectrum to maximize spectrum efficiency. From the general SD-SMSE expression, overlay-CR, underlay-CR and hybrid overlay/underlay expressions were derived.
- Derived an analytic expression for Bit Error Rate (BER) to evaluate a overlay-CR and underlay-CR performance in AWGN and fading channels.
- Demonstrated feasibility of overlay-CR and underlay-CR waveforms via numerical simulation, and validated its performance by comparison with the newly derived CR centric analytic expressions.
- Finally, presented the performance enhancement and spectrum efficiency improvement gained by using the hybrid overlay/underlay waveform with channel coding.

1.5 Dissertation Outline

This document is organized into seven chapters. The first chapter introduces the dynamic spectrum access (DSA) problem and provides an overview of different components involved in cognitive radio development. Chapter 2 provides an overview of the background information relevant to this dissertation, including an overview of Multi- Carrier (MC) modulations such as OFDM, MC-CDMA, CI/MC-CDMA and TDCS. This is followed

by the general analytic expression for Spectrally Modulated, Spectrally Encoded (SMSE) waveforms which encompasses all the multi-carrier waveforms used in this research. Chapter 3 provides development of the new SD-SMSE framework that accounts for both *unused* and *underused* spectral region. Using the SD-SMSE framework, Overlay-CR, Underlay-CR and hybrid Overlay/Underlay waveforms are presented. Chapter 4 presents evaluation of overlay and underlay waveforms under AWGN channel conditions. Chapter 5 presents the evaluation of overlay and underlay waveforms in frequency selective fading channels. Chapter 6 covers evaluation of a hybrid overlay/underlay waveforms in both AWGN and frequency selective fading channels. Finally Chapter 7 provides concluding remarks followed by open problems for future research.

Overview of Multi-Carrier Modulations

2.1 Introduction

This chapter starts with a brief overview of multi carrier modulations. In particular, the modulations used in this dissertation include OFDM, MC-CDMA, CI/MC-CDMA and TDCS. This will be followed by a discussion involving a general "Spectrally Modulated, Spectrally Encoded" (SMSE) expression from which a number of multi-carrier modulations can be formulated.

2.2 Overview of Multi-Carrier(MC) Modulations

Orthogonal Frequency Division Multiplexing (OFDM) is a popular Discrete Fourier Transform (DFT)-based technique that was initially proposed in the 1970s [6]. It's main use was for providing bandwidth reduction as an alternative to conventional multi-carrier techniques such as Frequency Division Multiplexing (FDM). OFDM has gained popularity with the emergence of wireless communications and wide band systems because of its inherent ability to compensate for multipath. In 1993, Linnartz et al. [71] combined OFDM with Code Division Multiple Access (CDMA) and proposed a new modulation scheme called Multi-Carrier CDMA (MC-CDMA). MC-CDMA effectively mitigates multipath interference while providing multiple access capability. Besides OFDM and MC-CDMA, there are

other variations of these approaches such as CI/OFDM, CI/MC-CDMA and TDCS found in the literature, which have been proposed to address the problems and limitations associated with OFDM and MC-CDMA. This chapter gives a brief overview of different multi carrier modulations. The general analytic expression to represent a number of these spectrally modulated, spectrally encoded multi-carrier signals is discussed.

2.2.1 Orthogonal Frequency Division Multiplexing (OFDM)

OFDM is a digital modulation scheme in which a wide-band signal is split into a number of narrow-band signals. Because the symbol duration of the narrow-band signal will be larger than the wide band signal, the amount of time dispersion caused by multi-path delay spread is reduced. OFDM is a special case of Multi-Carrier Modulation (MCM) in which multiple user symbols are transmitted in parallel using different sub-carriers with overlapping frequency bands that are mutually orthogonal. The origination of MCM or Frequency Division Multiplexing (FDM) dates back to 1950s and early 1960s for use in the military radios.

The overlapping multi-carrier technique implements the same number of channels as conventional Frequency Division Multiplexing (FDM), but with a much reduced bandwidth requirement. In conventional FDM, adjacent channels are well separated using a guard interval. In order to realize the overlapping technique, cross-talk between the adjacent channels must be reduced. Therefore, orthogonality between sub-carriers is required.

In OFDM each sub-carrier has an integer number of cycles within a given time interval T and the number of cycles each adjacent sub-carriers differ by is exactly one. This property assures OFDM sub-carrier orthogonality. The sub-carriers are data modulated using Phase Shift Keying (PSK) or Quadrature Amplitude Modulation (QAM). The amplitude spectrum of each modulated sub-carrier using either PSK or QAM has a $sinc^2$ shape. At the peak spectral response of each sub-carrier all other sub-carrier spectral responses are identically zero.

Following data modulation, symbols are fed through a serial-to-parallel conversion process. Each PSK or QAM symbol is assigned a sub-carrier, and an Inverse Discrete Fourier Transform (IDFT) is performed to produce a time domain signal. OFDM deals with multi-path delay spread by dividing a wide band signal into N narrow band channels where N is the number of sub-carriers. However, if the delay spread is longer than the symbol duration, multi-path will affect the performance. A guard-time is introduced to eliminate Inter-Symbol Interference (ISI) caused by delay spread. As a rule, the guard time is usually two to four times larger than the expected delay spread. This can take care of ISI but Inter-Carrier Interference (ICI) (cross-talk between sub-carriers) remains an issue. To reduce ICI, OFDM symbols are cyclically extended into the guard interval. This cyclic extension ensures that OFDM symbol will have an integer number of cycles in the DFT interval as long as the delay is less than the guard time.

At the receiver, after the RF and Analog to Digital (A/D) conversion stage, time and frequency synchronization between the transmitter and the receiver is very crucial with regard to performance of an OFDM link. A wide variety of techniques have been proposed for estimating and adjusting both timing and carrier frequency. Next, a DFT is used to demodulate all sub-carriers. To demodulate the sub-carriers using PSK or QAM modulations, reference phase and amplitude of the constellation on each sub-carriers are required. To overcome the unknown phase and amplitude ambiguities two techniques namely, coherent and differential detection are used [6].

Figure 2.1 illustrates the block diagram of a OFDM transmitter. As can be seen from Figure 2.1, each data symbol is transmitted via one narrow band subcarrier. Hence, each data symbol experiences a flat fade, leading to a simple OFDM receiver structure.

2.2.2 MC Code Division Multiple Access (MC-CDMA)

There are many possible ways to interpret and implement MC-CDMA. The approach used here to introduce MC-CDMA is by combining DS-CDMA and OFDM. Like OFDM, the

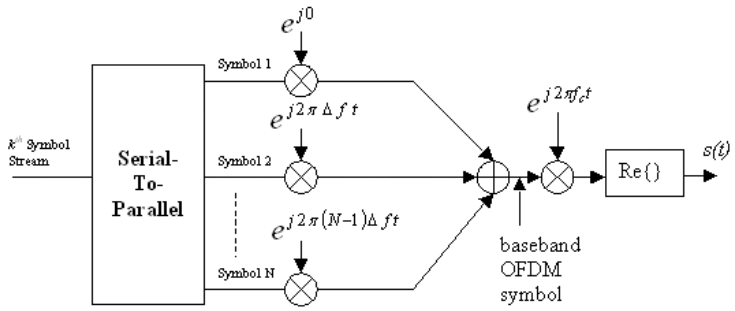

Figure 2.1: OFDM transmitter block diagram [6]

MC-CDMA signal is made up of a series of equal amplitude sub-carriers. Unlike OFDM where each sub-carrier transmits a different symbol, MC-CDMA transmits the same data symbol over each N sub-carrier. MC-CDMA applies spreading in the frequency domain by mapping a different chip of the spreading sequence to an individual OFDM sub-carrier [6].

The MC-CDMA transmitter can be implemented by concatenating a DS-CDMA spreader and an OFDM transmitter. The input data sequence is first converted into a number of parallel data sequence and then each data sequence is multiplied by a spreading code. The data in the spreading bits are modulated in baseband by IDFT and converted back to serial data. The spreading sequence in MC-CDMA provides multiple access capability. A guard interval with cyclic extensions similar to OFDM is inserted between symbols to counter ISI caused by multi-path fading. Similar to OFDM systems, MC-CDMA systems are very sensitive to non-linear amplification and require linear amplifiers. Two parameters that affect MC-CDMA design and performance are the guard interval and the number of sub carriers.

Figure 2.2 shows the block diagram of a MC-CDMA transmitter. It is clear that now each and every user's data symbol is spread over all subcarriers via the application of the spreading sequence. By choosing different spreading sequence, different versions of MC-CDMA can be implemented.

At the receiver a coherent detection method is employed to successfully de-spread the signal. The received signal after down conversion and digitization is first coherently detected with DFT and then multiplied by a gain factor. Equal Gain Combining (EGC)

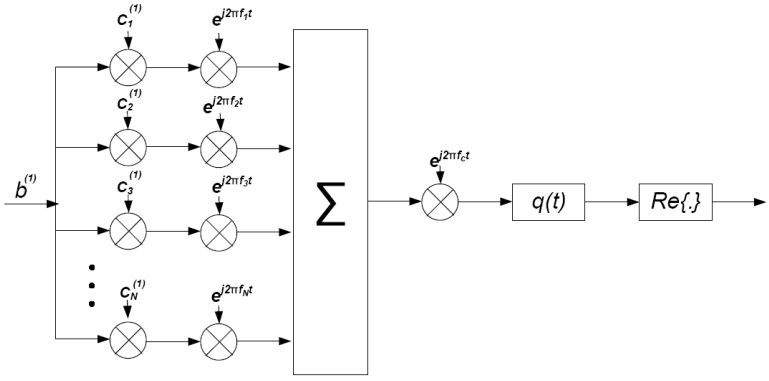

Figure 2.2: MC-CDMA transmitter block diagram [6]

and Maximum Ratio Combining (MRC) are standard combining techniques used in MC-CDMA receivers. The advantage of using combining techniques is that even though individual branches may not have sufficient SNR, their combined sum increases the probability of detection by increasing the SNR of a given signal. In EGC all branches are given equal weight (unity) irrespective of signal amplitude, but the signals from each branch are co-phased to avoid signals arriving at the same time. In MRC each signal is multiplied by a weight factor depending on the signal strength. Strong signals are amplified whereas weak signals are attenuated. Like EGC, MRC signals are also co-phased to avoid signal cancellations.

2.2.3 Carrier Interferometry (CI) MC-CDMA

Carrier Interferometry pulse shaping technique to reduce the interference and improve the performance has been applied to both OFDM and MC-CDMA [58, 59]. CI has been applied to OFDM (CI/OFDM) to minimize the peak to average power problem without reducing the data rate and also to provide narrow band interference suppression capability [72, 73]. CI has also been applied to MC-CDMA (CI/MC-CDMA). One difference between CI/MC-CDMA and MC-CDMA lies in the phase coding. MC-CDMA has different versions employing both pseudorandom (PN) as well as orthogonal codes. Each subcarrier is encoded with a -1 or +1. CI/MC-CDMA codes are polyphase orthogonal codes with

values ranging from $\{0, \pi\}$. Specifically, the polyphase orthogonal CI code of the k^{th} user corresponds to

$$\left\{ e^{j\frac{2\pi}{N}\cdot k\cdot 0}, e^{j\frac{2\pi}{N}\cdot k\cdot 1}, \cdots, e^{j\frac{2\pi}{N}\cdot k\cdot (N-1)} \right\} \tag{2.1}$$

When CI/MC-CDMA and MC-CDMA have both used orthogonal codes, CI codes have demonstrated superior performance than MC-CDMA in frequency selective fading channels [58]. MC-CDMA user limit is at $K = N$ where as CI/MC-CDMA provides added flexibility of supporting $k > N$ users by adding users with pseudo orthogonal signatures [58].

2.2.4 Transform Domain Communication System (TDCS)

Traditionally, communication waveforms are synthesized in the time domain using assigned frequency allocation(s) to the user(s). If interference is present, it can be mitigated using real-time transform domain filtering techniques to provide interference suppression. Such techniques can be traced back to [74, 75] where primary responsibility for achieving Signal-to-Noise Ratio (SNR) improvement rested on the receiver. Subsequent advances in processing power have enabled more computationally intense techniques [76, 77] whereby SNR improvement is achieved synergistically through transmit/receive waveform diversity to provide interference avoidance. The basic idea behind TDCS Fundamental Modulation Waveform (FMW) generation is to avoid existing users or jammers by operating dynamically over a given bandwidth. In 1988, German [77] proposed a system which uses spectral information to modify a Direct Sequence Spread Spectrum (DS-SS) waveform to avoid jammed frequencies. Subsequently in 1991, Andren of Harris Corporation patented a conceptual Low Probability of Intercept (LPI) Communication System for hiding the transmitted signal in noise using transform domain signal processing [76]. The patent does not provide theoretical analysis or address implementation issues associated with functional processing. The Air Force Research Laboratory (AFRL) and Air Force Institute of Tech-

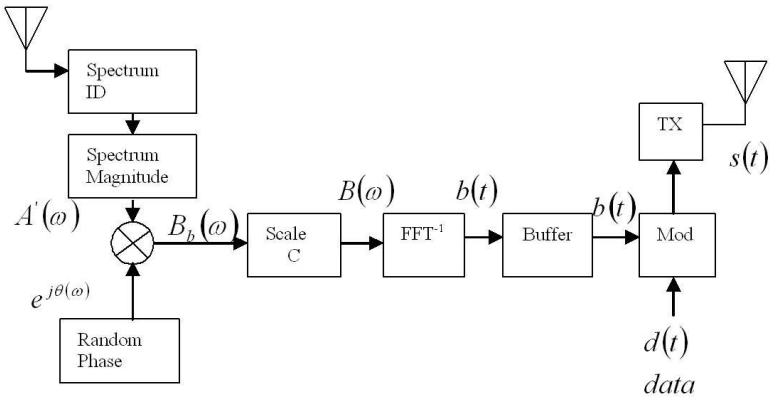

Figure 2.3: TDCS transmitter block diagram [7]

nology (AFIT) adopted Andren's framework for environmental sampling and waveform generation and German's transmit signal processing. Conventional time-domain matched filtering and Maximum Likelihood (ML) detection estimation are employed at the receiver [78, 79, 80, 81, 82, 83, 84, 85].

TDCS architecture assumes that both the transmitter and receiver are observing the same electromagnetic environment and thus produce similar spectral estimates and notches. In a basic TDCS implementation, spectral interference and friendly signal presence is estimated using Fourier-based or general spectral estimation techniques. Once the frequency bands containing interference or other signals are identified, typically through estimation and threshold detection, those bands are effectively "notched" (removed) prior to creating a clean or interference free spectrum. Then a complex poly-phase code is applied to the clean spectrum or sub-carriers in OFDM terms. Then a time-domain Fundamental Modulation Waveform (FMW) is obtained using the appropriate inverse transform (e.g., inverse DFT). Data then modulates the FMW to generate the digitally encoded waveforms. Since the FMW is spectrally synthesized to specifically avoid interference regions, transmitted communication symbols do not contain energy at spectral interference locations and received symbols are largely unaffected. Figure 2.3 shows the functional block diangram of TDCS signal generation and transmission, beginning with environmental sampling and spectral estimation. Once the interference-free spectral regions are established, the FMW

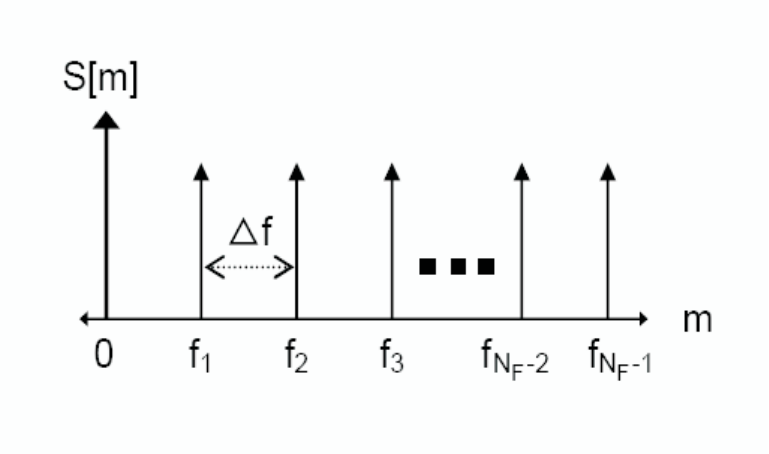

Figure 2.4: Discrete spectral components

b(t) is generated, stored, data modulated and transmitted [7].

2.3 A General SMSE Expression

The overview and discussion presented in this section is adapted from the Ph.D. dissertation by Roberts [10]. All the multi-carrier waveforms which have been discussed in this chapter fall under the "Spectrally Modulated Spectrally Encoded" framework [67, 68]. The first consideration in developing a general unifying framework, is the number and type of variables required to ensure that the desired level of diversity is achieved. There are a number of key variables associated with development of a SMSE analytic expression but the most important variable is the number of frequency components available in a given bandwidth of interest for a CR user. Identifying usable spectral components can be classified into two variables. The number of frequency components N_f in Figure 2.4 can be defined by the vector $\mathbf{a} = [a_1, a_2, \ldots, a_{N_f}]$, $a_i \in \{0, 1\}$. From this assigned frequency vector **a**, certain frequencies may be unavailable due to interference or by system design. The available frequency vector to be used can be expressed as $\mathbf{u} = [u_1, u_2, \ldots, u_{N_f}]$, $u_i \in \{0, 1\}$, where zeros indicate unused frequencies and there are $P \leq N_f$ used frequencies.

The other variables to consider in the design of the analytic expressions are the code

$\mathbf{c} = [c_1, c_2, \ldots, c_{N_f}]$, $c_i \in \mathbb{C}$, data modulation $\mathbf{d} = [d_1, d_2, \ldots, d_{N_f}], d_i \in \mathbb{C}$, windowing function for spectral shaping $\mathbf{w} = [w_1, w_2, \ldots, w_{N_f}], w_i \in \mathbb{C}$. These complex variables account for component-by-component amplitude and/or phase variations which are applied to frequency components. One last "phase only" variable to provide orthogonality among users is also considered and is represented by $\theta_{\mathbf{o}} = [o_1, o_2, \ldots, o_{N_f}], \theta_{o_i} \in [0, 2\pi)$.

Figure 2.4 illustrates a starting point where the spectrum bandwidth is divided into a number of equal sub-carriers or spectrum bins. A continuous time-domain expression for the discrete frequency-domain signal represented in Figure 2.4 is found via an inverse FFT (IFFT) of $S[m]$ as shown in 2.2.

$$s_k(t) = \sum_m Re\left[\mathcal{F}^{-1}\left\{r_m^{pos}\delta(f - f_m) + r_m^{neg}\delta(f + f_m)\right\}\right], \tag{2.2}$$

where $t_i \leq t \leq t_i + T$ and $T = N_f \triangle t$.

Using (2.2) as a starting point, an SMSE waveform was developed by applying the data modulation, coding, and windowing factors. The resultant expression for the k^{th} data modulated symbol $S_k[m]$ can be written as a sequence of terms

$$S_k[m] = \left\{c_m d_{m,k} w_m e^{-j(2\pi f_m t_n + \theta_{d_{m,k}} + \theta_{c_m} + \theta_{w_m})}\right\}_{m=0}^{N_f - 1}, \tag{2.3}$$

where m is the frequency component index, N_f is the total number of components, $f_m = m/(N_f \Delta t)$, $t_n = n\Delta t$ for $n = 0, 1, \ldots, N_f - 1$ [10], and $\mathbf{c}$, $\mathbf{d}$, and $\mathbf{w}$ denote complex code, data modulation, and windowing vectors (magnitudes and phases, as appropriate). By design, the coding and windowing factors only vary with frequency index m while data modulation factors are varied according to symbol index k as well. The expression in (2.3) can be further modified to incorporate *orthogonality* and account for frequency *assignment* and *use* via

$$S_k[m] = \left\{a_m u_m c_m d_{m,k} w_m e^{-j(\theta_{d_{m,k}} + \theta_{c_m} + \theta_{w_m} + \theta_{o_{m,k}})}\right\}_{m=0}^{N_f - 1}. \tag{2.4}$$

The general analytic expression for generating SMSE waveform is given by equation (2.4) where m is the frequency component index, N_f is the total number of components, $f_m = m/(N_f \Delta t)$, $t_n = n \triangle t$ for $n = 0, 1, \ldots, N_f - 1$ [86, 87], and $\mathbf{c}$, $\mathbf{d}$, and $\mathbf{w}$ denote complex code, data modulation, and windowing vectors (magnitudes and phases as appropriate) respectively. Once again, the coding and windowing factors only vary with frequency index m while data modulation factors are varied according to symbol index k as well. The variables $\mathbf{a}$ and $\mathbf{u}$ representing the usable spectral components can take on values $a_m u_m \in \{0, 1\}$ and $\theta_{o_{m,k}} = 2\pi k \cdot (a_m u_m / P) \sum_{i=1}^{m} a_m u_m$ with $P \leq N_f$. The phase term $\theta_{o_{m,k}}$ is used to ensure orthogonality between users.

The final expression for the spectral content of the SMSE transmitted symbol shown in (2.4) contains the spectral data modulation and encoding magnitude and phase factors. The sinusoid identifier F_{1m} contains the u_m term, which dictates frequencies that are used. A time domain version of the SMSE symbol is generated by applying an Inverse Discrete Fourier Transform (IDFT) to (2.4).

$$s_k[n] = \frac{1}{N_f} Re \left\{ \sum_{m=0}^{N_f - 1} a_m u_m c_m d_{m,k} w_m e^{j(2\pi f_m t_n + \theta_{d_{m,k}} + \theta_{c_m} + \theta_{w_m} + \theta o_{m,k})} \right\}. \tag{2.5}$$

for $t_k \leq t_n \leq t_k + T$, $f_m = f_c + m\Delta f$, and Δf is the frequency resolution [66].

2.3.1 OFDM via SMSE Analytic Expression

Using variables defined in Table 2.1 for a basic OFDM system, the analytic expression can be simplified by setting variables $u_i = a_i$, $w_i = 1$, and $\theta_{w_i} = 0 \ \forall \ i$. Since there is no windowing or coding in basic OFDM, the expression in (2.4) simplifies to expression shown in (2.6)

Table 2.1: Spectrally encoded waveform variables selection

Operation	**Basic OFDM**	**MC-CDMA**	**CI/MC-CDMA**	**TDCS**
Data Modulation	MPSK M-QAM relies on *m,k*	MPSK M-QAM relies on *k*	MPSK M-QAM relies on *k*	MPSK M-QAM relies on *k*
Coding	$\mathbf{c} = \mathbf{1}$ $\theta_{\mathbf{c}} = \mathbf{0}$	$\mathbf{c} = \mathbf{1}$ $\theta_{c_i} \in \{0, \pi\}$	$\mathbf{c} = \mathbf{1}$ $\theta_{c_i} \in [0, 2\pi)$	$\mathbf{c} = \mathbf{1}$ $\theta_{c_i} \in [0, 2\pi)$
Windowing	$\mathbf{w} = \mathbf{1}$ $\theta_{\mathbf{w}} = \mathbf{0}$	$\mathbf{w} = \mathbf{1}$ $\theta_{\mathbf{w}} = \mathbf{0}$	$\mathbf{w} = \mathbf{1}$ $\theta_{\mathbf{w}} = \mathbf{0}$	$\mathbf{w} = \mathbf{1}$ $\theta_{\mathbf{w}} = \mathbf{0}$
Orthogonality	$\theta_{\mathbf{o}} = \mathbf{0}$	$\theta_{\mathbf{o}} = \mathbf{0}$	$\theta_{\mathbf{o}} = \mathbf{0}$	$\theta_{\mathbf{o}} = \mathbf{0}$
Frequency Assignment	$\mathbf{a}$	$\mathbf{a}$	$\mathbf{a}$	$\mathbf{a}$
Frequencies Used	$\mathbf{u} = \mathbf{a}$	u_i depends on F-parameter	u_i depends on F-parameter	u_i depends on notching process 3mm

$$S_k[m] = \left\{ a_m d_{m,k} e^{-j\left(\theta_{d_{m,k}}\right)} \right\}_{m=0}^{N_f-1}, \tag{2.6}$$

Substituting for $d_i \in \mathbb{C}$, $d_{m,k}e^{-j\theta_{d_{m,k}}} = (\alpha_{m,k} + j\beta_{m,k})$ yields (2.7), where $\alpha_{m,k}$ and $\beta_{m,k}$ depend on the data modulation being used, e.g., $\alpha_{m,k}, \beta_{m,k} \in \{\pm 1\}$ for QPSK and $\alpha_{m,k}, \beta_{m,k} \in \{\pm 1, \pm 3\}$ for 16-QAM. Finally, applying an IFFT to (2.7) results in the discrete time domain OFDM expression (2.8) [67].

$$S_k[m] = \{(\alpha_{m,k} + j\beta_{m,k})\}_{m=0}^{N_f-1} \tag{2.7}$$

$$s_k[n] = \frac{1}{N_f} Re \left\{ \sum_{m=0}^{N_f-1} (\alpha_{m,k} + j\beta_{m,k}) e^{j(2\pi f_m t_n)} \right\} \tag{2.8}$$

2.3.2 MC-CDMA via SMSE Analytic Expression

Around 1993-94 time frame there were a number of hybrid MC-CDMA techniques proposed combining OFDM and CDMA [71, 88, 89]. The MC-CDMA technique considered here is based on the work presented in [71]. By inserting the variables listed in Table 2.1, $w_i = 1$ and $\theta_{w_i} = 0 \ \forall \ i$ (no windowing). Also, $\theta_{o_i} = 0 \ \forall \ i$ (no orthogonality control).

Finally, the data variable only depends upon k because of spectral spreading. Applying all these variables to (2.4).

$$S_k[m] = \left\{ a_m u_m c_m d_k e^{-j\left[\theta_{c_m} + \theta_{d_k}\right]} \right\}_{m=0}^{N_f - 1}, \tag{2.9}$$

Spectral spreading is accomplished using a random application of phases, 0 or π, such that $c_i = 1$ and $\theta_{c_i} \in \{0, \pi\} \; \forall \; i$. For $a_m u_m = 1$, this further simplifies equation (2.9) to

$$S_k[m] = \left\{ d_k e^{-j\left[\theta_{c_m} + \theta_{d_k}\right]} \right\}_{m=0}^{N_f - 1}, \tag{2.10}$$

For complex data modulation $d_k e^{-j\theta_{d_k}} = (\alpha_k + j\beta_k)$, (2.10) can be rewritten as

$$S_k[m] = \left\{ (\alpha_k + j\beta_k) e^{-j[\theta_{c_m}]} \right\}_{m=0}^{N_f - 1}, \tag{2.11}$$

where α_k and β_k depend on the modulation type being employed. After an IFFT operation on (2.11), the transmitted MC-CDMA signal is given by

$$s_k[n] = \frac{1}{N_f} Re \left\{ \sum_{m=0}^{N_f - 1} (\alpha_k + j\beta_k) e^{j(2\pi f_m t_n + \theta_{c_m})} \right\}. \tag{2.12}$$

2.3.3 Carrier Interferometry Signals via SMSE Analytic Expression

Carrier Interferometry has been applied to both OFDM (CI-OFDM) and MC-CDMA (CI/MC-CDMA). As in the case of OFDM, there are N_F equally spaced orthogonal subcarriers. However, in a CI/OFDM scenario, each data modulated symbol is simultaneously transmitted over all subcarriers. Orthogonality between the subcarriers is maintained via the inclusion of a phase term or carrier interferometry. Similar to the OFDM case the general expression is simplified by applying the following conditions. First, since the data is spread across all the subcarriers, $d_m, k \in \mathbb{C}$ only varies with k. Then the addition of CI phase term is accounted by changing $\theta_{o_m} = 0 \; \forall \; m$, to $\theta_{o_m,k} = m \triangle \theta_k$, where $\triangle \theta_k = k \, (2\pi / P_u)$. Sub-

stituting these condition in the general expression (2.4) yields the N_F spectral components for the k^{th} CI/OFDM communication symbol as

$$S_k[m] = \left\{ u_m d_k e^{-j\left(\theta_{d_k} + \theta_{o_{m,k}}\right)} \right\}_{m=0}^{N_f - 1}. \tag{2.13}$$

After an IFFT operation on (2.13), the transmitted CI/OFDM signal is given by

$$s_k[n] = \frac{1}{N_f} Re \left\{ \sum_{m=0}^{N_f - 1} d_k e^{j\left(2\pi f_m t_n + \theta_{d_k} + \theta_{o_{m,k}}\right)} \right\}. \tag{2.14}$$

One of the main differences between MC-CDMA and CI/MC-CDMA is the coding. There are number of MC-CDMA versions utilizing variety of pseudorandom as well as orthogonal codes, whereas the codes utilized in CI are orthogonal [58, 59, 72, 90]. CI coding coupled with MC-CDMA is termed as CI/MC-CDMA, which is also referred to as CI multiple access (CIMA). One of the key differences in implementing CI/MC-CDMA via the general SMSE expression is the inclusion of the orthogonal phase term and the deletion of the pseudorandom spreading code used in MC-CDMA.

$$s_k[n] = \frac{1}{N_f} Re \left\{ \sum_{m=0}^{N_f - 1} (\alpha_k + j\beta_k) e^{j\left(2\pi f_m t_n + \theta_{o_{m,k}}\right)} \right\}. \tag{2.15}$$

2.3.4 TDCS via SMSE Analytic Expression

The analytic expression of a basic TDCS implementation starts with setting the variables $w_i = 1$ and $\theta_{w_i} = 0 \; \forall \; i$ (no windowing). Coding is applied as random (or pseudo-random) phase variations between 0 and 2π and thus $c_i = 1 \; \forall \; i$. Data variables only depend upon k because of spreading. Orthogonality variable $\theta_{o_i} = 0 \; \forall \; i$ does not play a role in TDCS because the application of pseudo random phase accommodates orthogonality between users [79, 84]. Substituting these variables into (2.4) results in

$$S_k[m] = \left\{ a_m u_m d_k e^{-j\left(\theta_{c_m} + \theta_{d_k}\right)} \right\}_{m=0}^{N_f - 1}, \tag{2.16}$$

Spreading is performed in the frequency domain by using pseudo random phase distribution $\theta_{c_m} \in [0, 2\pi)$. The $a_m u_m$ term depends not only upon cognitive assignment, but also upon the adaptive TDCS notching process which deems specific frequency components as unusable based on channel interference characterization. For these "notched" components, $a_m u_m = 0$. Applying these conditions results in (2.17).

$$S_k[m] = \left\{ d_k e^{-j\left(\theta_{c_m} + \theta_{d_k}\right)} \right\}_{m=0}^{N_f - 1}, \tag{2.17}$$

After an IFFT operation on (2.17), the transmitted TDCS signal is given by

$$s_k[n] = \frac{1}{N_f} Re \left\{ \sum_{m=0}^{N_f - 1} d_k e^{j\left(2\pi f_m t_n + \theta_{c_m} + \theta_{d_k}\right)} \right\}, \tag{2.18}$$

which is consistent with the TDCS discrete-time analytic expression presented in [91].

Overlay-Underlay Waveforms

3.1 Introduction

In the hierarchial access model, interactions between primary and secondary users are considered to achieve spectrum efficiency. The basic idea here is to open up the licensed spectrum to secondary users while inducing minimum acceptable interference into the primary users. Spectrum overlay and spectrum underlay are two approaches under consideration to accomplish this. Spectrum overlay allows unlicensed secondary users to utilize unused spectrum simultaneously with primary users on a non-interference basis. This overlay approach was first adapted by [3] and subsequently researched under DARPA's Next Generation (XG) program as an "opportunistic spectrum access" approach. Similarly, spectrum underlay allows unlicensed secondary users to simultaneously operate in primary user bands but under strict transmit power constraints. Of all the spectrum access models presented, the hierarchical access model is perhaps the most compatible with current FCC policies and legacy wireless systems.

As proposed in [19, 20], CR technology fits within the hierarchial access method. Even though the present CR definition only considers overlay approaches, the research trend suggests that a hybrid technique combining overlay/underlay concepts can be employed to maximize spectral efficiency by using both white and gray spectral regions [2, 23]. Therefore, CR can be further categorized as being either overlay-CR or underlay-CR depending on the spectral region being used.

Channel capacity is directly related to bandwidth B and signal to noise ratio (SNR). This chapter starts with examining how the channel capacity can be maximized by utilizing both *unused* and *underused* portions of the spectrum. Then a general SD-SMSE framework is proposed followed by the implementation of Overlay, Underlay and hybrid Overlay/Underlay waveforms.

3.2 CR Channel Capacity

According to Shannon's channel capacity condition given by (3.1), channel capacity can be optimized by increasing the signal-to-noise ratio (S/N) and/or channel bandwidth (W).

$$C = W \log\left(1 + S/N\right) \tag{3.1}$$

In the current CR framework, the transmitter continuously monitors the radio spectrum and identifies frequency bands as being in one of two categories, either *used* or *unused*. The *unused* frequency bands are identified as CR bands for secondary users as shown in Fig. 3.1. The channel capacity when utilizing unused CR bands can be written as [62]

$$C_{CR} = \left(\sum_{k=1}^{N} W_{u_k}\right) \log\left(1 + \frac{\sum_{k=1}^{N} \Phi_{CR_k} W_{u_k}}{n_0 \sum_{k=1}^{N} W_{u_k}}\right) \tag{3.2}$$

where N is the total number of unused spectral bands in the total CR monitored bandwidth W, W_{u_k} is the bandwidth of the k^{th} unused band and Φ_{CR1_k} is the power spectral density of the CR transmission in the k^{th} unused band.

UWB signaling can be used as underlay technique to support CR transmission. In UWB signaling, a very large contiguous bandwidth is used in a coexistence manner such that the spectrum is simultaneously shared with primary narrow band transmissions as

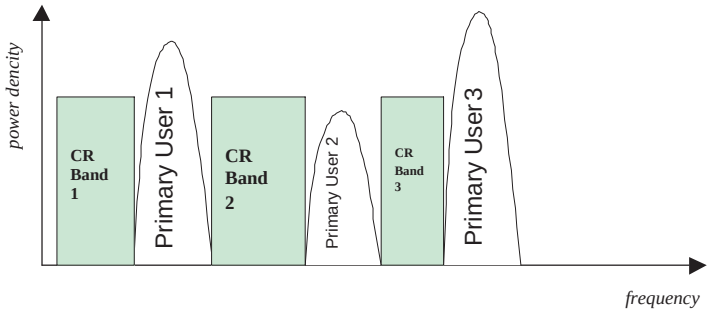

Figure 3.1: Illustration of notional Cognitive Radio Overlay concept

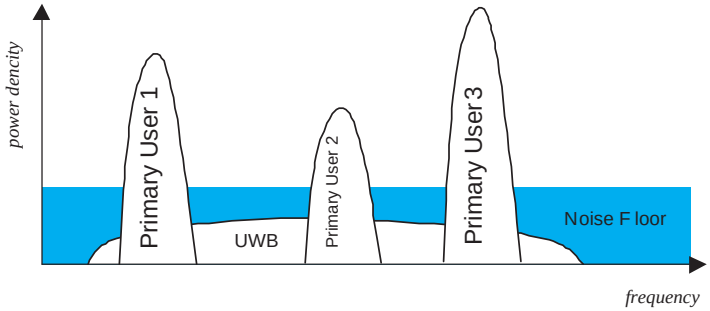

Figure 3.2: Illustration of notional Cognitive Radio Underlay concept

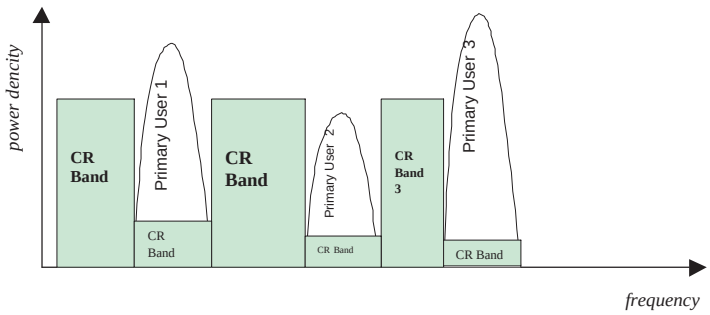

Figure 3.3: Illustration of notional Cognitive Radio Overlay/underlay concept

shown in Fig. 3.2. In this way, the total bandwidth W in (1) is maximized. However, to avoid interferences to primary (licensed) users, UWB transmissions are regulated by the FCC which limits the UWB transmitted power spectral density to a very low level. Hence, the channel capacity of UWB transmission is extremely limited and is given by (3.3) [62].

$$C_{UWB} = W \log \left(1 + \frac{\Phi_{UWB} W}{n_0 W + \sum_{i=1}^{M} \Phi_{p_i} W_{p_i}} \right) \tag{3.3}$$

where n_0 is the additive Gaussian noise power spectral density, Φ_{UWB} is the average power spectral density of the UWB transmission, M is the total number of primary users operating within total bandwidth W, Φ_{p_i} is the narrow band average power spectral density of the i^{th} primary user and W_{p_i} is the corresponding bandwidth of i^{th} primary user.

The coexistence of an UWB transmission with primary narrow band transmissions suggests that most of the narrow band transmission can tolerate a certain level of interference, i.e., even though some frequency bands are occupied by primary users they are likely to be *underused*. To maximize channel capacity, the so called *used* bands also need to be considered, this concept is illustrated in Fig. 3.3. Accounting for both *unused* and *underused* bands, the new SDCR [62] channel capacity for a given Cognitive Radio transmitter can be written as [62],

$$C_{SDCR} = W \log \left(1 + \frac{\sum_{k=1}^{N} \Phi_{CR1_k} W_{u_k} + \sum_{i=1}^{M} \Phi_{CR2_i} W_{p_i}}{n_0 W + \sum_{i=1}^{M} \Phi_{p_i} W_{p_i}} \right) \tag{3.4}$$

where Φ_{CR1_k} is the CR transmitted power spectral density in the k^{th} *unused* band, and Φ_{CR2_i} is the CR transmitted power spectral density in the i^{th} *underused* band. The following constraints are imposed to maximize overall channel capacity while minimizing mutual interference between CR users and other primary users:

$$\Phi_{CR2_i} \leq I_i, \forall i \tag{3.5}$$

$$\Phi_{CR1_k} \leq \phi_k, \forall k$$

$$\sum_{k=1}^{N} \Phi_{CR1_k} W_{u_k} + \sum_{i=1}^{M} \Phi_{CR2_i} W_{p_i} \leq S$$

where I_i is the interference tolerance level in the i^{th} used band, ϕ_k is the maximum allowed transmitted power spectral density (e.g., FCC mandated interference temperature) in the k^{th} unused band, and S is the total transmit power of the cognitive user across all unused and underused frequency bands.

Our objective is to maximize the channel capacity C_{SDCR} of the proposed system (3.4) subject to the constraints in (3.5). Assuming Φ_{p_i}, the power spectral density of the primary is fixed, this is a standard optimization of a convex function subject to convex constraints which can be solved using the technique of Lagrange multipliers [92].

The results of this standard optimization can be implemented in the form of the following algorithm [93].

1. Initialize all values $\Phi_{CR_{2j}} = 0$ and $\Phi_{CR_{1j}} = 0, \forall j$.

2. Construct the two lists

$$L_1 = \{W_{u_i} \log\left(1 + \frac{1}{W_{u_i} n_0}\right)\}, i = 1, \ldots, N$$

and

$$L_2 = \{W_{p_i} \log\left(1 + \frac{1}{W_{p_i}(n_0 + \Phi_{p_i})}\right)\}, i = 1, \ldots, M$$

for unused and used bands respectively.

3. Sort L_1 and L_2 in *non-increasing* order and merge the two lists.

Let $L = \{l_1, l_2, \ldots, l_{N+M}\}$ be the resultant sorted list.

4. Starting from the front of list L, (i.e $j = 1, 2 \ldots$), for the j^{th} element set $\Phi_{CR_{2_j}} = I_j$ if l_j corresponds to a used band or set $\Phi_{CR_{1_j}} = \phi_i$ if l_j corresponds to an unused band. Compute $S' = \sum_{i=1}^{j} \Phi_{CR_i} W_i$, where Φ_{CR_i} and W_i are chosen appropriately depending on whether l_i is a used or unused band.

5. If $S' < S$, then choose $j = j + 1$ and go back to step 4.

6. If $S' \geq S$, reduce Φ_{CR_j} such that $S' = S$, set $\Phi_{CR_k} = 0, \forall j < k \leq N + M$ and exit.

3.3 Overlay-Underlay Framework

Multi-carrier modulations such as OFDM and MC-CDMA are hailed as promising candidates [28] for realizing CR applications. To satisfy high data rate requirements, improve spectrum efficiency and at the same time avoid interference to primary and other secondary users, non-contiguous multi-carrier waveforms have been proposed [50, 54, 60, 62]. Software defined radio (SDR) is another promising DSA enabling technology where the radio transceivers perform baseband processing in software. SDR has the ability to quickly reconfigure its operating parameters, which is a fundamental requirement in the CR scenarios. The synergistic union of these two DSA technologies is termed *"CR-based SDR"*. That is, the SDR provides the software controlled communication vehicle (core technology for air interface and waveform generation), the control and application of which is based on CR principles guided by spectral monitoring to achieve efficient spectrum usage [66].

Driven by SDR principles, a general analytic framework was developed to encompass a myriad of multi-carrier signals. The framework is applicable to a broad class of waveforms that are called *Spectrally Modulated, Spectrally Encoded* (SMSE) signals [66, 67, 68]. Depending on CR user needs various multi-carrier waveforms can be generated, e.g., OFDM, MC-CDMA, CI/MC-CDMA or TDCS, using this SMSE framework. Since this

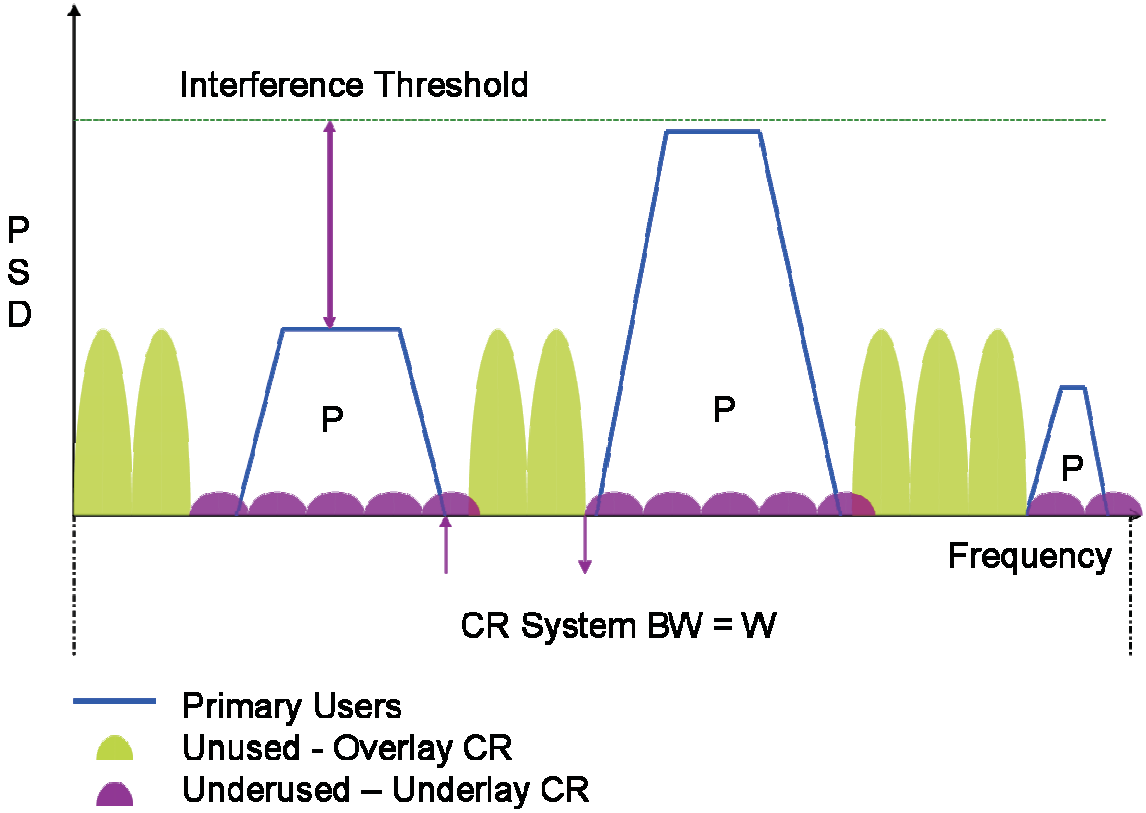

Figure 3.4: Identification of primary users, *unused* and *underused* spectral regions.

original SMSE framework employed hard decision frequency allocation, its applicability is limited to overlay-CR signals. To extend its applicability and maximize spectrum efficiency by utilizing both *unused* and *underused* regions, a soft decision SMSE (SD-SMSE) framework was subsequently developed to realize overlay-CR, underlay-CR and hybrid overlay/underlay CR signals [8].

The SMSE framework provides a unified expression for generating and implementing a host of multi-carrier type waveforms (e.g., OFDM, MC-CDMA, CI/OFDM, TDCS, etc) and satisfies current CR goals of exploiting *unused* spectral bands. However, it does not exploit *underused* spectrum. This section revisits the original SMSE framework development and the frequency assignment variables to exploit both *unused* and *underused* spectrum to generate both overlay and underlay type waveforms.

Fig. 3.4 illustrates a conceptual view of the *unused* and *underused* spectrum utilization

using an arbitrary interference threshold (IT). IT is assumed to be a limit set forth by the primary users based on the measured power spectrum density in a given bandwidth. Two cases of under-utilized spectrum are demonstrated: 1) when the spectral assignment is based on a binary decision the bands adjacent to the primary users are unavailable to overlay CR users and 2) primary users bands which are below the IT are also unavailable to the CR users. A soft decision CR (SDCR) will be able to exploit these *underused* frequency bands to increase channel capacity and improve performance. To support the envisioned SDCR system, the original SMSE framework is extended to account for both *unused* and *underused* frequency bands.

The proposed SD-SMSE framework is first illustrated using Fig. 3.5 and Fig. 3.6, by re-defining the design variables to extend the SMSE expression to account for both *unused* and *underused* spectrum. Fig. 3.5a and Fig. 3.5b show how the current CR framework identifies the *used* and *unused* spectrum based on binary decisions. Fig. 3.5c shows the weighted spectrum estimation resulting from spectrum sensing block shown in Fig. 3.6. The weighted spectrum estimate (WSE) (**a**) is further processed taking into account inputs from the IT estimator, primary users, other secondary users requirements and channel conditions. Specifically, the weighted spectrum estimate provides a metric of the allowable transmission power density at each and every frequency component in the entire bandwidth. Hence, the WSE divides the entire bandwidth into *unused* (**u**) and *underused* (**b**) frequency components and both the *unused* and *underused* spectrum can be exploited. Notice in Fig. 3.5 that different *underused* frequency components have different allowable CR transmission power densities. It is envisioned that any CR-based SDR will have the option to choose overlay-CR, underlay-CR or hybrid overlay/underlay waveforms to improve performance depending on the scenario, situation and need.

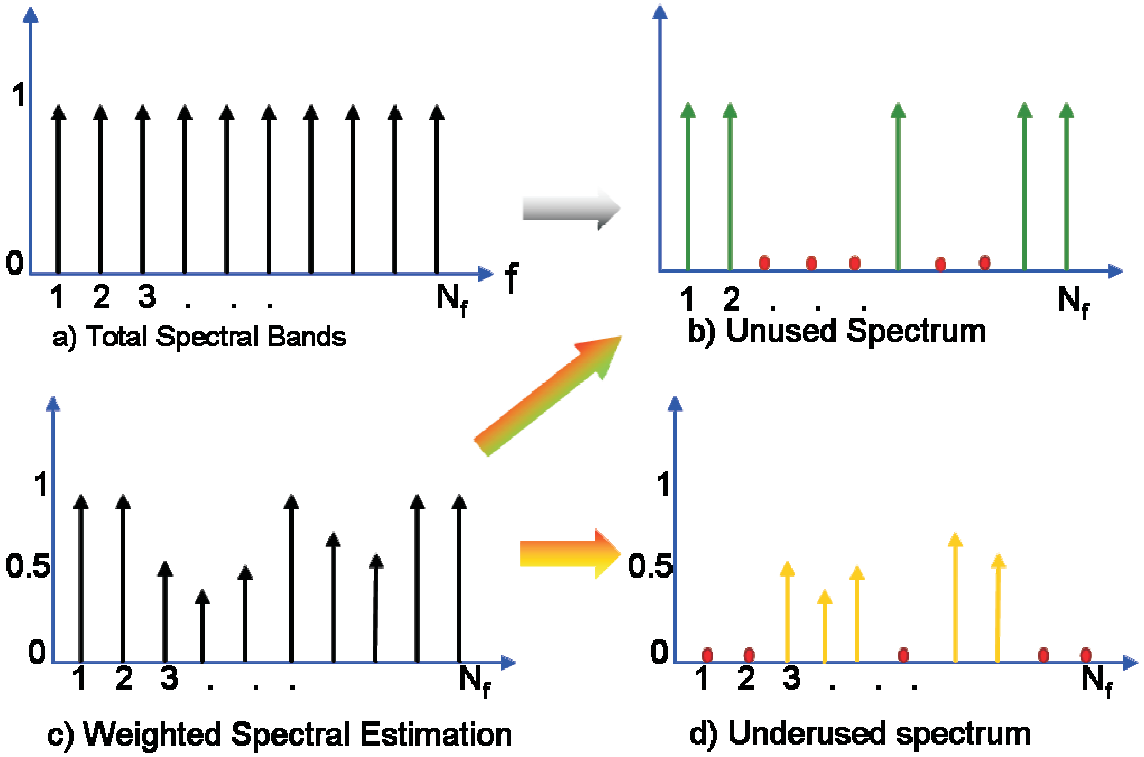

Figure 3.5: Spectrum parsing using weighted spectrum estimation in realization of SD-SMSE waveform.

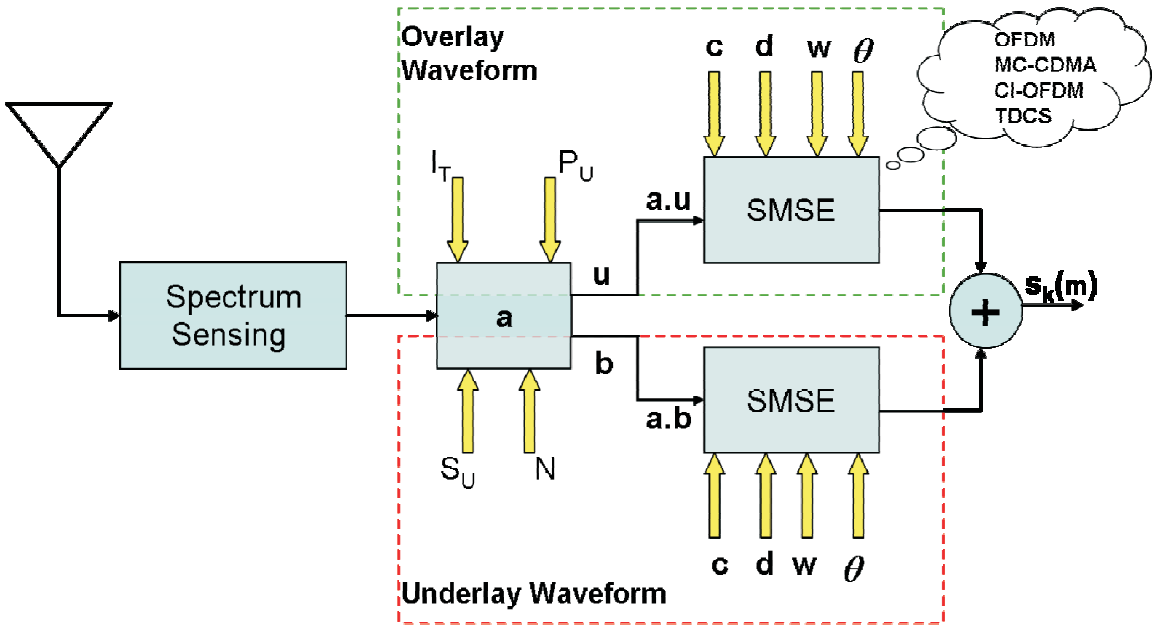

Figure 3.6: Block diagram representation of SD-SMSE framework [8].

3.3.1 Spectrum Sensing

Spectrum sensing is one of the most critical and important function in the implementation of a CR. The first challenge is to detect if a signal is present or not, which is particulary challenging if the primary and secondary users adopt sophisticated spread spectrum techniques and operate below the noise. Once the presence of a signal is detected, feature extraction plays the role of information assimilation, such that salient characteristics of the signals can be identified [22]. Almost all deterministic signals exhibit cyclostationary features arising from underlying periodicities within those signals. In addition to the inherent cyclic properties, a cyclostationary signature, intentionally embedded in the physical properties of a digital signal will aid in coordination of multiple secondary user sets [33]. Feature detection by itself is a very challenging research problem, especially when the received signal is under noise levels or thresholds which are below the sensitivity levels of the primary devices [34, 94]. If a signal exhibits cyclostationary properties, it can be detected at very low signal-to-noise ratios (SNR) and fading channels [11, 12, 38, 95]. A detailed cyclostationary signal detection theory is presented in Appendix 8.1. Spectrum sensing function is beyond the scope of this research. It is assumed that the usable spectrum is provided by the spectrum sensing block.

3.3.2 Interference Threshold

Spectrum sensing techniques are helpful in detection of spectrum holes and identification of other primary and secondary users. In order to know if a certain portion of the spectrum is *unused* or *underused*, the power spectrum density (PSD) in a given bandwidth needs to be compared to a predetermined threshold called interference threshold. This interference threshold can be set forth by primary users or in conjunction with primary and secondary users.

The concept of noise floor provides a means for evaluating the background noise in

over-utilized portions of the spectrum. Secondary user (SU) usage of the spectrum will raise the noise floor of the primary user (PU). To quantify this interference phenomenon, FCC spectrum policy task force has recommended interference temperature (IT) as a new performance metric [19].

In May 2007 FCC issued another notice stating that it has terminated the IT concept. Even though, there are few supporters for adopting the IT approach to measure or set a threshold, there appears to be no clear cut method or rules to implement IT. The community in general (technical as well as user) argued that the IT approach is not practical and would only result in increased interference in its operating ranges. Even though FCC has temporarily abandoned the interference temperature concept, research community in general is still considering IT as a viable metric, since IT is basically a measure of PSD in a receiver [17, 21, 37]. There are a number of cooperative/collabarative sensing approaches being proposed in the literature to share information between secondary users and also between primary and secondary users [39, 40].

3.3.3 A General SD-SMSE Analytic Expression

The first step in SD-SMSE framework development is to re-examine the design variables in the original SMSE framework. For the SD-SMSE development, frequency related factors are termed primary variables, while amplitude and phase related factors are termed secondary variables. Since the objective here is to optimize the spectrum usage, only frequency components related design variables are considered. From this point forward the SD-SMSE framework development is based on the scenario depicted in Fig. 3.5. As shown in Fig. 3.5c, the weighted spectrum estimate represents all frequency components which can be utilized for secondary user applications. It is represented by variable $\mathbf{a}$ with the range changed from binary values (hard decision) to real values (soft decision), i.e.:

$$\mathbf{a} = [a_0, a_1, \ldots, a_{N_f-1}], 0 \leq a_m \leq 1. \tag{3.6}$$

From the weighted spectrum estimate $\mathbf{a}$, the *unused* spectrum vector $\mathbf{u}$ can be derived as

$$\mathbf{u} \;=\; [u_0, u_1, \ldots, u_{N_f-1}] \tag{3.7}$$

where,

$$u_m = \begin{cases} 1 & if \quad a_m = 1 \\ 0 & else \end{cases} \quad m = 0, 1, \cdots N_f - 1 \tag{3.8}$$

In SMSE, hard decision CR design is employed by transmitting over the unused spectrum specified by $\mathbf{u}$.

Now a new variable $\mathbf{b}$ is introduced to account for the *underused* spectrum, i.e.,

$$\mathbf{b} \;=\; [b_0, b_1, \ldots, b_{N_f-1}] \tag{3.9}$$

where,

$$b_m = \begin{cases} 0 & if \quad a_m = 1 \\ a_m & else \end{cases} \quad m = 0, 1, \cdots N_f - 1 \tag{3.10}$$

Note that when $a_m = 1$ the value of $b_m = 0$, because when $a_m = 1$ the spectral component is termed as *unused* and is assigned to u_m. It is obvious that if one frequency component is *underused*, it cannot also accounted as *unused* and vice versa, i.e., $u_m = 0$ if $b_m > 0$ and $b_m = 0$ if $u_m = 1$.

The remaining waveform design variables, i.e., code ($\mathbf{c}$), data ($\mathbf{d}$), window ($\mathbf{w}$) and orthogonality ($\mathbf{o}$), remain unchanged from the original SMSE framework.

Applying all these design variables, the m^{th} component of the k^{th} data symbol of the SD-SMSE can be expressed as

$$S_k[m] = a_m c_m d_{m,k} w_m e^{j(\theta_{d_{m,k}} + \theta_{c_m} + \theta_{w_m} \theta o_{m,k})} \tag{3.11}$$

This equation can be rewritten in terms of u_m and b_m as,

$$S_k[m] = \begin{cases} u_m c_m d_{m,k} w_m e^{j(\theta_{d_{m,k}} + \theta_{c_m} + \theta_{w_m} \theta o_{m,k})} & if \quad a_m = 1 \\ b_m c_m d_{m,k} w_m e^{j(\theta_{d_{m,k}} + \theta_{c_m} + \theta_{w_m} \theta o_{m,k})} & else \end{cases} \tag{3.12}$$

The expression in (3.12) can be decomposed into *unused* and *underused* SMSE waveform representing the new SDCR architecture shown in Fig. 3.6. Applying the IDFT to (3.12) results in the discrete time domain waveform given by:

$$s_k[n] = \frac{1}{N_f} Re \left\{ \sum_{m=0}^{N_f - 1} a_m c_m d_{m,k} w_m e^{j(2\pi f_m t_n + \theta_{d_{m,k}} + \theta_{c_m} + \theta_{w_m} + \theta o_{m,k})} \right\} \tag{3.13}$$

$$\begin{aligned} s_k[n] = \frac{1}{N_f} Re \left\{ \sum_{m=0}^{N_f - 1} u_m c_m d_{m,k} w_m e^{j(2\pi f_m t_n + \theta_{d_{m,k}} + \theta_{c_m} + \theta_{w_m} + \theta o_{m,k})} \right\} \\ + \frac{1}{N_f} Re \left\{ \sum_{m=0}^{N_f - 1} b_m c_m d_{m,k} w_m e^{j(2\pi f_m t_n + \theta_{d_{m,k}} + \theta_{c_m} + \theta_{w_m} + \theta o_{m,k})} \right\} \end{aligned} \tag{3.14}$$

where the first summation represents the unused frequency components and the second summation accounts for the *underused* frequency components.

The SMSE expression in (3.13) was demonstrated by applying it to a number of OFDM based multi-carrier signals [66]. The process of generating these waveforms can be viewed as a two-step approach: 1) generating the frequency related primary variables and 2) applying the secondary variables such as the code, data modulation, windowing and orthogonality to the frequency vector. Since the SD-SMSE only focused on manipulating the primary variables, all the OFDM based multi-carrier modulations expressions such as NC-OFDM, NC-MC-CDMA, CI/MC-CDMA and NC-TDCS are applicable to both overlay and underlay scenarios.

SD-SMSE Overlay Waveform

Current CR techniques only employ overlay waveforms that exploit unused spectral bands. It is apparent that current CR transmission is just a special case of the soft decision CR when no *underused* frequency components are exploited. In the SMSE framework, if the *underused* variable $\mathbf{b}$ is forced to be zero and the frequency assignment variable $\mathbf{a}$ to be binary:

$$\mathbf{b} = [0, 0, \ldots, 0] \tag{3.15}$$

$$\mathbf{a} = [a_0, a_1, \ldots, a_{N_f-1}], a_m \in \{0, 1\} \tag{3.16}$$

the second summation in (3.14) is eliminated and reduces to current hard decision CR overlay:

$$s_k[n] = \frac{1}{N_f} Re \left\{ \sum_{m=0}^{N_f-1} u_m c_m d_{m,k} w_m e^{j(2\pi f_m t_n + \theta_{d_{m,k}} + \theta_{c_m} + \theta_{w_m} + \theta o_{m,k})} \right\}. \tag{3.17}$$

SD-SMSE Underlay Waveform

Unlike the overlay waveforms which only operate in the unused bands of the spectrum, the underlay waveform operates in the *underused* portions of the spectrum. An underlay waveform spreads its signal over a wide bandwidth to minimize its interference to the existing primary users and also to achieve the required processing gain to improve its performance. In general, UWB technology has been associated with underlay approaches. By definition, a signal is defined as UWB if it occupies a bandwidth that is greater than 500 MHz. Therefore, not all underlay waveforms are UWB by this definition. For example, a low data rate underlay waveform used as a control channel might only require a few mega hertz of bandwidth. In the SD-SMSE context, UWB is a special implementation of an underlay

waveform. An UWB transmission uses underlay waveform which operates across all spectral components but minimizes its interference by limiting its transmission power spectral density to avoid interference to all primary users. Hence, its transmission power spectral density is determined by the primary user most sensitive to interference. In this case, all frequency components are treated as *underused* components. Hence, by setting

$$\mathbf{u} = [0, 0, \ldots, 0] \tag{3.18}$$

$$\mathbf{b} = [K, K, \ldots, K], 0 < K < 1 \tag{3.19}$$

the first summation in (3.14) can be eliminated and the CR underlay signal corresponds to an UWB transmission:

$$s_k[n] = \frac{1}{N_f} Re \left\{ \sum_{m=0}^{N_f-1} K d_{m,k} w_m e^{j(2\pi f_m t_n + \theta_{d_{m,k}} + \theta_{c_m} + \theta_{w_m} + \theta o_{m,k})} \right\}, \tag{3.20}$$

where K is a constant obtained by taking the minimum value of the weighted power spectral density shown in Fig. 3.5. Note that although **b** was assumed to be constant for simplicity purpose, in general each *underused* spectral component can have different spectral weights capable of employing adaptive baseband modulations.

SD-SMSE Overlay/Underlay

In the proposed soft decision CR, the waveform achieves benefits of both overlay and underlay waveforms by taking advantage of both *unused* and *underused* spectrum. This is done by employing soft decision criteria at each and every frequency component while minimizing the interference to primary users [50, 54, 60]. The expression shown in (3.14) represents the hybrid overlay/underlay utilizing the SD-SMSE framework.

Evaluation of Overlay and Underlay Waveforms in AWGN Channel

4.1 Introduction

In this chapter analytic BER performance for overlay-CR and underlay-CR in AWGN channel is derived. Simulation analysis of overlay-CR and underlay-CR are performed and validated with the newly derived analytic expressions. Co-existence analysis of primary and secondary users in a multi-user scenario is demonstrated.

4.2 Performance Analysis of Overlay and Underlay Waveforms

This section starts with the applications of the general SMSE and SD-SMSE framework to a number of multi-carrier modulations such as OFDM, MC-CDMA, CI/MC-CDMA and TDCS. It has been shown that these multi-carrier modulations can be easily adapted to a non-contiguous spectrum environment by de-activating undesired sub carriers interfering with the primary user bands [50, 54, 60, 62, 64].

Here, the BER performance of Overlay and Underlay waveforms are evaluated. The

total received signal in a cognitive radio scenario in AWGN channel is

$$r(t) = \sum_{k=1}^{K} S_{p_k}(t) + \sum_{l=1}^{L} S_{s_l}(t) + n(t) \tag{4.1}$$

where K is the total number of primary users, L is the total number of secondary users, $S_{p_k}(t)$ represents the k^{th} primary user's signal, $S_{s_l}(t)$ is the l^{th} secondary user's signal, and $n(t)$ represents the additive Gaussian noise. Fig. 4.1 illustrates such a dynamic spectrum access scenario. As shown in Fig. 4.1, there are two primary users occupying two non-contiguous frequency bands, and two spectrum holes are available for secondary user transmission. it is assumed that the k^{th} primary user transmits an OFDM signal with BPSK modulation over its M_k subcarriers, so the k^{th} primary user's signal corresponds to:

$$S_{p_k}(t) = \sqrt{\frac{E_{b_k}}{T}} Re\left\{ \sum_{i=0}^{M_k-1} b_i^{(k)} e^{j2\pi f_{k_i}} g(t) \right\} \tag{4.2}$$

where E_{b_k} is the k^{th} user's bit energy, $b_i^{(k)}$ is the k^{th} user's i^{th} bit, f_{k_i} is the i^{th} subcarrier of the k^{th} user, $g(t)$ is a rectangular waveform of unity height which time-limits the code to one symbol duration T, and the subcarrier bandwidth $\Delta f = f_{k_i} - f_{k_{i-1}} = 1/T$.

4.2.1 Performance Analysis of Overlay Waveforms

When the secondary user employs overlay waveform for its transmissions, only spectrum holes are used. Here it is assumed that one secondary user transmitting over all the available spectrum holes. The signal corresponding to the secondary user waveform employing NC-OFDM can be written as:

$$S_s(t) = \sqrt{\frac{E_{b_s}}{T}} Re\left\{ \sum_{i=0}^{M_h-1} b_i^{(s)} e^{j2\pi f_{h_i} t} g(t) \right\} \tag{4.3}$$

where E_{b_s} is the secondary user's bit energy, $b_i^{(s)}$ is the secondary user's i^{th} bit, f_{h_i} is the i^{th} subcarrier of the spectrum holes, and M_h is the total number of subcarriers of all spectrum

holes.

Similarly, a secondary user employing NC-MC-CDMA can be written as

$$S_s(t) = \sqrt{\frac{E_{b_s}}{M_h T}} Re\left\{ b^{(s)} \sum_{i=0}^{M_h-1} \beta_i e^{j2\pi f_{h_i} t} g(t) \right\} \tag{4.4}$$

where β_i is the i^{th} component of the spreading code of the secondary user.

Since the secondary user's transmission is assumed to be synchronized in time with the primary users' transmission, and the secondary user only transmits over spectrum holes, there is no interference from the secondary user to primary users and vice versa. Hence, the BER performance of the secondary user (and the primary users) is simply as shown in (4.5) for BPSK modulatons or (4.6) for 8PSK modulation with Gray coding [43].

$$P(b) = Q\left(\sqrt{\frac{2E_b}{N_0}}\right) \tag{4.5}$$

$$P(b) = \frac{2}{3} Q\left(\sqrt{\frac{6E_b}{N_0}} \sin\frac{\pi}{8}\right). \tag{4.6}$$

4.2.2 Performance Analysis of Underlay Waveforms

When underlay waveform is employed by the secondary users for transmission, the transmission occupies the entire bandwidth instead of only the spectrum holes. Here, multiple secondary users can be accommodated using MC-CDMA. The total secondary users' signal corresponds to:

$$S_s(t) = \sum_{l=1}^{L} S_{s_i}(t) = \sqrt{\frac{E_{b_s}}{N_f T}} Re\left\{ \sum_{l=1}^{L} b^{(l)} \sum_{i=0}^{N_f-1} \beta_i^{(l)} e^{j2\pi(f_c+i\Delta f)t} g(t) \right\} \tag{4.7}$$

N_f is the total number of subcarriers over the entire bandwidth, $\beta_i^{(l)}$ is the i^{th} component of l^{th} user's spreading code.

At the receiver side, the received signal is first decomposed to N_f subcarriers, then recombined together to create the final decision variable for the desired secondary user. Specifically, the n^{th} secondary user's decision variable is:

$$R^{(n)} = \sum_{i=0}^{N_f-1} r_i^{(n)}. \tag{4.8}$$

When one subcarrier is in a spectrum hole, there is no primary user's signal:

$$r_i^{(n)} = \sqrt{\frac{E_{b_s}}{N_f}} b^{(n)} + \sqrt{\frac{E_{b_s}}{N_f}} \sum_{l=1, l\neq n}^{L} b^{(l)} \beta_i^{(l)} \beta_i^{(n)} + n_i \tag{4.9}$$

where the first term is the desired signal, the second term is the Multiple Access Interference (MAI), and the third term represents the additive Gaussian noise.

However, if one subcarrier is not in a spectrum hole, the secondary users' signal coexist with one primary user's signal:

$$r_i^{(n)} = \sqrt{\frac{E_{b_s}}{N_f}} b^{(n)} + \sqrt{\frac{E_{b_s}}{N_f}} \sum_{l=1, l\neq n}^{L} b^{(l)} \beta_i^{(l)} \beta_i^{(n)} + \sqrt{E_{b_k}} b_i^{(k)} + n_i \tag{4.10}$$

When orthogonal spreading codes are employed for secondary users, the n^{th} secondary user's decision variable after recombining now corresponds to:

$$R^{(n)} = \sum_{i=0}^{N_f-1} r_i^{(n)} = N_f \sqrt{\frac{E_{b_s}}{N_f}} + \sum_{k=1}^{K} \sqrt{E_{b_k}} \sum_{i=0}^{M_k-1} b_i^{(k)} + \sum_{i=0}^{N_f-1} n_i. \tag{4.11}$$

The first term in (4.11) is the desired signal, the second term represents the interference from primary users to the secondary user and the third term is the noise contribution where $E[{n_i}^2] = \frac{N_0}{2}$. Note that there is no MAI in the final decision variable due to the orthogonality among spreading codes.

Using a Gaussian approximation [43], the interference power from the primary user on the secondary user given by the second term in (4.11) is [73]:

$$E\left[\left(\sum_{k=1}^{K}\sqrt{E_{b_k}}\sum_{i=0}^{M_k-1}b_i^{(k)}\right)^2\right]=\sum_{k=1}^{K}M_kE_{b_k}. \tag{4.12}$$

If all primary users have equal bit energy E_{b_p}, the above expression in (4.12) reduces to

$$\sum_{k=1}^{K}M_kE_{b_k}=ME_{b_p} \quad , \tag{4.13}$$

where $M=\sum_{k=1}^{K}M_k$ is the total number of subcarriers occupied by primary users.

It is easy to show that the signal-to-interference plus noise ratio (SINR) is

$$SINR=\frac{N_fE_{b_s}}{\sum_{k=1}^{K}M_kE_{b_k}+N_f\frac{N_0}{2}} \quad . \tag{4.14}$$

With the BER performance of the n^{th} secondary given by

$$P(e)=Q(\sqrt{SINR})=Q\left(\sqrt{\frac{N_fE_{b_s}}{\sum_{k=1}^{K}M_kE_{b_k}+N_f\frac{N_0}{2}}}\right)=Q\left(\sqrt{\frac{2E_{b_s}}{\frac{2\sum_{k=1}^{K}M_kE_{b_k}}{N_f}+N_0}}\right). \tag{4.15}$$

When all primary users have the same bit energy, the BER reduces to:

$$P(e)=Q\left(\sqrt{\frac{2E_{b_s}}{\frac{2ME_{b_p}}{N_f}+N_0}}\right). \tag{4.16}$$

4.3 Overlay-CR and Underlay-CR Simulation Analysis

Performance of all three overlay and underlay waveforms is demonstrated via simulation under AWGN channel conditions. Perfect synchronization is assumed between primary and secondary users. Analytic versus simulated P_b versus E_b/N_o is used as a performance metric to validate these waveforms. When the secondary user is perfectly synchronized with the primary user, there is no interference from the secondary user to primary user when secondary user employs overlay waveform, hence, the performance of the non-contiguous overlay waveform secondary user follows the theoretical performance under AWGN channel conditions.

4.3.1 Overlay-CR Simulation Results

In current CR methods only the unused spectrum is allocated for secondary users. The overlay spectrum allocation scenario is illustrated in Fig. 4.1. The spectral bins having a value of one identify secondary user bands and the zeroed-out bins identify primary user bands. It is assumed that at any given time, 32 non-contiguous sub-carriers will be available for secondary CR users. Performance of four non-contiguous overlay waveforms is demonstrated in Figs. 4.2 through Fig. 4.5. The results demonstrate that with perfect synchronization between primary and secondary users, non-contiguous waveforms such as NC-OFDM, NC-MCCDMA, NC-CI/MC-CDMA and TDCS employing BPSK and 8PSK modulation, match the theoretical expressions of BPSK and 8PSK modulations under AWGN channel conditions.

4.3.2 Analysis of Underlay Waveform

A CR underlay waveform utilizes the *underused* portion of the spectrum, operating on top of the other primary user waveform. In the previous overlay case, since perfect synchronization was assumed, there was no interference between primary and CR overlay

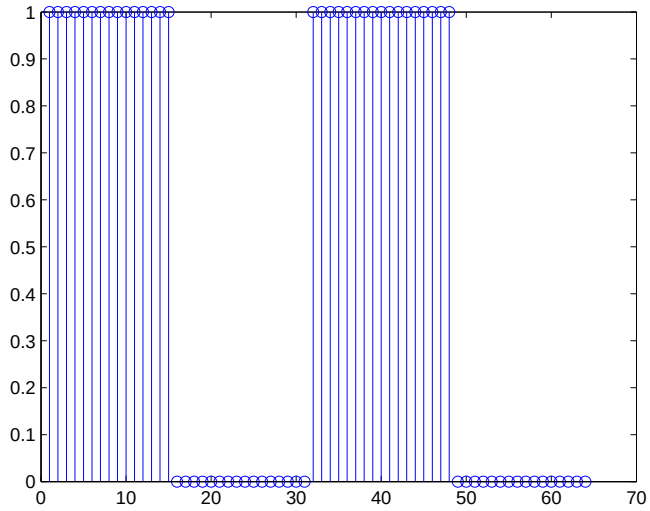

Figure 4.1: Spectrum response for scenario with non-contiguous spectrum available for CR users.

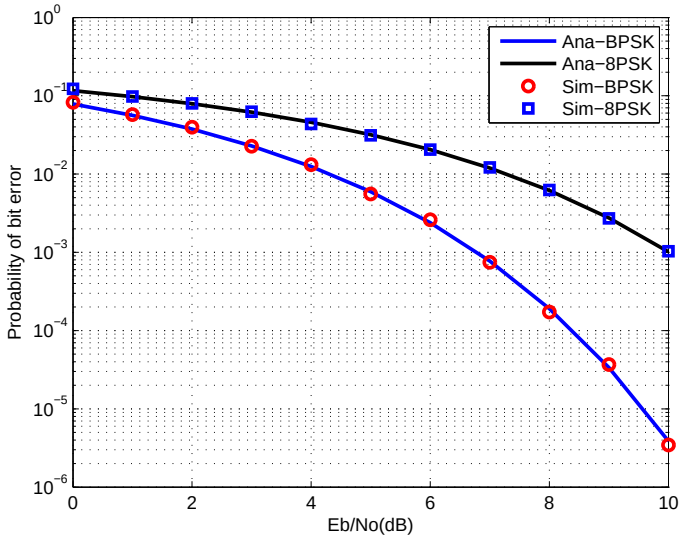

Figure 4.2: Performance of overlay NC-OFDM waveform in AWGN channel.

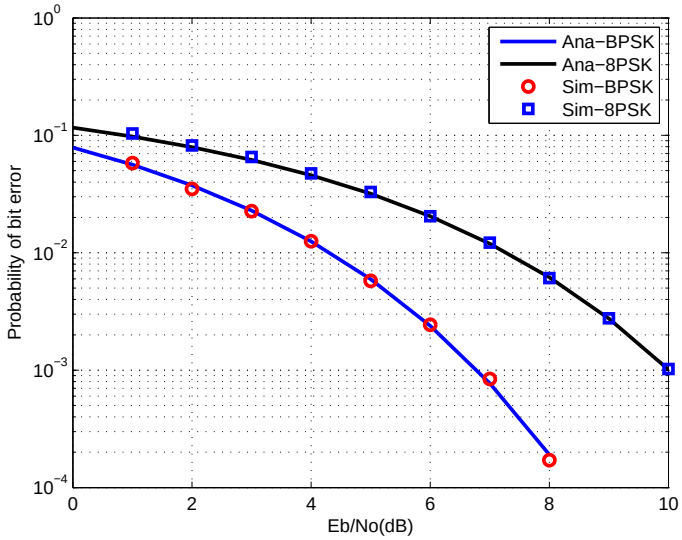

Figure 4.3: Performance of overlay NC-MC-OFDM waveform in AWGN channel.

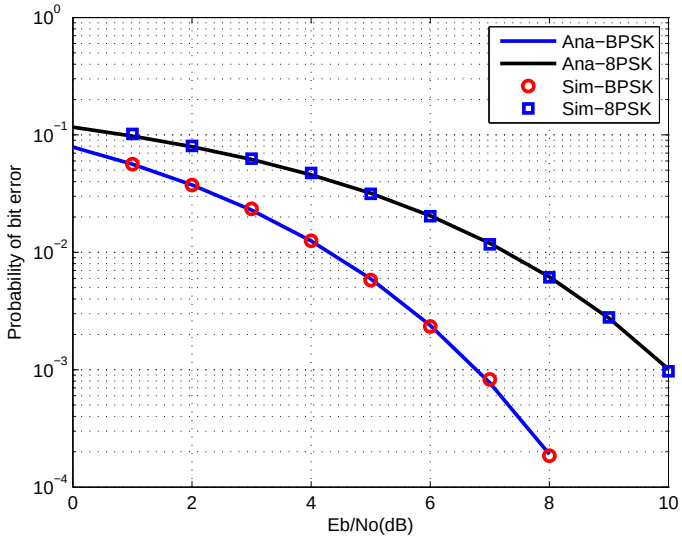

Figure 4.4: Performance of overlay NC-CI/MC-CDMA waveform in AWGN channel.

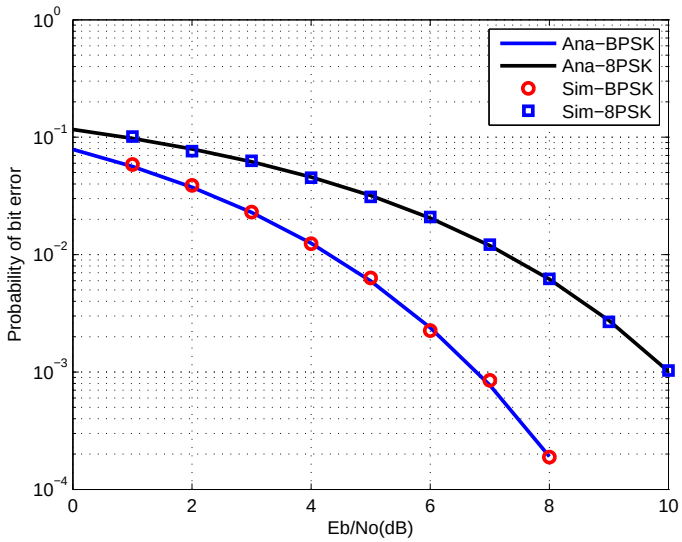

Figure 4.5: Performance of overlay NC-TDCS waveform in AWGN channel.

secondary user. However, in the CR underlay case, primary and secondary underlay user will be interfering with each other causing performance degradation to each other. To get an insight and understanding of the mutual interference to each other, three scenarios have been considered. The first two scenarios examine CR underlay waveform with primary user as interference and the third scenario analyzes primary user performance in the presence of CR underlay as interference.

In the first scenario, the primary user is modeled as OFDM with BPSK modulation using a contiguous 32 sub-carrier spectrum. The underlay waveform is modeled as MC-CDMA with BPSK modulation. The underlay waveform uses much lower power and will spread its spectrum while maintaining its own performance requirements and minimizing its interference to the primary user. Figure 4.7 and Fig. 4.8 illustrate the performance of an underlay secondary user under AWGN channel conditions with primary user interference. The underlay waveform in Fig. 4.7 is operating at -20dB transmission power relative to that of the primary user. It can be seen that as the underlay waveform spectrally spreads, its performance improves and approaches the theoretical baseline at $N = 512$. Similarly, in Fig. 4.8 the underlay waveform operating at -30dB relative to the primary user has to

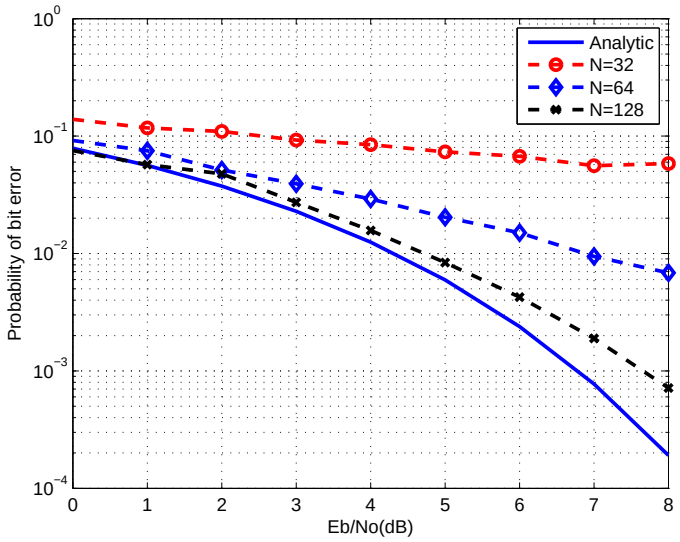

Figure 4.6: Performance of underlay NC-MCCDMA BPSK as a secondary user. Primary to secondary user power ratio is 10dB.

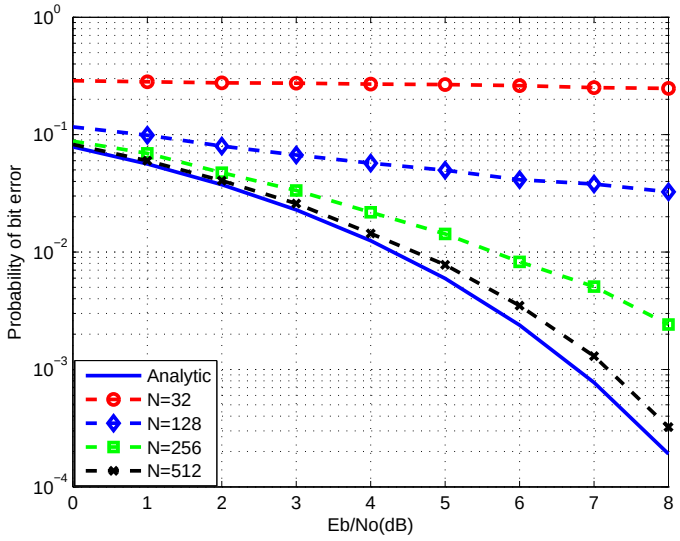

Figure 4.7: Performance of underlay NC-MCCDMA BPSK as a secondary user. Primary to secondary user power ratio is 20dB.

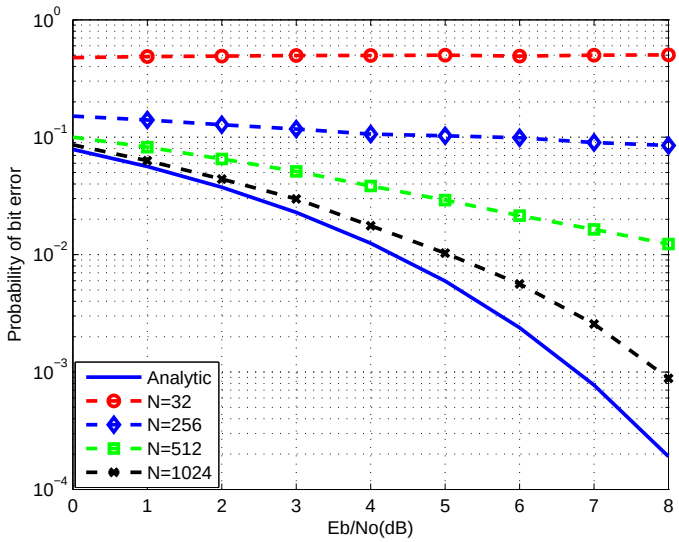

Figure 4.8: Performance of Underlay NC-MCCDMA bpsk as a secondary user. Primary to secondary user power ratio is 30dB.

increase its spreading length to $N = 1024$ to improve its performance to come close to the theoretical expression.

Results in Fig. 4.12 and Fig. 4.13 enable the comparison of theoretical and simulated BER performance of a secondary user using an underlay waveform. Figure 4.12 shows results when the secondary user's transmission power is 20dB lower than that of the primary user, and Fig. 4.13 shows the case of 30dB power difference. The solid lines in Fig. 4.12 represent theoretical BER performance of the secondary user specified by (4.15), the circles represent the simulation results when the secondary user spreads to 128 subcarriers, the stars represent the simulation results when the secondary user spreads to 256 subcarriers, and the squares represent the case of 512 subcarriers. Fig. 4.13 shows the case of secondary user spreading to 256, 512 and 1024 subcarriers. As can be seen in these figures, the simulation results are well predicted by the theoretical analysis derived in the previous section.

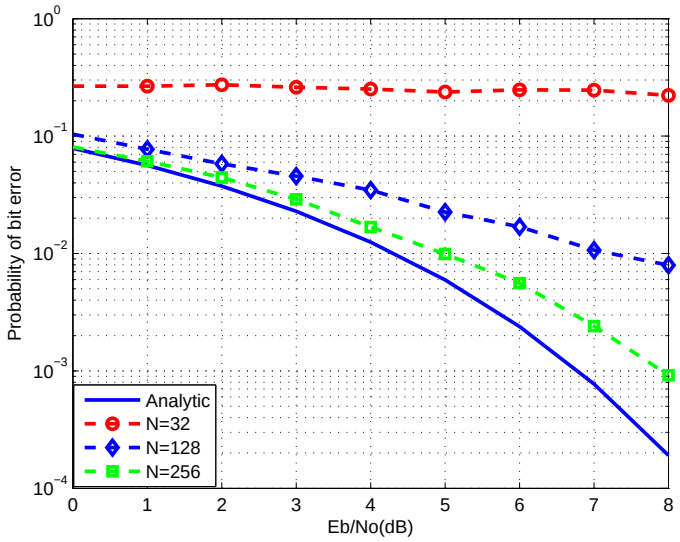

Figure 4.9: Performance of Underlay NC-CI/MCCDMA bpsk as a secondary user. Primary to secondary user power ratio is 20dB.

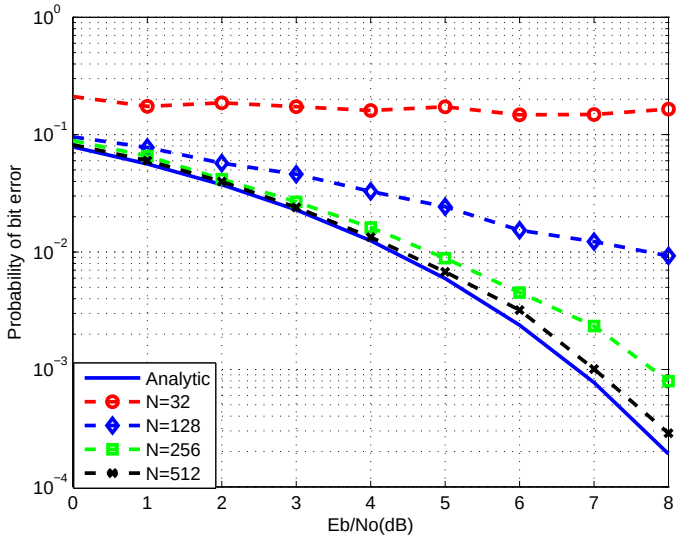

Figure 4.10: Performance of Underlay NC-TDCS bpsk as a secondary user. Primary to secondary user power ratio is 20dB.

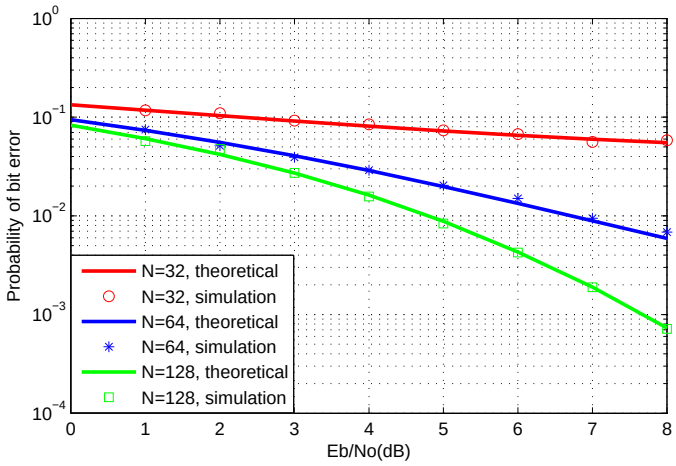

Figure 4.11: Comparing analytic with simulated results for Underlay secondary user performance (at power -10dB below primary user) .

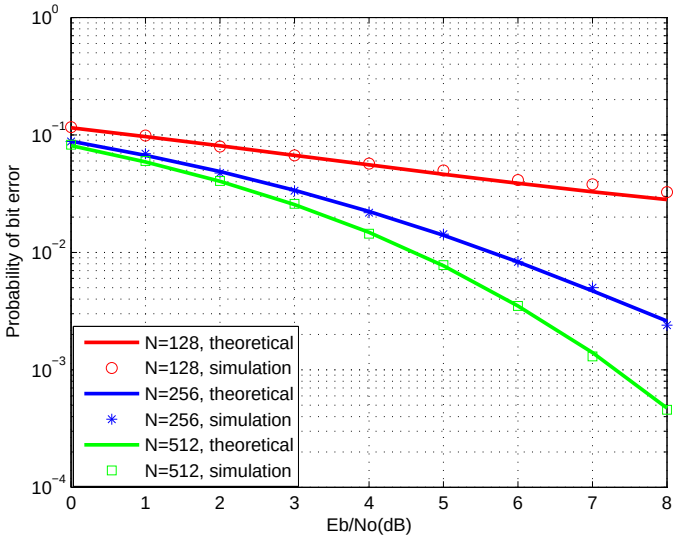

Figure 4.12: Comparing analytic with simulated results for Underlay secondary user performance (at power -20dB below primary user) .

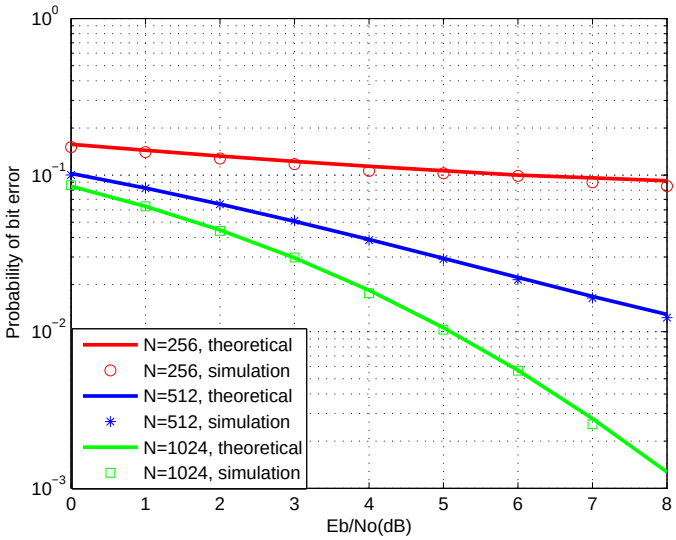

Figure 4.13: Comparing analytic with simulated results for Underlay secondary user performance (at power -30dB below primary user) .

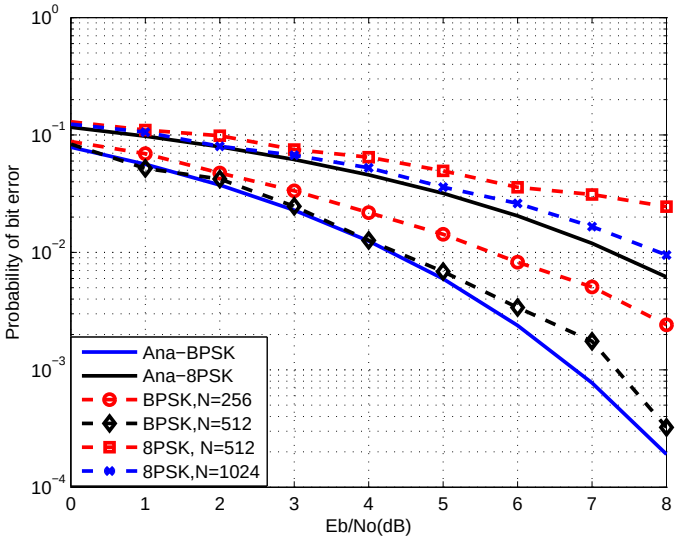

Figure 4.14: Performance of Underlay NC-MCCDMA 8PSK as a secondary user. Primary to secondary user power ratio is 20dB.

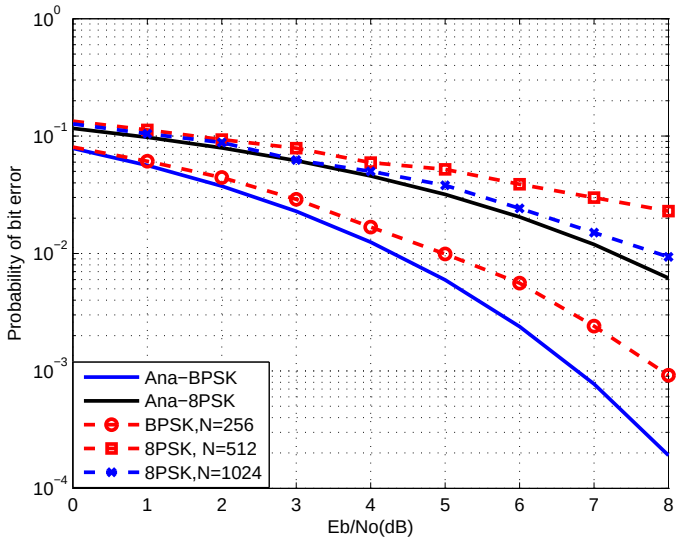

Figure 4.15: Performance of Underlay NC-CI/MCCDMA 8PSK as a secondary user. Primary to secondary user power ratio is 20dB.

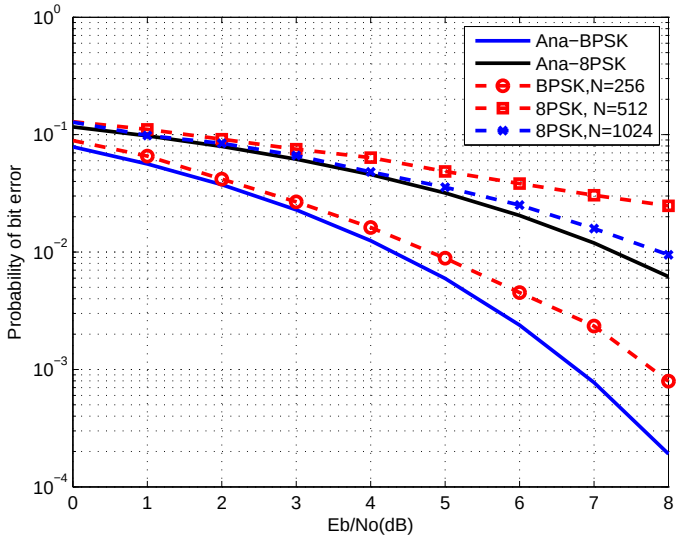

Figure 4.16: Performance of Underlay NC-TDCS 8PSK as a secondary user. Primary to secondary user power ratio is 20dB.

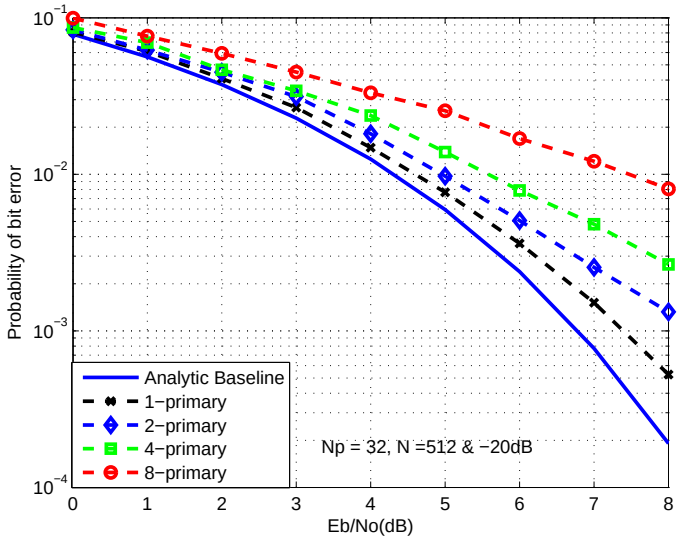

Figure 4.17: Performance of underlay NC-MCCDMA BPSK as a secondary user in the presence multiple primary users.

Multiple Primary Users

The second scenario also models the primary user as OFDM-BPSK consisting of 32 contiguous sub-carriers. In this case the underlay spread length is fixed to $N = 512$ and the secondary to primary power ratio is set at -20dB. In the previous scenario there was just one single primary user in the entire underlay spread bandwidth, whereas in this case the entire bandwidth is populated with multiple primary users, each operating over 32 sub-carriers. It is evident from Fig. 4.17 that as the number of primary users increases, underlay performance goes down, prompting the underlay user to employ other means such as spread further or add channel coding to improve the performance.

Fig. 4.18 shows the theoretical BER performance and the simulation results of the secondary user using underlay waveform with multiple primary users. All primary users are assumed to have the same transmission power and each primary user occupies 32 subcarriers. The solid lines in Fig. 4.18 represent theoretical curves, the circles represent simulation results when one primary user is present, the stars represent the simulation results with two primary users present, the squares represent simulation results with four primary users, and

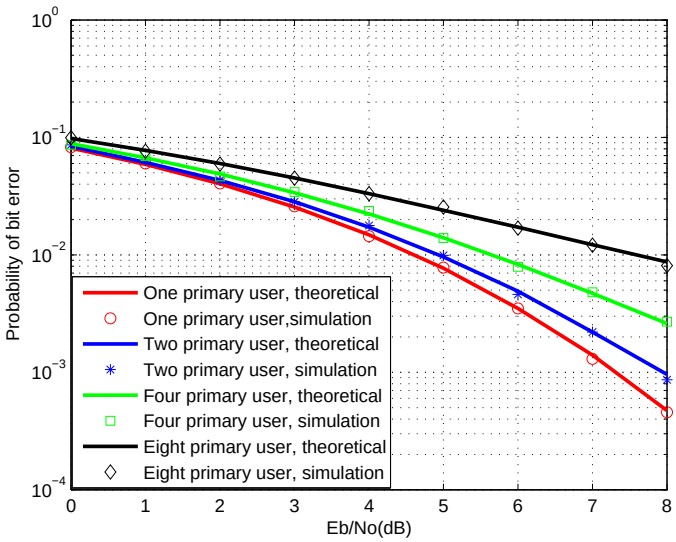

Figure 4.18: Comparing analytic with simulated results for underlay secondary user performance with multiple primary users.

the diamonds represent simulation result with eight primary users. It is evident from these curves that the simulation results perfectly match the theoretical analysis presented in the previous section.

Secondary Interference to Primary

The first two scenarios examined the effects of primary user interference to the secondary underlay waveform. The effect of secondary underlay interference to the primary user is shown in Fig. 4.19. As in the previous cases primary user is modeled as length 32 sub-carrier OFDM-BPSK and secondary underlay is modeled as MC-CDMA BPSK with length $N = 512$. Orthogonal Hadamard-Walsh codes are used to support the multiple users MC-CDMA underlay waveform. It can be seen from Fig. 4.19 that as the number of secondary users increases to 10 (at primary to secondary power ratio of 20dB) the primary user performance severely degrades and at that point the secondary underlay users drop their power level to -30dB to lessen interference to the primary user.

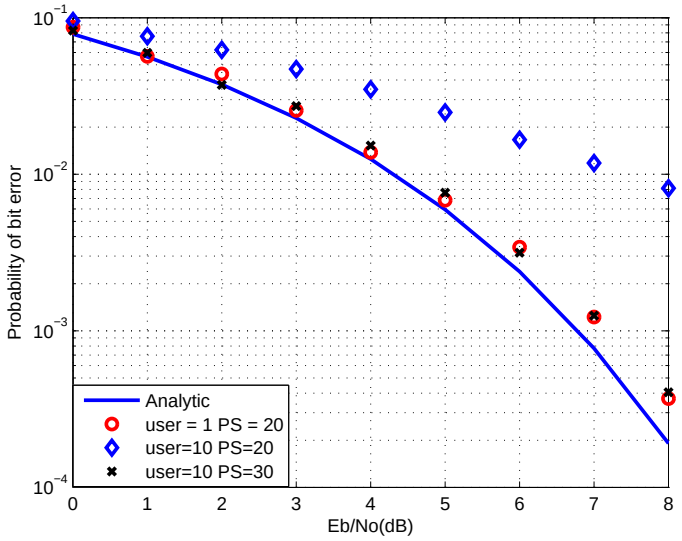

Figure 4.19: Performance of primary users with multiple secondary users present.

Evaluation of Overlay and Underlay Waveforms in Fading Channel

5.1 Introduction

This chapter starts with an overview of fading concepts and diversity techniques to mitigate the effects of fading. Then in the next few sections analytic expressions to calculate bit error rate (BER) performance curves for overlay-CR and underlay-CR in both flat and frequency selective fading channels are presented. Finally, simulation results are presented to demonstrate performance of overlay-CR and underlay-CR waveform in frequency selective fading channel. The flexibility of the overlay/underlay framework is demonstrated by applying it to a family of SMSE signals including OFDM, MC-CDMA, CI/MC-CDMA and TDCS.

5.2 Fading Channel Overview

In a wireless communication system a transmitted signal usually travels through a medium called ”Channel” before it is received and processed for extracting the information content. Usually, Additive White Gaussian Channel Noise (AWGN) serves as a starting point to evaluate the performance of a communication system in an ideal channel conditions. In a

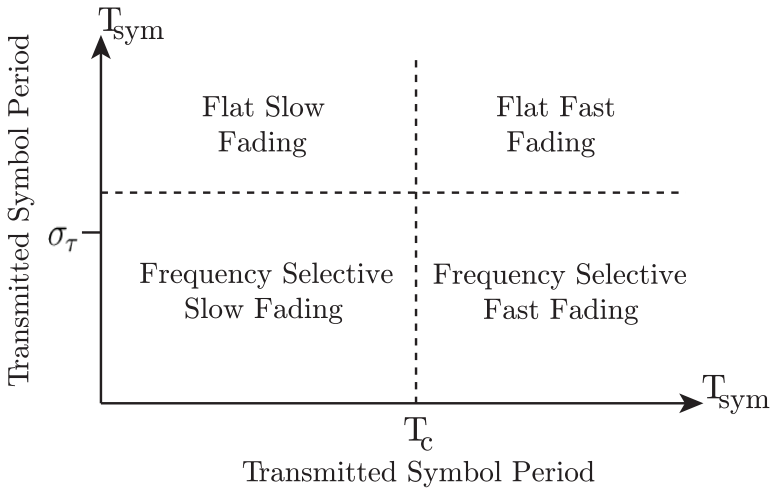

Figure 5.1: Fading Type 1. [9]

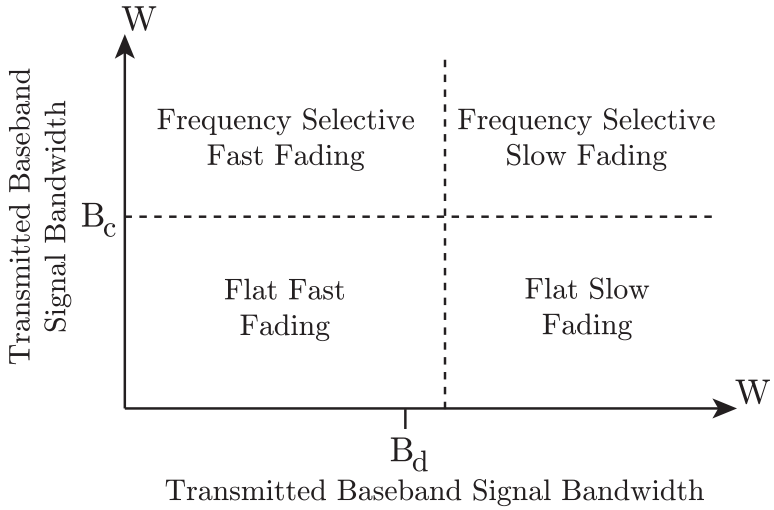

Figure 5.2: Fading Type 2. [9]

practical scenario, the wireless medium between the transmitter and the receiver can vary from a simple line of sight to a severely obstructed medium influenced by building, mountains, foliage and motion (if the wireless systems are on a mobile platform). A wireless communication system will experience performance degradation due to propagation loss resulting from the distance from the transmitter and receiver and also the multipath effects due to the obstruction.

The variations in the received power due to propagation loss and obstruction over a long distance is referred to as large scale propagation loss or large scale fading. A num-

ber of propagation models are available to mitigate the effects of large scale fading effects [9, 96]. Rapid fluctuations of the amplitude, phase or multipath delays over a short period or distance is referred to as small scale fading. The three important effects in small scale fading due to multipath phenomenon are: 1)Rapid changes in signal strength, 2)Random frequency modulation due to Doppler shift on different multipath signals and 3)Time dispersion or echoes caused by multipath delays [9]. In order to identify and understand of different aspects of multipath fading, a good understanding of key parameters and terminologies is necessary. Small scale fading effects can be characterized either in the time or frequency domain. Signal bandwidth, coherence bandwidth and Doppler bandwidth are frequency domain parameters. Similarly, symbol period, multipath delay spread and coherence time are time domain parameters which are used in characterization of small scale fading effects.

- **Signal Bandwidth**: Range of frequencies predominantly occupied by a wireless communications system. In general, the communication occupies bandpass signal bandwidth W that is inversely proportional to the symbol period T or duration.

$$W \approx \frac{1}{T}. \tag{5.1}$$

- **Coherence Bandwidth**: Coherence bandwidth B_c is a statistical measure of the range of frequencies over which the channel is considered to be "flat". In other words, coherence bandwidth is the range of frequencies over which two frequency components have a strong potential to be correlated in amplitude [9]. Coherence bandwidth is usually expressed in terms of σ_τ, the root mean square (rms) delay spread.

$$B_c \approx \frac{1}{5\sigma_\tau}. \tag{5.2}$$

- **Doppler Bandwidth**: Doppler bandwidth B_d or Doppler spread is a measure of the spectral broadening caused by the time rate of change due to wireless system mobility. It is defined as the range of frequencies over which the received spectrum is essentially non-zero, expressed as

$$B_d \approx \frac{\upsilon}{\lambda}, \tag{5.3}$$

where υ is relative velocity and λ is wavelength.

- **Symbol Period**: Symbol period is the time duration of one symbol and is inversely proportional to the bandwidth.

$$T \approx \frac{1}{W}. \tag{5.4}$$

- **Delay Spread**: The time period or the delay during which the multipath components exceeds a specified power relative to the strongest multipath component is called the delay spread. Multipath spread T_m is inversely proportional to the coherence bandwidth.

$$T_m \approx \frac{1}{B_c}. \tag{5.5}$$

Since channels with identical delay spread can have different signal intensity profiles, delay spread may not be an ideal metric to measure system performance. Therefore, rms delay spread as in (5.6) is usually used when discussing delay spread. It is important to note that coherence bandwidth and delay spread exhibit duality property.

$$\sigma_\tau \approx \frac{1}{5B_c}. \tag{5.6}$$

- **Coherence Time**: Coherence time is the time period during which the channel remains constant meaning no temporal or spectral variations occur during this time period.

$$T_c = \sqrt{\frac{9}{16\pi B_d^2}} = \frac{0.423}{B_d}. \tag{5.7}$$

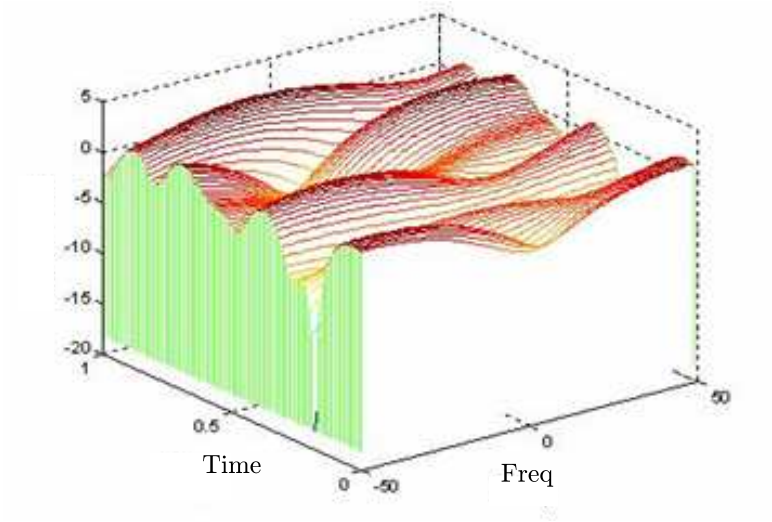

Figure 5.3: Flat Fading - fast.[10]

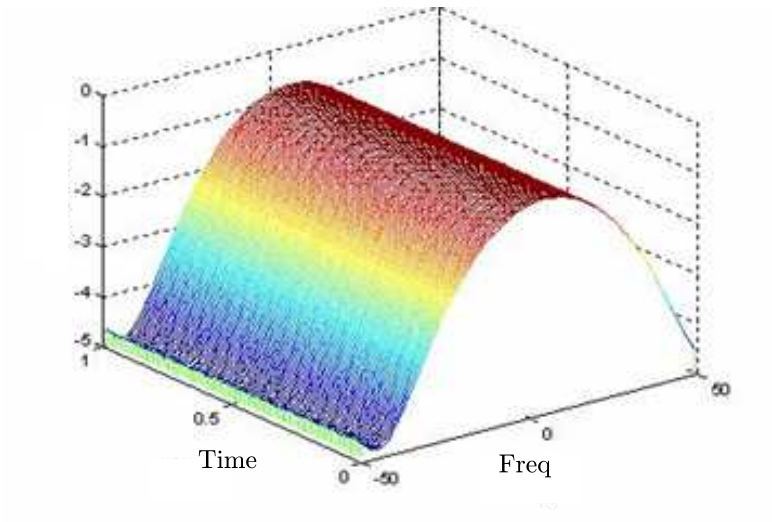

Figure 5.4: Flat Fading -slow. [10]

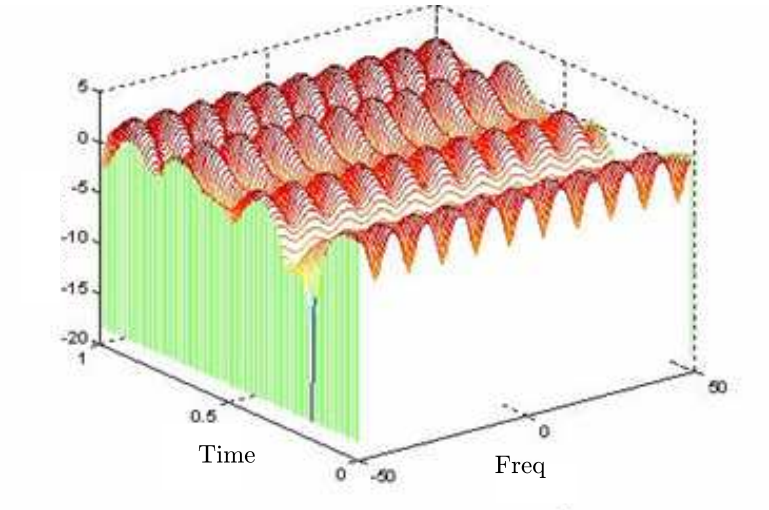

Figure 5.5: Fading type - Frequency Selective fast fading. [10]

Now that all key parameters have been introduced, as required to characterize small scale fading effects, the two type of fading namely flat and frequency selective can be discussed. The fading phenomenon experienced by the small scale fading can be expressed as shown in (5.1) using time domain parameters such as rms delay σ_τ and coherence time T_c, or as shown in (5.2) using frequency domain parameters such as doppler bandwidth B_d and coherence bandwidth B_d. A channel is said to be experiencing frequency selective fading if the channel bandwidth is greater than the coherence bandwidth $W > B_c$, or in time domain, if the symbol period is less the rms delay spread $T < \sigma_\tau$. Wideband or high data rate signals (e.g., MC-CDMA, CI/MC-CDMA and TDCS) usually experience frequency selective fading. On the other hand a channel is said to be experiencing flat fading. If the coherence bandwidth is greater than the channel bandwidth ($B_c > W$). Similarly, in the time domain the channel is considered flat fading if the symbol duration is greater than the delay spread $T >> \sigma_\tau$. Narrow band channels (e.g., OFDM) will experience flat fading. If the wireless system is in motion it will experience Doppler shifting according to (5.3). Since doppler introduces a change in the frequency, it will also affect how fast or slow the channel fluctuates. Depending on how fast the transmitted signal changes as compared to the rate of change of the channel, the channel may be classified as

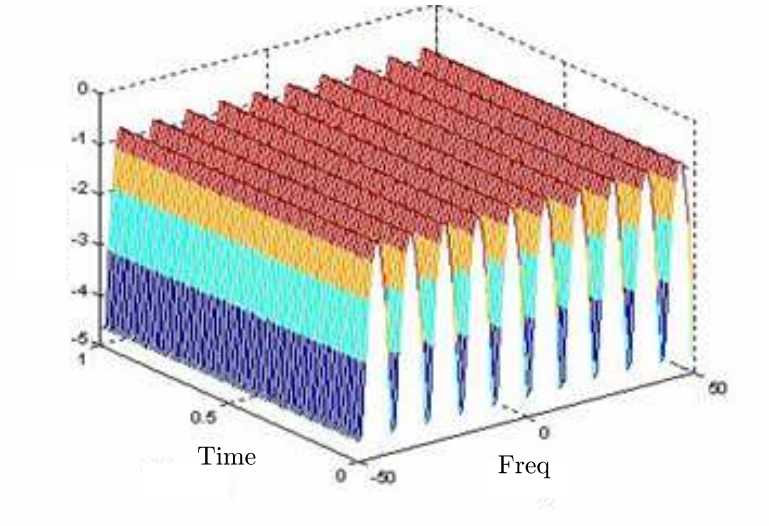

Figure 5.6: Fading type - FS slow fading. [10]

fast fading or slow fading. Figure 5.3 and 5.4, illustrate the fast and slow versions of the flat fading channel [10]. Similarly, Fig. 5.5 and Fig. 5.6, illustrates fast and slow fading in a frequency selective fading channel [10].

5.2.1 Overview of Diversity Combining

In wireless communication systems, the RF signal usually suffers from multi-path fading. In designing the SMSE multi-carrier transmission schemes, the bandwidth of each and every subcarrier Δf is carefully chosen so that $\Delta f << (\Delta f)_c$, where $(\Delta f)_c$ is the coherence bandwidth of the fading channel. Hence, while the total transmitted SMSE signal is transmitted through a multi-path fading channel, each subcarrier only experiences a flat fading channel. This feature significantly simplifies the design and implementation of the SMSE multi-carrier transmission transceiver.

Specifically, the i^{th} subcarrier observes a flat fading characterized by $\alpha_i e^{j\theta_i}$, where α_i is the fading gain which is characterized as a Rayleigh random variable, and θ_i is the phase offset introduced by the fading which is characterized as a uniform random variable. Hence, the received signal on the i^{th} subcarrier $r_i(t)$ is:

$$r_i(t) = Re[\alpha_i e^{j\theta_i} s_i(t)] + n(t) \tag{5.8}$$

where $s_i(t)$ is the transmitted signal on the i^{th} subcarrier, and $n(t)$ is the additive Gaussian noise.

At the SMSE receiver side, the phase offset θ_i is first tracked and removed, then the fading gain α_i is estimated via different methods (such as blind estimation, pilot tones, training sequences, etc).

The simplest SMSE waveform is OFDM. OFDM has been adopted by a wide variety of applications because it enables both high data rates and reliability over multipath fading channels. For example, HIPERLAN/2 and IEEE802.11 standards employ OFDM as their modulation technique. In its basic form, OFDM transmits each data symbol on one of N narrowband subcarriers, which in turn experiences a flat fade. Thus, each data symbol arrives at the receiver with a unique fade amplitude, leading to a poor performance in deep fades.

Traditionally, OFDM's poor performance is resolved by a combination of interleaving and channel coding. The resulting Coded OFDM (COFDM) system benefits from frequency diversity at the cost of reduced throughput. An attractive alternative to OFDM and COFDM is MC-CDMA (multi-carrier CDMA) and its variations (CI/MC-CDMA, TDCS, etc). In these schemes, each data symbol is simultaneously modulated onto all N carriers, exploiting large frequency diversity gains without any loss in throughput.

The transmitted signal for a K user MC-CDMA system at carrier frequency f_c is

$$S_{MC-CDMA}(t) = A \sum_{k=1}^{K} b^{(k)} \sum_{i=1}^{N} \beta_i^{(k)} e^{j2\pi(f_c + i\Delta f)t} g(t) \tag{5.9}$$

where A is the transmission amplitude ensuring unit energy, $\beta_i^{(k)}$ is the i^{th} chip of the k^{th} user's spreading code, and $g(t)$ is the rectangular pulse shape.

After transmission through a multipath fading channel, the received MC-CDMA signal is simply:

$$R_{MC-CDMA}(t) = A\sum_{k=1}^{K} b^{(k)} \sum_{i=1}^{N} \alpha_i \beta_i^{(k)} e^{j(2\pi(f_c+i\Delta f)t+\theta_i)} g(t) + n(t). \tag{5.10}$$

After phase offset removal, each subcarrier's matched filter output is

$$r_i = \sum_{k=1}^{K} b^{(k)} \sum_{i=1}^{N} \alpha_i \beta_i^{(k)} + n_i. \tag{5.11}$$

To decode the l^{th} user's data $b^{(l)}$, the l^{th} user's spreading code is being applied to all r_i and recombined to exploit frequency diversity:

$$R^{(l)} = \sum_{i=0}^{N-1} W_i \cdot r_i \cdot \beta_i^{*(k)}. \tag{5.12}$$

Different combining schemes can be used in the frequency combining, such as EGC (equal gain combining), MRC (maximum ratio combining), ORC (orthogonal restoration combining), MMSEC (minimized mean square error combining), etc [6].

In EGC, each combining weights is equal to one which is suitable for scenarios where fading gain is not obtained:

$$W_i = 1. \tag{5.13}$$

In MRC, the combining weight is the fading gain:

$$W_i = \alpha_i. \tag{5.14}$$

MRC is optimal for a single user MC-CDMA system [6].

In ORC, MAI (multiple access interference) is eliminated, however, the BER perfor-

mance is poor due to noise amplification:

$$W_i = \frac{1}{\alpha_i}. \tag{5.15}$$

MMSEC has been considered the best combining scheme for MC-CDMA when channel information is known at the receiver [6]:

$$W_i = \frac{\alpha_i}{K\alpha_i + \frac{N_0}{2}}. \tag{5.16}$$

To model realistic wireless environments, the Rayleigh fading channel employed in our simulation demonstrates frequency selectivity over the entire bandwidth, W, but flat fading over each of the N_f carriers. As a result, the α_i's in the N_f carriers are correlated according to $\rho_{i,j} = \frac{1}{1+((f_i-f_j)/(\Delta f)_c)^2}$ where $\rho_{i,j}$ denotes the correlation between the i^{th} carrier and the j^{th} carrier, and $(f_i - f_j)$ is the frequency separation between these two carriers [97].

5.3 Performance Anlalysis of Overlay and Underlay Waveforms in Flat Fading Channels

In this section, analytic bit error rate (BER) performance of non-contiguous Overlay and Underlay waveforms in flat fading channels is presented.

The total received signal in a cognitive radio scenario is

$$r(t) = \sum_{k=1}^{K} r_{p_k}(t) + \sum_{l=1}^{L} r_{s_l}(t) + n(t) \tag{5.17}$$

where K is the total number of primary users, L is the total number of secondary users, $r_{p_k}(t)$ represents the received signal of the k^{th} primary user, $r_{s_l}(t)$ is the received signal of the l^{th} secondary user, and $n(t)$ represents the additive Gaussian noise. Here, it is assumed that the primary users' signals are not going through the fading channel. Hence, the

received secondary user signals are altered by the fading gain α as:

$$r_{s_l}(t) = \alpha s_{s_l}(t) \tag{5.18}$$

while the primary users received signal stays the same as the transmitted signal:

$$r_{p_k}(t) = s_{p_k}(t). \tag{5.19}$$

Here, α is the fading gain, $s_{p_k}(t)$ represents the k^{th} primary user's transmitted signal, $s_{s_l}(t)$ is the l^{th} secondary user's transmitted signal. We assume that the k^{th} primary user transmits an OFDM signal with BPSK modulation over its M_k subcarriers, so the received signal of the k^{th} primary user corresponds to:

$$r_{p_k}(t) = \sqrt{\frac{E_{b_k}}{T}} Re\left\{ \sum_{i=0}^{M_k-1} b_i^{(k)} e^{j2\pi f_{k_i}} g(t) \right\} \tag{5.20}$$

where E_{b_k} is the k^{th} user's bit energy, $b_i^{(k)}$ is the k^{th} user's i^{th} bit, f_{k_i} is the i^{th} subcarrier of the k^{th} user, $g(t)$ is a rectangular waveform of unity height which time-limits the code to one symbol duration T, and the subcarrier bandwidth $\Delta f = f_{k_i} - f_{k_{i-1}} = 1/T$.

5.3.1 Performance Analysis of Overlay Waveforms

When the secondary user employs overlay waveform for its transmissions, only spectrum holes are used. Here it is assumed that one secondary user is transmitting over all the available spectrum holes. The received signal corresponding to the secondary user waveform employing NC-OFDM can be written as:

$$r_s(t) = \alpha \sqrt{\frac{E_{b_s}}{T}} Re\left\{ \sum_{i=0}^{M_h-1} b_i^{(s)} e^{j2\pi f_{h_i} t} g(t) \right\} \tag{5.21}$$

where E_{b_s} is the secondary user's bit energy, $b_i^{(s)}$ is the secondary user's i^{th} bit, f_{h_i} is the i^{th} subcarrier of the spectrum holes, and M_h is the total number of subcarriers of all spectrum holes.

Similarly, the received signal of a secondary user employing NC-MC-CDMA can be written as

$$r_s(t) = \alpha\sqrt{\frac{E_{b_s}}{M_h T}} Re\left\{ b^{(s)} \sum_{i=0}^{M_h-1} \beta_i e^{j2\pi f_{h_i} t} g(t) \right\} \tag{5.22}$$

where β_i is the i^{th} component of the spreading code of the secondary user.

Since the secondary user's transmission is assumed to be synchronized in time with the primary users' transmission, and the secondary user only transmits over spectrum holes, there is no interference from the secondary user to primary users and vice versa.

Hence, the BER performance of the secondary user (and the primary users) is simply

$$P(e) = \frac{1}{2}\left(1 - \sqrt{\frac{\bar{\gamma}/2}{1+\bar{\gamma}/2}},\right) \tag{5.23}$$

where $\bar{\gamma}$ is the average signal-to-noise ratio, defined as

$$\bar{\gamma} = \frac{E_b}{N_0} E\left[\alpha^2\right]. \tag{5.24}$$

5.3.2 Performance Analysis of Underlay Waveforms

When underlay waveform is employed by the secondary users for transmission, the transmission occupies the entire bandwidth instead of only the spectrum holes. Here, multiple secondary users can be accommodated using MC-CDMA. The total secondary users' signal corresponds to:

$$r_s(t) = \alpha \sum_{l=1}^{L} S_{s_i}(t) = \alpha \sqrt{\frac{E_{b_s}}{N_f T}} Re \left\{ \sum_{l=1}^{L} b^{(l)} \sum_{i=0}^{N_f-1} \beta_i^{(l)} e^{j2\pi(f_c+i\Delta f)t} g(t) \right\} \tag{5.25}$$

N_f is the total number of subcarriers over the entire bandwidth, $\beta_i^{(l)}$ is the i^{th} component of l^{th} user's spreading code.

At the receiver side, the received signal is first decomposed to N_f subcarriers, then recombined together to create the final decision variable for the desired secondary user. Specifically, the n^{th} secondary user's decision variable is:

$$R^{(n)} = \sum_{i=0}^{N_f-1} r_i^{(n)} \tag{5.26}$$

When one subcarrier is in a spectrum hole, there is no primary user's signal:

$$r_i^{(n)} = \alpha \sqrt{\frac{E_{b_s}}{N_f}} b^{(n)} + \alpha \sqrt{\frac{E_{b_s}}{N_f}} \sum_{l=1, l\neq n}^{L} b^{(l)} \beta_i^{(l)} \beta_i^{(n)} + n_i \tag{5.27}$$

where the first term is the desired signal, the second term is the MAI, and the third term represents the additive Gaussian noise.

However, if one subcarrier is not in a spectrum hole, the secondary users' signal co-exists with one primary user's signal:

$$r_i^{(n)} = \alpha \sqrt{\frac{E_{b_s}}{N_f}} b^{(n)} + \alpha \sqrt{\frac{E_{b_s}}{N_f}} \sum_{l=1, l\neq n}^{L} b^{(l)} \beta_i^{(l)} \beta_i^{(n)} + \sqrt{E_{b_k}} b_i^{(k)} + n_i. \tag{5.28}$$

When orthogonal spreading codes are employed for secondary users, the n^{th} secondary user's decision variable after recombining now corresponds to:

$$R^{(n)} = \sum_{i=0}^{N_f-1} r_i^{(n)} = N_f \alpha \sqrt{\frac{E_{b_s}}{N_f}} + \sum_{k=1}^{K} \sqrt{E_{b_k}} \sum_{i=0}^{M_k-1} b_i^{(k)} + \sum_{i=0}^{N_f-1} n_i. \tag{5.29}$$

The first term in (5.29) is the desired signal, the second term represents the interference from primary users to the secondary user and the third term is the noise contribution where $E[{n_i}^2] = \frac{N_0}{2}$. Note that there is no MAI in the final decision variable due to the orthogonality among spreading codes.

Using a Gaussian approximation, the interference power from primary user on the secondary user, second term in (5.29) is given by

$$E\left[\left(\sum_{k=1}^{K}\sqrt{E_{b_k}}\sum_{i=0}^{M_k-1}b_i^{(k)}\right)^2\right] = \sum_{k=1}^{K} M_k E_{b_k}. \tag{5.30}$$

If all primary users have the same bit energy E_{b_p}, equation (5.30) reduces to

$$\sum_{k=1}^{K} M_k E_{b_k} = M E_{b_p} \quad , \tag{5.31}$$

where $M = \sum_{k=1}^{K} M_k$ is the total number of subcarriers occupied by primary users.

It is easy to show that the average signal-to-interference-and-noise ratio SINR (signal to interference and noise ratio) $\bar{\gamma}'$ is

$$\bar{\gamma}' = \frac{N_f E[\alpha^2] E_{b_s}}{\sum_{k=1}^{K} M_k E_{b_k} + N_f \frac{N_0}{2}}. \tag{5.32}$$

Hence, the BER for the secondary user in flat fading channel corresponds to

$$P(e) = \frac{1}{2}\left(1 - \sqrt{\frac{\bar{\gamma}'/2}{1+\bar{\gamma}'/2}}\right) = \frac{1}{2}\left(1 - \sqrt{\frac{\frac{N_f E[\alpha^2] E_{b_s}}{2\sum_{k=1}^{K} M_k E_{b_k} + N_f N_0}}{1 + \frac{N_f E[\alpha^2] E_{b_s}}{2\sum_{k-1}^{K} M_k E_{b_k} + N_f N_0}}}\right) \tag{5.33}$$

$$P(e) = \frac{1}{2}\left(1 - \sqrt{\frac{N_f E[\alpha^2] E_{b_s}}{2\sum_{k=1}^{K} M_k E_{b_k} + N_f N_0 + N_f E[\alpha^2] E_{b_s}}}\right) \tag{5.34}$$

$$P(e) = \frac{1}{2}\left(1 - \sqrt{\frac{E[\alpha^2]\frac{E_{b_s}}{N_0}}{E[\alpha^2]\frac{E_{b_s}}{N_0} + 2\sum_{k=1}^{K} \frac{M_k}{N_f}\frac{E_{b_k}}{N_0} + 1}}\right). \tag{5.35}$$

When all primary users have the same bit energy, the BER reduces to:

$$P(e) = \frac{1}{2}\left(1 - \sqrt{\frac{E[\alpha^2]\frac{E_{b_s}}{N_0}}{E[\alpha^2]\frac{E_{b_s}}{N_0} + 2\frac{M}{N_f}\frac{E_{b_k}}{N_0} + 1}}\right). \tag{5.36}$$

5.4 Performance Analysis of Overlay and Underlay Waveforms in Multipath Fading Channels

In this section, the analytic expression to evaluate the BER performance of Overlay and Underlay waveforms in multipath fading channels is derived. The total received signal in a cognitive radio scenario is

$$r(t) = \sum_{k=1}^{K} r_{p_k}(t) + \sum_{l=1}^{L} r_{s_l}(t) + n(t) \tag{5.37}$$

where K is the total number of primary users, L is the total number of secondary users, $r_{p_k}(t)$ represents the received signal of the k^{th} primary user, $r_{s_l}(t)$ is the received signal of the l^{th} secondary user, and $n(t)$ represents the additive Gaussian noise. Here, it is assumed that the primary users' signals are not going through the fading channel. Hence, the

received secondary user signals after transmission through a multipath fading channel is:

$$r_{s_l}(t) = h(t) * s_{s_l}(t) \tag{5.38}$$

while the primary users received signal stays the same as the transmitted signal:

$$r_{p_k}(t) = s_{p_k}(t). \tag{5.39}$$

Here, $h(t)$ is the impulse response of the fading channel, $*$ represents convolution, $s_{p_k}(t)$ represents the k^{th} primary user's transmitted signal, $s_{s_l}(t)$ is the l^{th} secondary user's transmitted signal. It is assumed that the k^{th} primary user transmits an OFDM signal with BPSK modulation over its M_k subcarriers, so the received signal of the k^{th} primary user corresponds to:

$$r_{p_k}(t) = \sqrt{\frac{E_{b_k}}{T}} Re\left\{ \sum_{i=0}^{M_k-1} b_i^{(k)} e^{j2\pi f_{k_i}} g(t) \right\} \tag{5.40}$$

where E_{b_k} is the k^{th} user's bit energy, $b_i^{(k)}$ is the k^{th} user's i^{th} bit, f_{k_i} is the i^{th} subcarrier of the k^{th} user, $g(t)$ is a rectangular waveform of unity height which time-limits the code to one symbol duration T, and the subcarrier bandwidth $\Delta f = f_{k_i} - f_{k_{i-1}} = 1/T$.

5.4.1 Performance Analysis of Overlay Waveforms

When the secondary user employs overlay waveform for its transmissions, only spectrum holes are used. Here, it is assumed that one secondary user transmitting over all the available spectrum holes. The received signal corresponding to the secondary user waveform employing NC-OFDM can be written as:

$$r_s(t) = \sqrt{\frac{E_{b_s}}{T}} Re \left\{ \sum_{i=0}^{M_h - 1} \alpha_i b_i^{(s)} e^{(j2\pi f_{h_i} t + \theta_i)} g(t) \right\} \tag{5.41}$$

where α_i is the fading gain on the i^{th} subcarrier, θ_i is the phase offset introduced by the fading channel on the i^{th} subcarrier, E_{b_s} is the secondary user's bit energy, $b_i^{(s)}$ is the secondary user's i^{th} bit, f_{h_i} is the i^{th} subcarrier of the spectrum holes, and M_h is the total number of subcarriers of all spectrum holes.

Similarly, the received signal of a secondary user employing NC-MC-CDMA can be written as

$$r_s(t) = \sqrt{\frac{E_{b_s}}{M_h T}} Re \left\{ b^{(s)} \sum_{i=0}^{M_h - 1} \alpha_i \beta_i e^{(j2\pi f_{h_i} t + \theta_i)} g(t) \right\} \tag{5.42}$$

where β_i is the i^{th} component of the spreading code of the secondary user.

Since the secondary user's transmission is assumed to be synchronized in time with the primary users' transmission, and the secondary user only transmits over spectrum holes, there is no interference from the secondary user to primary users and vice versa.

Since the NC-OFDM does not provide frequency diversity, the BER performance of the secondary user (and the primary users) employing NC-OFDM is the same as in a flat fading channel:

$$P(e) = \frac{1}{2} \left(1 - \sqrt{\frac{\bar{\gamma}/2}{1 + \bar{\gamma}/2}} \right) \tag{5.43}$$

where $\bar{\gamma}$ is the average signal-to-noise ratio, defined as

$$\bar{\gamma} = \frac{E_b}{N_0} E \left[\alpha^2 \right]. \tag{5.44}$$

On the other hand, in NC-MC-CDMA, the signal is recombined across all subcarriers to exploit frequency diversity:

$$R^{(n)} = \sum_{i=0}^{M_h-1} W_i \cdot r_i^{(n)} \tag{5.45}$$

where

$$r_i^{(n)} = \alpha_i \sqrt{\frac{E_{b_s}}{M_h}} b^{(n)} + \alpha_i \sqrt{\frac{E_{b_s}}{M_h}} \sum_{l=1, l\neq n}^{L} b^{(l)} \beta_i^{(l)} \beta_i^{(n)} + n_i \tag{5.46}$$

and W_i is the i^{th} combining weight. Maximum Likelihood Combining (MLC) is employed, since it offers the best BER performance in multipath fading channels:

$$W_i = \frac{\alpha_i \sqrt{\frac{E_{b_s}}{M_h}}}{(L-1)\alpha_i^2 \frac{E_{b_s}}{M_h} + \frac{N_0}{2}}. \tag{5.47}$$

It is important to note that when there is only one secondary user (i.e., $L = 1$), MLC reduces to maximum ratio combining (MRC) which is well known as the optimal frequency diversity combining scheme [6, 96]:

$$W_i = \alpha_i. \tag{5.48}$$

After frequency combining, the final decision variable corresponds to:

$$\begin{aligned} R^{(n)} &= \sum_{i=0}^{M_h-1} W_i \cdot r_i^{(n)} \qquad (5.49) \\ &= \sum_{i=0}^{M_h-1} W_i \alpha_i \sqrt{\frac{E_{b_s}}{M_h}} b^{(n)} + \sum_{i=0}^{M_h-1} W_i \alpha_i \sqrt{\frac{E_{b_s}}{M_h}} \sum_{l=1, l\neq n}^{L} b^{(l)} \beta_i^{(l)} \beta_i^{(n)} + \sum_{i=0}^{M_h-1} W_i n_i \end{aligned}$$

where the first term is the desired signal, the second term is the MAI (multiple access interference), and the third term is the noise contribution. The power of the desired signal corresponds to:

$$P_{Signal} = \left(\sum_{i=0}^{M_h-1} W_i \alpha_i \sqrt{\frac{E_{b_s}}{M_h}} b^{(n)} \right)^2 = \frac{E_{b_s}}{M_h} \left(\sum_{i=0}^{M_h-1} W_i \alpha_i \right)^2 . \tag{5.50}$$

The power of the MAI is

$$P_{MAI} = E \left[\sum_{i=0}^{M_h-1} W_i \alpha_i \sqrt{\frac{E_{b_s}}{M_h}} \sum_{l=1, l \neq n}^{L} b^{(l)} \beta_i^{(l)} \beta_i^{(n)} \right]^2 = (L-1) \frac{E_{b_s}}{M_h} \sum_{i=0}^{M_h-1} W_i^2 \alpha_i^2 \tag{5.51}$$

and the power of the noise contribution is

$$P_{Noise} = E \left[\sum_{i=0}^{M_h-1} W_i n_i \right]^2 = \frac{N_0}{2} \sum_{i=0}^{M_h-1} W_i^2 . \tag{5.52}$$

The instantaneous signal to interference and noise ratio (SINR) is thus

$$\begin{aligned} SINR &= \frac{P_{Signal}}{P_{MAI} + P_{Noise}} \\ &= \frac{\frac{E_{b_s}}{M_h} \left(\sum_{i=0}^{M_h-1} W_i \alpha_i \right)^2}{(L-1) \frac{E_{b_s}}{M_h} \sum_{i=0}^{M_h-1} W_i^2 \alpha_i^2 + \frac{N_0}{2} \sum_{i=0}^{M_h-1} W_i^2} . \end{aligned} \tag{5.53}$$

The expression for probability of error as a function of SINR corresponds to

$$P(e)_{\text{instant}} = Q\left(\sqrt{SINR} \right) \tag{5.54}$$

and the average $P(e)$ is the integration over the probability density function of SINR, i.e.,

$$P(e) = \int_0^\infty Q\left(\sqrt{SINR} \right) p(SINR) d(SINR). \tag{5.55}$$

The expression in (5.55) can be determined via numerical methods which can be easily implemented.

5.4.2 Performance Analysis of Underlay Waveforms

When underlay waveform is employed by the secondary users for transmission, the transmission occupies the entire bandwidth instead of only the spectrum holes. Here, multiple secondary users can be accommodated using MC-CDMA. The total secondary users' signal corresponds to:

$$r_s(t) = \sum_{l=1}^{L} r_{s_i}(t) = \sqrt{\frac{E_{b_s}}{N_f T}} Re \left\{ \sum_{l=1}^{L} b^{(l)} \sum_{i=0}^{N_f-1} \alpha_i \beta_i^{(l)} e^{(j2\pi(f_c+i\Delta f)t+\theta_i)} g(t) \right\} \tag{5.56}$$

N_f is the total number of subcarriers over the entire bandwidth, $\beta_i^{(l)}$ is the i^{th} component of l^{th} user's spreading code.

At the receiver side, the received signal is first decomposed to N_f subcarriers, then recombined together to create the final decision variable for the desired secondary user. Specifically, the n^{th} secondary user's decision variable is:

$$R^{(n)} = \sum_{i=0}^{N_f-1} r_i^{(n)}. \tag{5.57}$$

When one subcarrier is in a spectrum hole, there is no primary user's signal:

$$r_i^{(n)} = \alpha_i \sqrt{\frac{E_{b_s}}{N_f}} b^{(n)} + \alpha_i \sqrt{\frac{E_{b_s}}{N_f}} \sum_{l=1, l\neq n}^{L} b^{(l)} \beta_i^{(l)} \beta_i^{(n)} + n_i \tag{5.58}$$

where the first term is the desired signal, the second term is the MAI, and the third term represents the additive Gaussian noise.

However, if one subcarrier is not in a spectrum hole, the secondary users' signal co-

exists with one primary user's signal:

$$r_i^{(n)} = \alpha_i \sqrt{\frac{E_{b_s}}{N_f}} b^{(n)} + \alpha_i \sqrt{\frac{E_{b_s}}{N_f}} \sum_{l=1, l\neq n}^{L} b^{(l)} \beta_i^{(l)} \beta_i^{(n)} + \sqrt{E_{b_k}} b_i^{(k)} + n_i. \tag{5.59}$$

The secondary users' signal is then recombined across all subcarriers to exploit frequency diversity:

$$R^{(n)} = \sum_{i=0}^{N_f-1} W_i \cdot r_i^{(n)}. \tag{5.60}$$

After frequency combining, the final decision variable corresponds to:

$$\begin{aligned} R^{(n)} &= \sum_{i=0}^{N_f-1} W_i \cdot r_i^{(n)} \\ &= \sum_{i=0}^{N_f-1} W_i \alpha_i \sqrt{\frac{E_{b_s}}{N_f}} b^{(n)} + \sum_{i=0}^{N_f-1} W_i \alpha_i \sqrt{\frac{E_{b_s}}{N_f}} \sum_{l=1, l\neq n}^{L} b^{(l)} \beta_i^{(l)} \beta_i^{(n)} \\ &+ \sum_{k=1}^{K} \sum_{i \in P_k} \sqrt{E_{b_k}} b_i^{(k)} + \sum_{i=0}^{N_f-1} W_i n_i \end{aligned} \tag{5.61}$$

where P_k is the subcarrier set of the k^{th} primary user. The first term in (5.61) represents the desired signal, the second term represents the MAI from all other secondary users, the third term is the primary users' interference, and the fourth term is the noise contribution.

It can be easily show that the desired signal power is:

$$P_{Signal} = \left(\sum_{i=0}^{N_f-1} W_i \alpha_i \sqrt{\frac{E_{b_s}}{N_f}} b^{(n)} \right)^2 = \frac{E_{b_s}}{N_f} \left(\sum_{i=0}^{N_f-1} W_i \alpha_i \right)^2 \quad , \tag{5.62}$$

the MAI power is

$$P_{MAI} = E\left[\sum_{i=0}^{N_f-1} W_i \alpha_i \sqrt{\frac{E_{b_s}}{N_f}} \sum_{l=1, l\neq n}^{L} b^{(l)} \beta_i^{(l)} \beta_i^{(n)}\right]^2 = (L-1)\frac{E_{b_s}}{N_f} \sum_{i=0}^{N_f-1} W_i^2 \alpha_i^2 \quad , \quad (5.63)$$

and the power of the primary users' interference (PUI) is

$$P_{PUI} = E\left[\sum_{k=1}^{K} \sum_{i\in P_k} \sqrt{E_{b_k}} b_i^{(k)}\right]^2 = \sum_{k=1}^{K} M_k E_{b_k} \quad , \quad (5.64)$$

where M_k is the total number of subcarriers of the k^{th} primary user. If all primary users have the same bit energy, the PUI power reduces to

$$P_{PUI} = \sum_{k=1}^{K} M_k E_{b_k} = M E_{b_p} \quad , \quad (5.65)$$

where $M = \sum_{k=1}^{K} M_k$ is the total number of subcarriers occupied by primary users.

The power of the noise contribution is

$$P_{Noise} = E\left[\sum_{i=0}^{N_f-1} W_i n_i\right]^2 = \frac{N_0}{2} \sum_{i=0}^{N_f-1} W_i^2. \quad (5.66)$$

The instantaneous signal-to-interference and noise ratio (SINR) is thus

$$SINR = \frac{P_{Signal}}{P_{MAI} + P_{PUI} + P_{Noise}} = \frac{\frac{E_{b_s}}{N_f}\left(\sum_{i=0}^{N_f-1} W_i \alpha_i\right)^2}{(L-1)\frac{E_{b_s}}{N_f} \sum_{i=0}^{N_f-1} W_i^2 \alpha_i^2 + \sum_{k=1}^{K} M_k E_{b_k} + \frac{N_0}{2} \sum_{i=0}^{N_f-1} W_i^2}.$$

When all primary users have the same bit energy, the instantaneous SINR reduces to:

$$SINR = \frac{\frac{E_{b_s}}{N_f}\left(\sum_{i=0}^{N_f-1} W_i\alpha_i\right)^2}{(L-1)\frac{E_{b_s}}{N_f}\sum_{i=0}^{N_f-1} W_i^2\alpha_i^2 + ME_{b_p} + \frac{N_0}{2}\sum_{i=0}^{N_f-1} W_i^2}. \tag{5.67}$$

The expression for probability of error as a function of SINR corresponds to

$$P(e)_{\text{instant}} = Q\left(\sqrt{SINR}\right) \tag{5.68}$$

and the average $P(e)$ is the integration over the probability density function of SINR, i.e.,

$$P(e) = \int_0^\infty Q\left(\sqrt{SINR}\right) p(SINR)d(SINR). \tag{5.69}$$

The expression (5.69) can be determined (calculated) via numerical methods which are easily implemented.

5.5 Simulation Analysis of Overlay waveform in Multi-path Fading

In this section, overlay-CR waveforms in frequency selective fading channel is demonstrated. Multi-Carrier waveforms such as NC-OFDM, NC-MC-CDMA, CI/MC-CDMA and TDCS have all been implemented. The overlay spectrum allocation scenario is similar to the analysis performed in the previous chapter with total number of subcarrier, given by $N = 64$ and at any given time 32 subcarriers are allocated to primary user and 32 are allocated to overlay-CR user. Even though the multi-carrier overlay-CR waveforms are

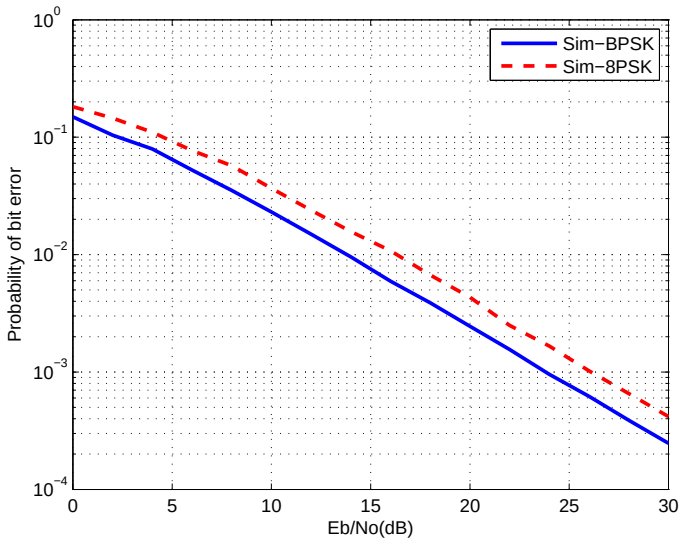

Figure 5.7: Performance of overlay NC-OFDM waveform in Frequency Selective Fading channel.

suitable for multi-user scenario, the scope of the simulations is limited to single primary and a single secondary user scenario. It is also assumed that the primary user signals which are modeled as OFDM-BPSK are not going through a fading channel and the primary and secondary users are perfectly synchronized.

In order to model a realistic wireless channel, the rayleigh fading channel employed in the simulations demonstrates frequency selectivity over the entire bandwidth BW, but flat fading over each of the subcarriers. This simulation assumes a channel model with coherence bandwidth characterized by $(\Delta f)_c$. It is assumed that the coherence bandwidth is eight times the subcarrier bandwidth, i.e. $(\Delta f)_c = 8\Delta f$. Hence, a primary user transmitting over 32 subcarriers observes 4-fold diversity and in the overall CR bandwidth of 64 subcarriers the frequency selectivity is 8 folds. In order to mitigate multipath fading effects and take advantage of the diversity, maximum ratio combining diversity approach was selected.

Figure 5.7 illustrates the performance of NC-OFDM using both BPSK and 8PSK modulations. Since NC-OFDM transmits a different symbol on each of the subcarriers and each subcarrier experiences flat fading, the diversity gain due to frequency selective combining

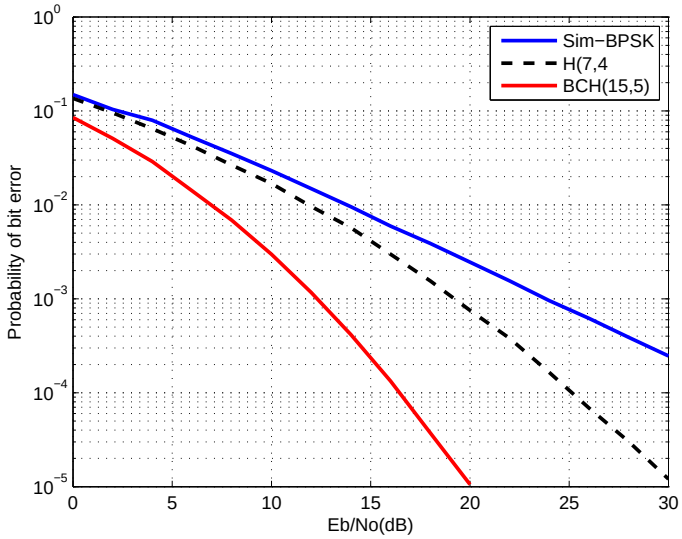

Figure 5.8: Performance of Overlay NC-OFDM waveform with channel coding in Frequency Selective Fading channel. This figure illustrates an OFDM waveform employing channel coding to take advantage of channel diversity .

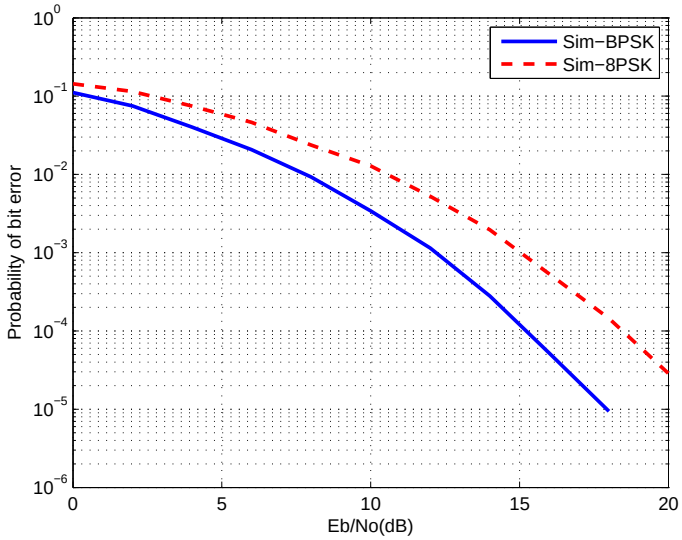

Figure 5.9: Performance of overlay NC-MC-CDMA waveform in Frequency Selective Fading channel.

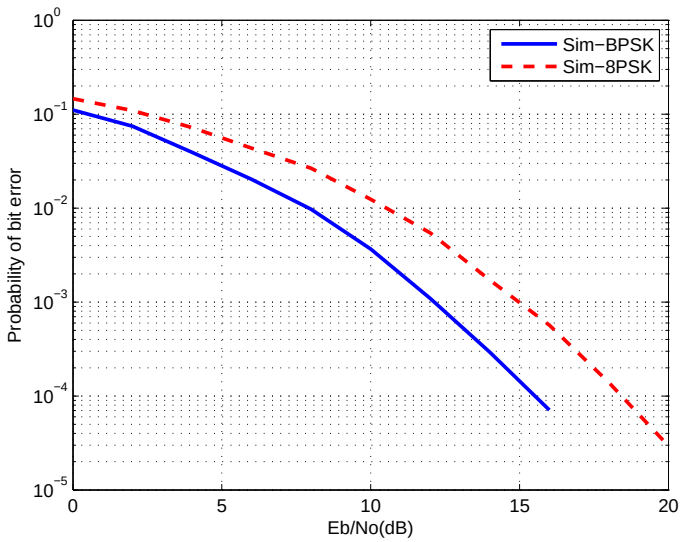

Figure 5.10: Performance of overlay NC-CI/MC-CDMA waveform in Frequency Selective Fading channel.

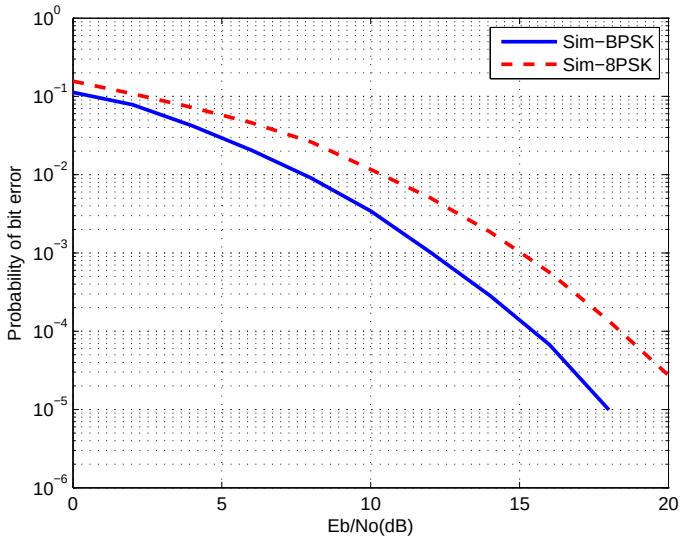

Figure 5.11: Performance of overlay NC-TDCS waveform in Frequency Selective Fading channel.

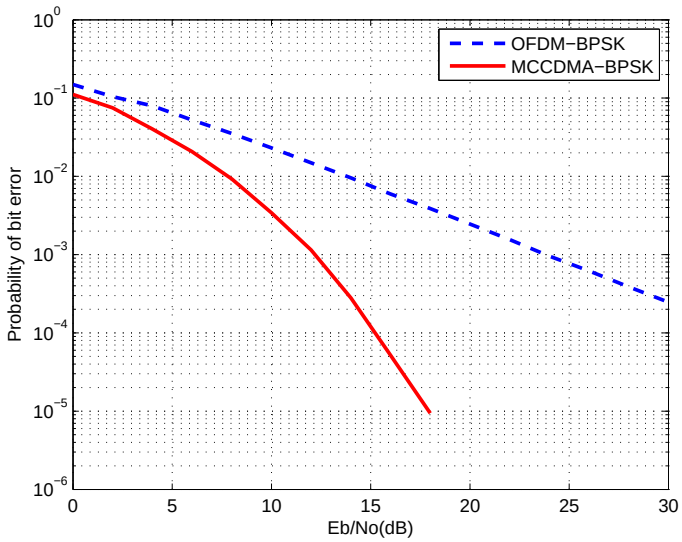

Figure 5.12: Performance of NC-OFDM and NC-MCCDMA waveform in Frequency Selective Fading channel. This figure illustrates the performance gained MC-CDMA dues to the diversity combining.

is not applicable here. Hence the performance of overlay-CR employing NC-OFDM experiences flat fading. One approach to take advantage of frequency diversity is to adopt coding schemes, which is demonstrated in Fig. 5.8. The top solid line in Fig. 5.8 is the uncoded version of NC-OFDM and the bottom two curves are NC-OFDM utilizing hamming(7,4) and BCH(15,5) codes. More about these codes will be discussed in the next chapter.

Figures 5.9 through 5.11, illustrate the performance of multi carrier waveforms such as NC-MC-CDMA, NC-CI/MC-CDMA and TDCS using both BPSK and 8PSK modulations. As expected, all three waveforms show performance improvement compared to the uncoded version of NC-OFDM show in Fig. 5.7. Figure 5.12 illustrates the performance of NC-OFDM-BPSK and NC-MC-CDMA BPSK modulations. The performance improvement due to the 8 folds frequency selectivity gains by employing MRC diversity technique is illustrated.

5.6 Simulation Analysis of Underlay waveform in Multi-path Fading

In this section simulation results are presented to demonstrate the performance of underlay-CR waveforms in a frequency selective fading environment. To recapitulate some of the underlay-CR properties, a underlay-CR waveform employed by the secondary user occupies the entire CR bandwidth or can adjust the bandwidth depending on data rate and interference requirements set forth by the primary users. In an overlay-CR waveform implementation and analysis, perfect synchronization is assumed between primary and overlay-CR secondary users, whereas in underlay-CR analysis, primary and secondary waveforms will be overlapping, increasing signal to interference noise ratio to both the systems To minimize the mutual interference, underlay waveform similar to UWB and spread spectrum signals will be expected to operate under the noise floor of the primary user signals.

The simulation analysis in this research is limited to single CR-primary user employing OFDM-BPSK modulations and a single secondary user employing multi-carrier waveforms such as NC-MC-CDMA, CI/MC-CDMA and TDCS employing BPSK and 8PSK modulations. Even though the underlay waveform employed in the simulations operate on a contiguous bandwidth, it has the ability to adapt to non-contiguous scenarios as demonstrated in the overlay simulations.

The frequency selective channel model assumed in the overlay-CR simulation analysis also applies to the underlay-CR analysis. Recall that in these simulations a four fold frequency diversity in a 32 subcarrier bandwidth was assumed. As the bandwidth increases due to spreading of the underlay waveforms, the number of diversity folds also increases, which results in performance improvements provided by utilizing an appropriate diversity combining technique.

Figure 5.13 and Fig. 5.14, illustrate the analytic results of MC-CDMA BPSK and MC-CDMA 8PSK, respectively, in a frequency selective fading channel employing MRC

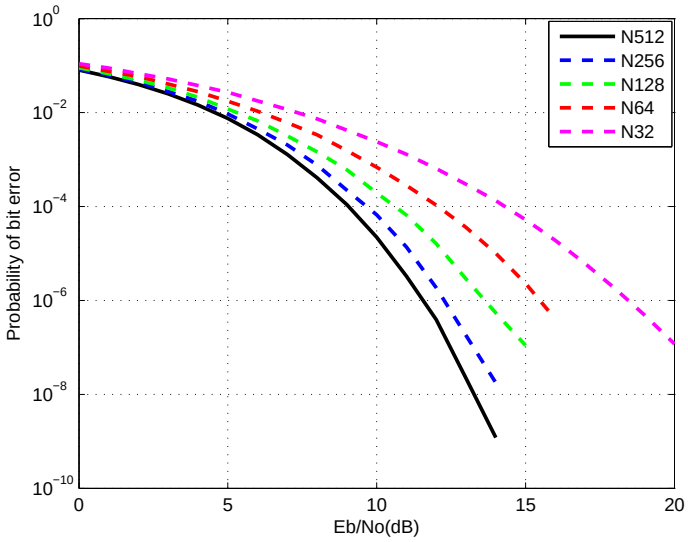

Figure 5.13: Analytic performance of MC-CDMA-BPSK due to diversity combining in frequency selective fading channel.

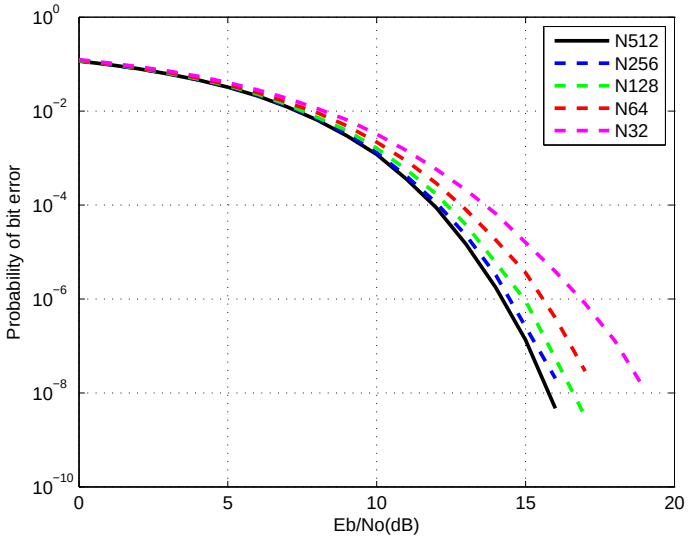

Figure 5.14: Analytic performance of MC-CDMA-8PSK due to diversity combining in frequency selective fading channel.

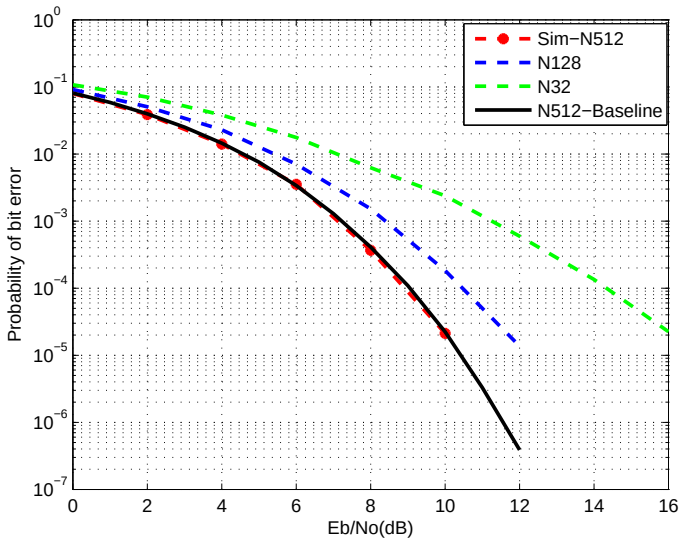

Figure 5.15: Illustration of performance gain due to spreading in Frequency Selective Fading channel. In this ideal underlay scenario there is no primary user interference.

diversity combining technique. It is evident from the figures that as the number of subcarriers increases, the performance gain due to frequency diversity also increases. It is also worth noting that the difference in performance improvement gets larger at higher E_b/N_o values. In order to validate the analytic results, underlay-CR simulations were also performed with primary user interference. Figure 5.15 demonstrates that the simulation results matches the analytic results, validating the assumption made in deriving the analytic expression as well as in the implementation. These analytic curves serve as a baseline to compare and contrast underlay-CR results.

Figures 5.16 through 5.18, illustrate simulation results for an underlay-CR waveform employing MC-CDMA BPSK, CI/MC-CDMA BPSK and TDCS BPSK modulations. The underlay-CR waveforms are assumed to be operating at -20dB relative to the primary user. The single primary user is modeled as 32 subcarrier OFDM-BPSK modulation. It is evident from the figures that as the underlay-CR waveform increases its spreading bandwidth by increasing the number of subcarrier there is a performance improvement, and at $N = 512$, the simulation results approaches the baseline results.

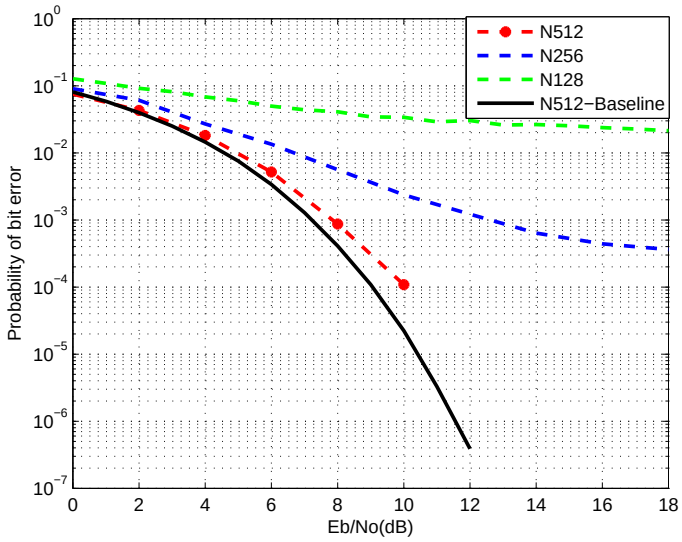

Figure 5.16: Performance analysis of Underlay waveform using MCCDMA-BPSK in Frequency Selective Fading channel.

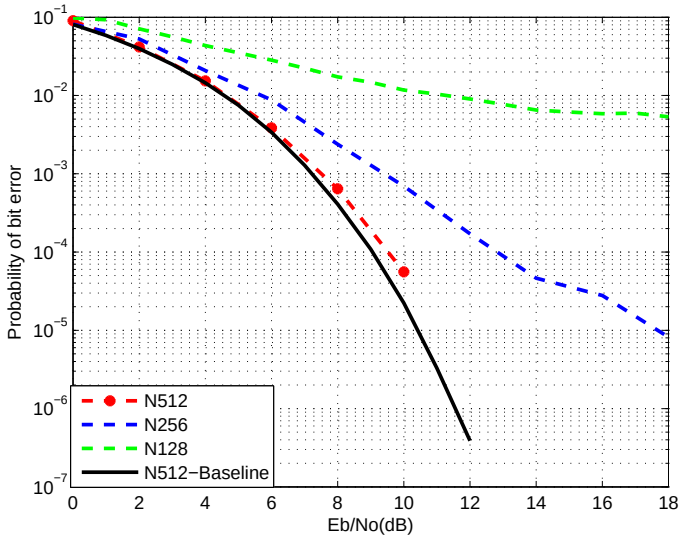

Figure 5.17: Performance analysis of Underlay waveform using CI/MCCDMA-BPSK in Frequency Selective Fading channel.

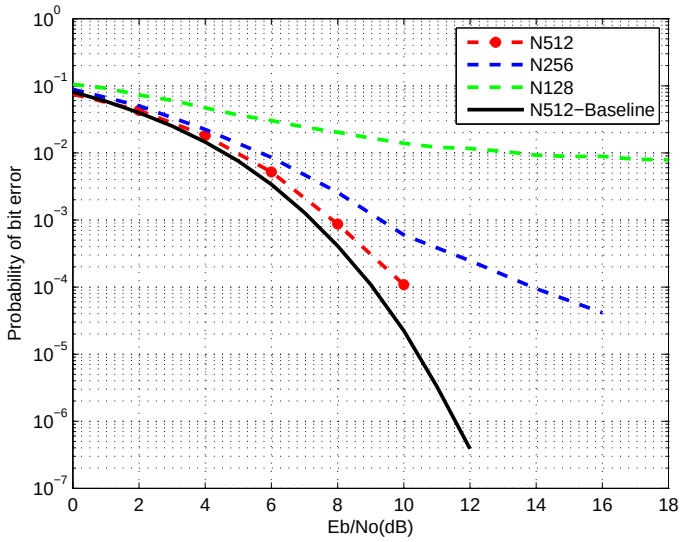

Figure 5.18: Performance analysis of Underlay waveform using TDCS-BPSK in Frequency Selective Fading channel.

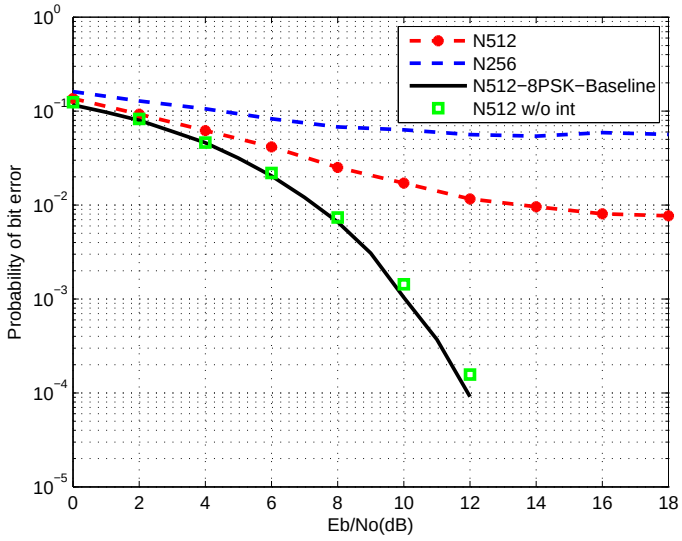

Figure 5.19: Performance analysis of Underlay waveform using MCCDMA-8PSK in Frequency Selective Fading channel.

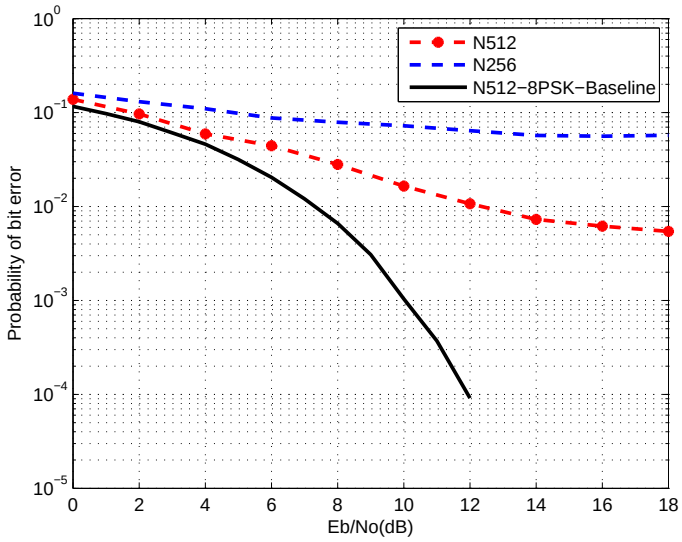

Figure 5.20: Performance analysis of Underlay waveform using CI/MCCDMA-8PSK in Frequency Selective Fading channel.

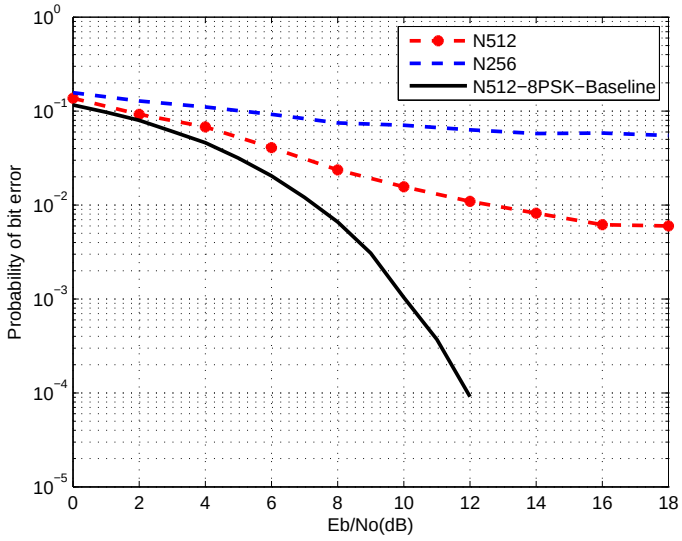

Figure 5.21: Performance analysis of Underlay waveform using TDCS-8PSK in Frequency Selective Fading channel.

Similarly, Figures 5.19 through 5.21, illustrate simulation results employing MC-CDMA 8PSK, CI/MC-CDMA 8PSK and TDCS 8PSK modulations. It can be seen from the figures that even though the performance starts to improve it does not come close to the baseline results. It should be noted that employing higher modulation schemes or lowering the secondary to primary interference ratio, will result in an increase in the bandwidth or the number of subcarriers in order to satisfy the performance requirements. For example, if the performance requirement for underlay-CR waveforms was to achieve a minimum BER of 10^{-3}, then the number of subcarriers has to be increased, since at $N = 512$ it has reached the irreducible noise floor.

Evaluation of Hybrid Overlay-Underlay Waveforms

6.1 Introduction

To maximize both spectrum efficiency and channel capacity, both *unused* and *underused* portion of the spectrum has to be utilized. This chapter via simulation demonstrates the performance enhancement utilizing both *unused* and *underused* spectrum using hybrid underlay/overlay waveform.

6.2 Channel Coding Overview

Channel coding is usually associated with forward error correction (FEC) codes. FEC are structured sequences which are added to the data to transform the overall sequence with error detection and error correction capability. To accomplish this, the encoder transmits not only the information symbols, but also one or more redundant symbols. The decoder uses the redundant symbols to detect and possibly correct whatever errors occurred during transmission. FEC codes can be divided into two categories, Block Codes and Convolution Codes [43, 96].

Block coding is simply an extension of single bit parity-check codes for error detec-

tion. Linear block codes extend this concept by using large number of parity bits to either detect or correct more than one error. A linear block code can be functionally described by two integer variables and a generator matrix or polynomial. The integer k represents the number of input data or information bits and the integer n represents the total number of bits associated with the output codeword.

A binary block code generates n coded bits from k information bits. This mapping is termed as (n, k) binary block code. The rate of the code $R_c = k/n$ represents information bits per codeword symbol. If for example, the coded symbols are transmitted at a rate of R_s symbols per second, then the information rate associated with an (n, k) block code is $R_b = R_c R_s = (k/n)R_s$ bits per second. The ratio k/n is called the rate of the code and also a measure of redundancy. Block codes improve the performance with a penalty of reduced data rate. Hamming, Bose-Chadhuri-Hocquenghem (BCH), Golay and extended Golay are few examples of linear block code. This research has considered hamming and BCH codes in implementing and demonstrating the hybrid overlay/underlay concept.

Hamming codes are the simplest from of linear block codes characterized by $(n, k) = (2^m - 1, 2^m - 1 - m)$ where $m = 2, 3, ...$ All hamming codes have a minimum distance $d_{min} = 3$, which indicates they are capable of correcting all single digit errors and can detect up to two errors in a single block of codeword. Error correction capability is related to the minimum distance.

BCH codes can be viewed as an extension to hamming codes which facilitates multiple error correction capabilities. They are a class of cyclic codes that provide a large selection of block length, code rates, alphabet sizes and error correction capability [43]. BCH codes are considered as very powerful linear block codes because at a few hundred block length, BCH outperforms all other block codes with the same block length and code rate.

Figure 6.1 illustrates a number of hamming and BCH codes with varying error correction capabilities. The top solid curve represents OFDM-BPSK in AWGN channel and the bottom solid curve represents OFDM-BPSK with BCH(15,5) channel coding with an error

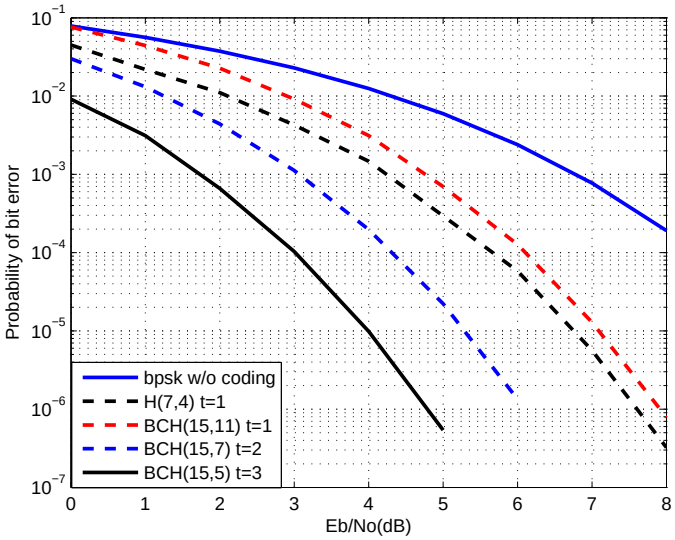

Figure 6.1: Performance of overlay NC-OFDM employing number of channel coding methods in AWGN channel conditions.

correction capability of three.

6.3 Evaluation of Hybrid Overlay/Underlay

The block diagram representations in Fig. 6.2 and Fig. 6.3 illustrate the conceptual view of the hybrid overlay/underlay approach. Systematic block channel coding is introduced to demonstrate the performance improvement gained by combining overlay and underlay techniques. Two popular block codes, namely a (7,4) Hamming code with $t = 1$ error correction capability and a (15,5) BCH code with $t = 3$ error correction capability were chosen for evaluation. In general, channel coding improves performance by adding redundant or parity bits. For a given communication system this translates to increase in transmission bandwidth or decrease in effective data rate. Hence, the overlay systems experience a reduction in effective date rate by a factor of k/n where k and n represent the number of output encoded and input information bits, respectively.

However, in the proposed overlay/underlay system in Fig. 6.3, the information bits are transmitted via overlay waveform (over unused frequency bands), and the redundant bits are

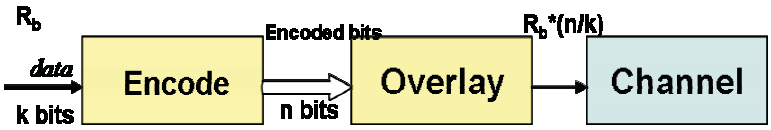

Figure 6.2: Block diagram representation of Overlay with channel coding.

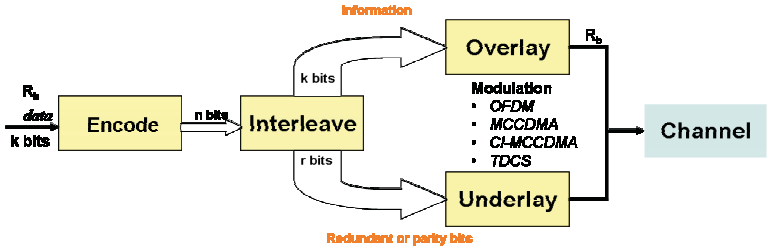

Figure 6.3: Hybrid overlay/underlay technique using channel coding.

transmitted via underlay waveform (over *underused* frequency bands). This way, both the *unused* and the *underused* frequency bands are utilized. Compared to pure overlay system, the new overlay/underlay system exploits channel coding gain without sacrificing data rate. More importantly, the overlay/underlay system possesses an increased degree of flexibility in receiver design. If preferred, no channel decoding needs to be implemented and the receiver simply demodulates the data from the overlay transmission. On the other hand, with a channel decoder present the overlay/underlay receiver can improve the performance significantly.

6.3.1 Overlay/Underlay in AWGN

Figure. 6.4 shows simulation results for the overlay and overlay/underlay concepts illustrated in Fig. 6.2 and Fig. 6.3. The top solid line represents the OFDM-BPSK overlay system without channel coding. The bottom two solid lines represents OFDM-BPSK overlay systems using H(7,4) and BCH(15,5) channel coding, respectively. The dashed lines represent the overlay/underlay combinations. The underlay waveform spread length was at $N = 256$ and $N = 512$, respectively. It is evident from the results in the figure that applying channel coding improves performance significantly but at the cost of reduced ef-

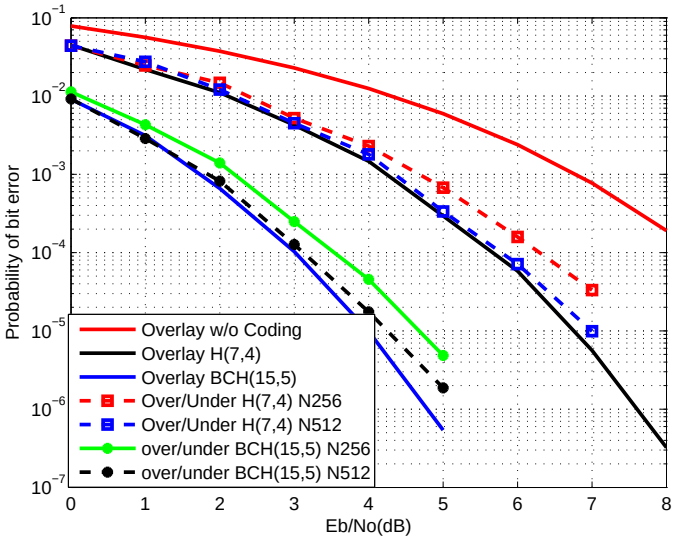

Figure 6.4: Performance of hybrid overlay/underlay waveform in AWGN channel conditions. Overlay is implemented using NC-OFDM and underlay is implemented using NC-MC-CDMA waveform.

fective data rate. Performance of the proposed overlay/underlay system approaches that of the channel coded overlay system without undergoing the reduced data rate.

Similarly, Fig. 6.5 and Fig. 6.6 illustrate the performance of hybrid overlay/underlay waveform. In both the figures OFDM-BPSK is used to model overlay-CR waveform, whereas the underlay-CR waveforms in Fig. 6.5 and Fig. 6.6 are modeled using CI/MC-CDMA BPSK and TDCS BPSK, respectively. Again, as in the previous scenario this simulation only considered a single user environment and comparisons between the different MC modulations can only be made in multi-user scenarios. The intent here was to demonstrate that using SDR-based CR platforms any of these multicarrier waveforms can be easily implemented.

6.3.2 Overlay/Underlay in Fading channel

In the previous chapter the performance improvements gained by overlay-CR and underlay-CR waveforms employing diversity combining in a frequency selective channel was demon-

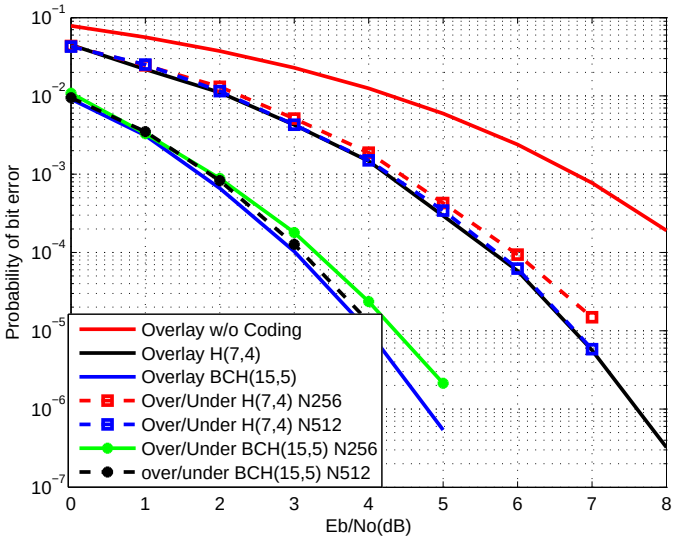

Figure 6.5: Performance of hybrid overlay/underlay waveform in AWGN channel conditions. Overlay is implemented using NC-OFDM and underlay is implemented using NC-CI/MC-CDMA waveform.

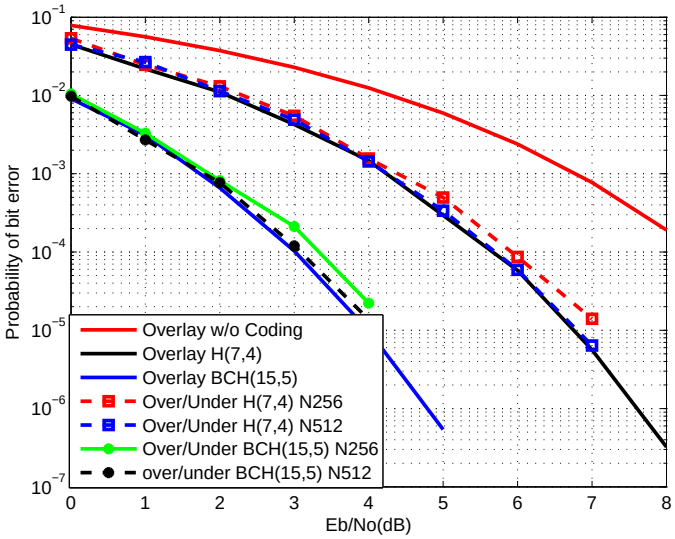

Figure 6.6: Performance of hybrid overlay/underlay waveform in AWGN channel conditions. Overlay is implemented using NC-OFDM and underlay is implemented using NC-TDCS waveform.

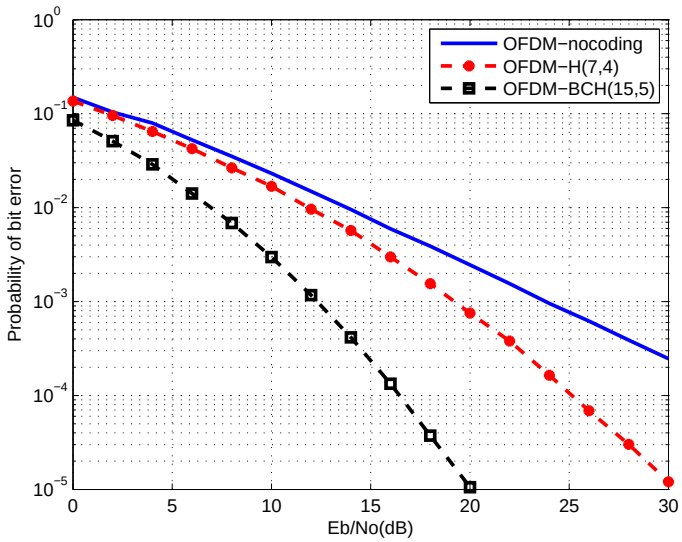

Figure 6.7: Performance of coded overlay NC-OFDM waveform in frequency selective fading channel.

strated. In this section, the performance improvement gained by *combining* both overlay-CR and underlay-CR in a frequency selective fading channel using diversity combining is demonstrated.

As mentioned in the previous chapter, a multipath channel is assumed to experience four folds frequency diversity. The single primary user interference is modeled as OFDM-BPSK consisting of 32 subcarriers. It is also assumed that the primary user is not experiencing fading effects. In order to demonstrate the robustness of the hybrid approach, two systematic block codes namely, hamming H(7,4) code with one error correction ability and BCH(15,5) with up to three error correction capability were implemented.

Figure 6.7 illustrates how coding improves the performance in a frequency selective (FS) fading channel. The top solid line is NC-OFDM experiencing fading whereas the bottom two curves represent coded NC-OFDM performance.

From the above discussions it is evident that coding enhances performance of overlay-CR systems in FS channels, but at the same time the overlay-CR systems experience a reduction in effective date rate by a factor of k/n.

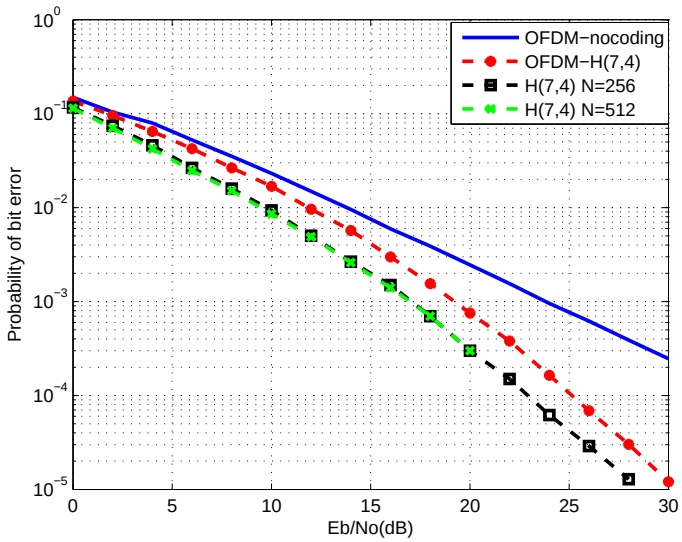

Figure 6.8: Performance of hybrid overlay/underlay waveform using hamming codes in Frequency selective fading channel. Overlay is implemented using NC-OFDM BPSK and underlay is implemented using NC-MC-CDMA BPSK.

Figure 6.8, illustrates the performance of hybrid overlay/underlay by employing NC-OFDM BPSK as a overlay-CR waveform, MC-CDMA BPSK as a underlay-CR waveform and hamming code H(7,4) was employed as an encoder. Underlay spreading length of 256 and 512 sub carriers was used. The top solid line represents OFDM with flat fading results. The red curve labeled as ”OFDM(7,4)” represents coded OFDM and the labels ”H(7,4) N = 256” and ”H(7,4) N = 512” represent overlay/underlay with spreading length 256 and 512 subcarriers. It is evident from the simulation results that the hybrid overlay/underlay not only offers performance improvements over overlay-CR but it also outperformed overlay-CR with channel coding. Moreover, the hybrid performance gain is not at the expense of reduced throughput as in the case of coded overlay-CR systems. Similarly, Fig. 6.9, illustrates hybrid overlay/underlay by employing NC-OFDM BPSK as the overlay-CR waveform and CI/MC-CDMA as the underlay-CR waveform.

Figure 6.10 and Fig. 6.11 illustrate performance of hybrid overlay/underlay using OFDM BPSK as overlay-CR, MC-CDMA BPSK and CI/MC-CDMA BPSK as underlay-CR employing BCH(15,5) encoder.

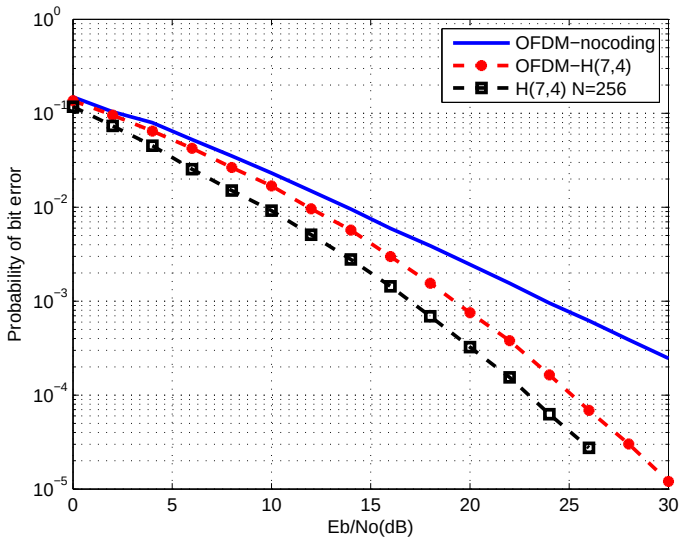

Figure 6.9: Performance of hybrid overlay/underlay waveform using hamming codes in Frequency selective fading channel. Overlay is implemented using NC-OFDM BPSK and underlay is implemented using NC-CI/MC-CDMA BPSK.

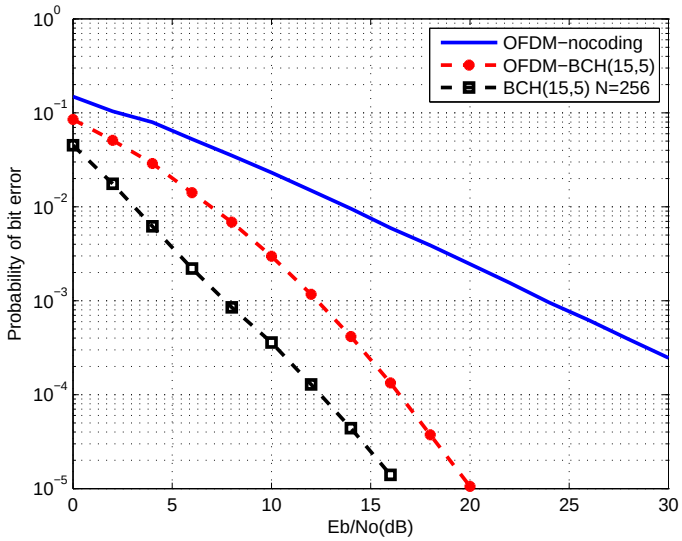

Figure 6.10: Performance of hybrid overlay/underlay waveform using BCH(15,5) codes in Frequency selective fading channel. Overlay is implemented using NC-OFDM BPSK and underlay is implemented using NC-MC-CDMA BPSK.

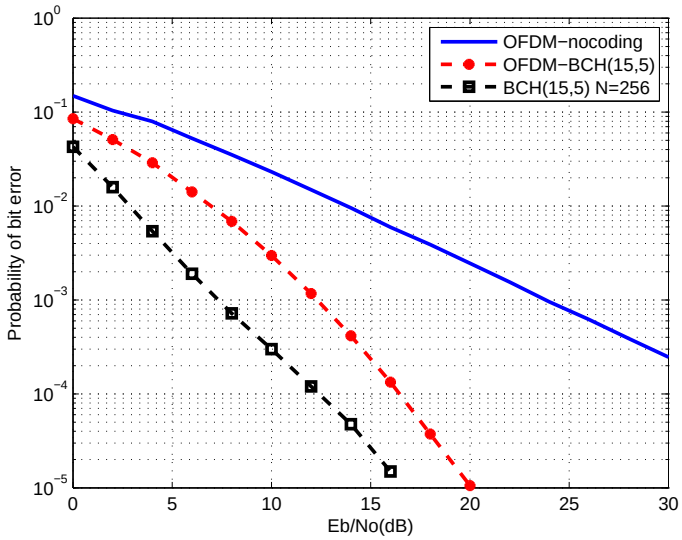

Figure 6.11: Performance of hybrid overlay/underlay waveform using BCH(15,5) codes in Frequency selective fading channel. Overlay is implemented using NC-OFDM BPSK and underlay is implemented using NC-CI/MC-CDMA BPSK.

Conclusions

To improve spectrum efficiency and maximize channel capacity, both *unused* (white) and *underused* (gray) spectral regions need to be exploited. An existing SMSE framework based on hard decision spectrum usage has been extended to soft decision SMSE framework (SD-SMSE) for physical layer waveforms that are well-suited for *"CR-based SDR"* applications. Given an established set of SD-SMSE design variables, the *"CR-based SDR"* is capable of dynamically generating overlay, underlay and hybrid overlay/underlay waveforms based on user requirements. Each of these three waveforms is evaluated using the SD-SMSE framework in a CR context under AWGN and frequency selective fading channel conditions. In general, the underlay-CR waveform is associated with UWB technology. However, results here demonstrate that the underlay-CR waveform is able to adapt its bandwidth based on user requirements and environmental conditions. It was also demonstrated that the hybrid overlay/underlay waveform can be used to improve spectrum efficiency.

7.1 Future Research Topics

This research has provided a SD-SMSE framework with the ability to utilize both *unsed* and *underused* spectrum of opportunity via Overlay/Underlay waveform design. Even though this research has demonstrated that spectrum efficiency and performance enhancement can be realized by combining overlay/underlay waveforms. A number of assumptions were made and a number of issues remain unanswered.

- **Synchronization**: This research assumed perfect synchronization between the secondary and primary user, which leads to two open problems: 1)Synchronization issues related to the co-existence of primary and secondary users, and 2)Synchronization of non-contiguous multi-carrier waveforms such as NC-OFDM, NC-MC-CDMA, NC-CI/MC-CDMA and NC-TDCS.

- **Multi-User Environment**: This research was limited to a single secondary user scenario. A thorough multi-user co-existence analysis with multiple primary and multiple secondary users presents challenges not only at the physical layer but also at the medium access control (MAC) layer. Metrics to measure interference threshold and co-existence analysis also need to be considered.

- **Multipath Fading**: This research evaluated CR-overlay and CR-Underlay analytically in both flat and frequency selective fading channels and validated by simulation the performance of frequency selective fading channels. It was assumed that only the secondary user was experiencing fading and that the primary user was operating over an AWGN channel. Even though this analysis serves as a baseline, other open problems include 1) analysis of primary user fading effects on the secondary user and 2) secondary user fading effects on primary users.

- **Spectrum Sensing**: In this work, the spectrum sensing function was assumed to be available. For more realistic implementation of the SD-SMSE, the spectrum sensing function needs to be integrated into the SD-SMSE framework.

- **Adaptive Modulation**: In the SD-SMSE framework, a weighted spectrum estimate of the channel was assumed. This means that depending on the utilization and interference, each of the spectral bins or subcarriers will have a different power requirement. In order to maximize the channel capacity, subcarrier level adaptive modulation is desired.

- **Primary User Interference**: In this research, secondary user interference was limited to a primary user employing OFDM-BPSK modulation. Other practical primary user interference sources could include other multi carrier waveforms, licensed users such as TV, radio, cell phones, and unlicensed users might be considered as well.

- **Applications of Overlay/Underlay Waveforms**: One common CR research assumptions is that either 1) all the secondary users will have the knowledge of primary users, secondary users and their channel conditions, or 2) there will exist some control channel to exchange this information. While this assumption might help in formulating or solving a particular problem, the question remains "What does this control channel look like?". The CR-underlay waveform proposed in this research might be an appropriate candidate to serve as the control channel for the secondary users.

Appendix

8.1 Cyclostationary based signal detection

This section provides an in depth analysis of cyclostationary (CS) based signal detection method in low SNR conditions. A modulated signal as received by the classifier can modeled as:

$$\begin{aligned} y(t) = &\quad Re\{\tilde{y}(t)\} \\ \tilde{y}(t) = &\quad s(t-t_0)e^{j2\pi f_c t}e^{j\phi} + \tilde{n}(t) \end{aligned} \tag{8.1}$$

where $y(t)$ is the received signal, $\tilde{y}(t)$ is the analytic signal of $y(t)$, f_c is the carrier frequency, ϕ is the carrier phase, t_0 is the signal time offset, $n(t)$ is additive Gaussian noise, and $s(t)$ denotes the time-varying message signal. For digital signals, this can be further specified as:

$$\tilde{y}(t) = e^{j2\pi f_c t}e^{j\phi}\sum_{-\infty}^{\infty} s_k p(t - kT_s - t_0) + \tilde{n}(t) \tag{8.2}$$

where $p(t)$ is the pulse shape, T_s is the symbol period, and s_k is the digital symbol transmitted at time $t \in (kT - T/2, kT + T/2)$. Here, the symbols s_k are assumed to be zero-mean, identically distributed random variables.

CS based approaches are based on the fact that communications signals are not ac-

curately described as stationary, but rather more appropriately modeled as cyclostationary. While stationary signals have statistics that remain constant in time, the statistics of CS signals vary periodically. These periodicities occur for signals of interest in well defined manners due to underlying periodicities such as sampling, scanning, modulating, multiplexing and coding. This resulting periodic nature of signals can be exploited to determine the modulation scheme of the unknown signal.

8.1.1 Second Order Cyclic Features

The autocorrelation function of a CS signal $x(t)$ can be expressed in terms of its Fourier Series components [98]:

$$R_x(t,\tau) = E\{x(t+\tau/2)x^*(t-\tau/2)\} = \sum_{\{\alpha\}} R_x^\alpha(\tau)e^{j2\pi\alpha t} \tag{8.3}$$

where $E\{\cdot\}$ is the expectation operator, $\{\alpha\}$ is the set of Fourier components, and the function $R_x^\alpha(\tau)$ giving the Fourier components is termed the cyclic autocorrelation function (CAF), given by:

$$R_x^\alpha(\tau) = 1/T_0 \int_{-T_0/2}^{T_0/2} R_x(t,\tau)e^{-j2\pi\alpha t}, \tag{8.4}$$

In the case of multiple incommensurate periodicities, (8.4) can be expressed as the limit:

$$R_x^\alpha(\tau) = \lim_{T\to\infty} 1/T \int_{-T/2}^{T/2} R_x(t,\tau)e^{-j2\pi\alpha t}, \tag{8.5}$$

The CAF Fourier Transform, denoted the Spectral Correlation Function (SCF) is given by:

$$S_x^\alpha(f) = \int_{-\infty}^{\infty} R_x^\alpha(\tau)e^{-j2\pi f\tau}d\tau, \tag{8.6}$$

This can be shown to be equivalent (assuming cyclo-ergodicity) to [98]:

$$S_X^{\alpha}(f) = \lim_{T\to\infty} \lim_{\Delta t\to\infty} \frac{1}{\Delta t} \int_{-\Delta t/2}^{\Delta t/2} \frac{1}{T} X_T\left(t, f+\frac{\alpha}{2}\right) X_T^*\left(t, f-\frac{\alpha}{2}\right) dt \tag{8.7}$$

$$X_T(t,f) = \int_{t-T/2}^{t+T/2} x(u) e^{j2\pi f u} du. \tag{8.8}$$

Here it can be seen that S_x^{α} is in fact a true measure of the correlation between the spectral components of $x(t)$. A significant benefit of the SCF is its insensitivity to additive noise. Since the spectral components of white noise are uncorrelated, it does not contribute to the resulting SCF for any value of $\alpha \neq 0$. This is even the case when the noise power exceeds the signal power, where the signal would be undetectable using a simple energy detector. At $\alpha = 0$, where noise is observed, the SCF reduces to the ordinary Power Spectral Density (PSD).

To derive a normalized version of the SCF, the Spectral Coherence Function (SOF) is given as:

$$C_X^{\alpha}(f) = \frac{S_X^{\alpha}(f)}{\left[S_X^0\left(f+\frac{\alpha}{2}\right)^* S_X^0\left(f-\frac{\alpha}{2}\right)\right]^{1/2}}. \tag{8.9}$$

The SOF is seen to be a proper coherence value with a magnitude in the range of $[0, 1]$. To account for the unknown phase of the SOF, the absolute value of $C_X^{\alpha}(f)$ is computed and used for classification. The SOF of some typical modulation schemes are shown in Fig. 8.1 and Fig. 8.2. The SOF of each modulation scheme generates a highly distinct image. These images can then be used as spectral fingerprints to identify the modulation scheme of the received signal.

An additional benefit to using the SOF is its insensitivity to channel effects. Wireless signals are typically subject to severe multipath distortion. Taking this into consideration, the SCF of a received signal is given as:

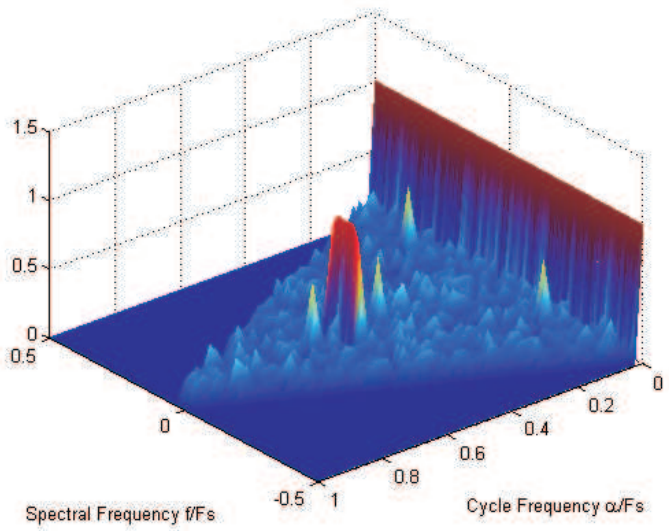

Figure 8.1: Spectrum coherence function of BPSK in AWGN channel [11].

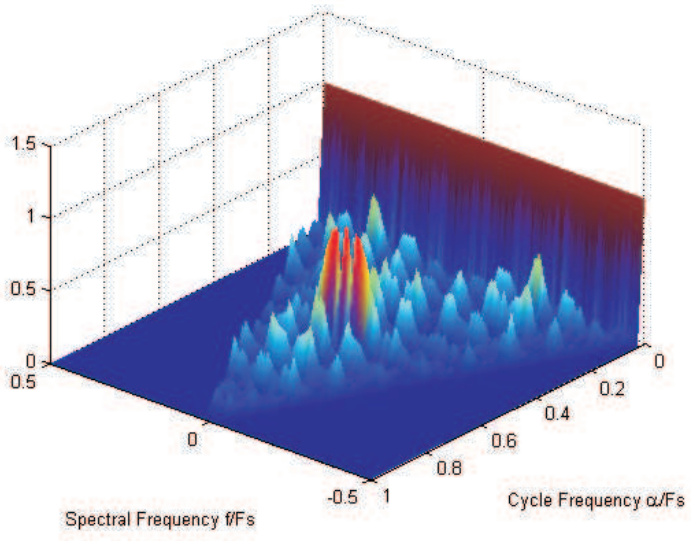

Figure 8.2: Spectrum coherence function of FSK in AWGN channel [11].

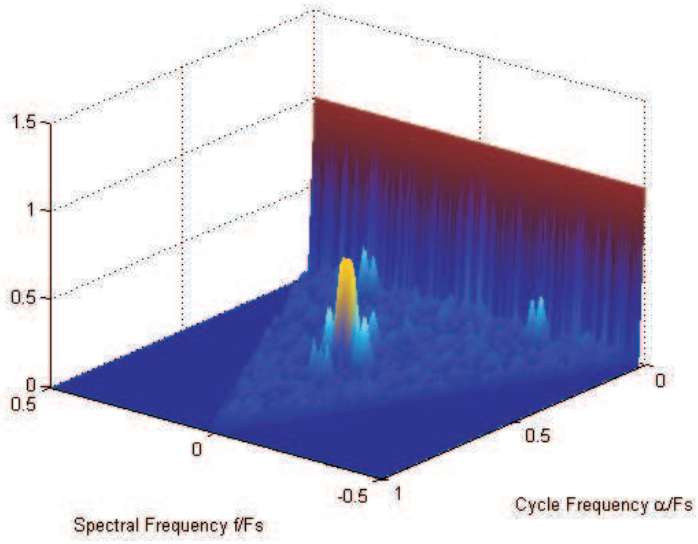

Figure 8.3: Spectrum coherence function of BPSK in Multipath channel [12].

$$S_Y^\alpha(f) = H\left(f + \frac{\alpha}{2}\right) H^*\left(f - \frac{\alpha}{2}\right) S_x^\alpha(f) \tag{8.10}$$

$$y(t) = x(t) \otimes h(t) \tag{8.11}$$

where $h(t)$ is the unknown channel response, and $H(f)$ is the Fourier Transform of $h(t)$. Here it can be seen that the resulting SOF of the received signal can be significantly distorted depending on the channel. However, when forming the SOF, by substituting (8.10) into (8.9) it is evident that the channel effects are removed, and the resulting SOF is equal to that of the original undistorted signal. As a result, the SOF is preserved as a reliable feature for identification even when considering propagation through multipath channels, so long as no frequency of the signal of interest is completely nullified by the channel. The SOF of some typical signals undergoing multipath fading are shown in Fig. 8.3 and Fig. 8.4.

To compute the SOF for a sampled signal, a sliding windowed FFT of length N can be used to compute X_T, and a sum taken over the now discrete versions of X_T gives the

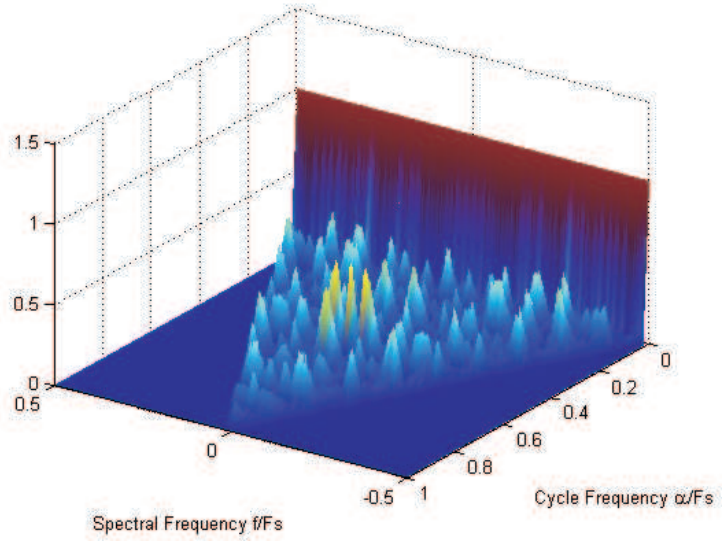

Figure 8.4: Spectrum coherence function of FSK in Multipath channel [12].

resulting equation for $S_X^\alpha(f)$. Additionally, the limits in (8.7) and (8.8) must be made finite, and an estimate of the SCF is obtained. This has the effect of limiting the temporal and spectral resolution of the SCF. In (8.7), Δt is the amount of time over which the spectral components are correlated. This limits the temporal resolution of the signal to Δt. In [99] the cyclic resolution is shown to be approximately $\Delta\alpha = \Delta t$. Similarly, the spectral resolution is limited to $\Delta f = 1/T$, where $1/T$ is the resolution of the FFT used to compute X_T.

To obtain a reliable estimate of the SCF, the random fluctuations of the signal must be averaged out. The resulting requirement is that the time-frequency resolution product must be made very large, with $\Delta t \Delta f \gg 1$, or equivalently, $\Delta f \gg \Delta\alpha$. This has the effect of requiring a much finer resolution for the cycle frequencies than would be provided by the FFT operation. To compensate for this, in [100] it was proposed to zero-pad the input to the FFTs out to the full length of the original signal. However, this leads to a computationally infeasible task. A more suitable method is to first estimate the cycle frequencies of interest using the method outlined in [101]. After the appropriate cycle frequencies have been located, the SCF can be computed using the equivalent method of frequency smoothing on

the reduced amount of data:

$$S_X^{\alpha}(f) = \frac{1}{\Delta f} \int_{f-\Delta f/2}^{f+\Delta f/2} X_{\Delta t}\left(t, f + \frac{\alpha}{2}\right) X_{\Delta t}^{*}\left(t, f - \frac{\alpha}{2}\right) dt \tag{8.12}$$

where $X_{\Delta t}(t, f)$ is defined in (8.8) with T replaced by Δt.

The resulting feature derived from the SOF is a three-dimensional image. This presents an unreasonable amount of data for a classifier to operate on in real-time. Therefore, it must be further reduced to provide a more computationally manageable feature. The work in [100] the authors proposed using merely the cycle frequency profile of the SOF. However, in our previous work [95] demonstrated that with a minimal increase in computational complexity, both the frequency profile as well as the cycle frequency profile can be used, creating a pseudo three-dimensional image of the SOF which performs at a significantly higher degree of reliability for classification. The resulting feature used for classification are then defined as the cycle frequency profile:

$$\overrightarrow{\alpha} = max_f[C_X^{\alpha}] \tag{8.13}$$

and the spectral frequency profile

$$\overrightarrow{f} = max_{\alpha}[C_X^{\alpha}] \tag{8.14}$$

These features can then be analyzed using a pattern recognition-based approach. Due to its ease of implementation, and its ability to generalize to any carrier frequency or symbol rate, a neural network-based system is proposed to process the feature vectors.

8.1.2 Higher Order Cyclic Features

While the SOF produces highly distinct images for different modulation schemes, some modulation schemes produce identical images, as well as different orders of a single modulation scheme. Therefore, while the SOF is able to reliably classify each of the analog signals as well as classify the digital schemes into a modulation family, it will not be able to distinguish between some digital schemes (namely QAM and M-PSK, $M > 4$), or determine the order of the modulation.

8.2 Interference Temperature

In 2003 has proposed Interference Temperature (IT) as a metric to aid in interference analysis and for establishing a threshold on the allowable interference induced by secondary users. IT is "a measure of the RF power generated by undesired emitters plus noise sources that are present in a receiver system $(I + N)$ per unit bandwidth," or in other words, the temperature equivalent of such RF power measured in unit of "Kelvin" (K) [19].

Finally, on May 2007 FCC issued another notice saying that it has terminated the IT concept. Even though, there are few supporters for adopting the IT approach to measure or set a threshold, there is no clear cut method or rules to implement IT. The community in general (technical as well as user) argued that the IT approach is not practical and would only result in increased interference in its operating ranges

8.2.1 View of IT Opponents

This section is adapted from discussion by Krenik in EE times [102]. From the very beginning there was lot of opposition to this concept, with arguments that interference and noise behave differently and cannot be completely characterized with single measurement. Then there are arguments on implementation of such a concept. The difficulty lies in effectively

measuring the interference temperature. A CR is naturally aware of its transmit power level and, with a global-positioning system, also knows its precise location. With this information, a CR can compute the probability that its transmission could cause interference to a neighboring receiver on the same frequency. The concept is similar to UWB, in which transmit power is kept so low that no damaging interference normally would occur. However, there is no practical way for CR to locate all receivers of communications from the transmitter in question or to assess the capabilities of those receivers. Some may generate significant internal noise and, as a result, tolerate little interference. Some may be located so far from the transmitter that their reception is marginal to begin with. Unless a CR can measure the effect of its transmission on all possible receivers, taking a useful interference temperature measurement may not be feasible .

For this reason, many system operators oppose shared use of their licensed frequencies. Interference at the edges of their coverage areas could force them to drop service to some customers or to build more towers. To address this concern, some flavors of cognitive radio abandon the idea of sharing channels. Instead, they rely on identifying an unused channel and transmitting at that frequency until a licensed user wants it. When the CR detects other activity, it jumps to another channel not in use. Even this approach allows for the possibility that an unlicensed CR user may deprive a licensee of access to channels for which it has paid significant sums. In extreme cases, CR may not be able to detect a competing signal even when a channel is actively in use. Such a situation can easily occur when the CR transmits at high power levels while existing users of the channel are quite far away and at low power levels.

Take the case of a television station's remote news van. The van sends a signal to the station, which then broadcasts the report to viewers at home. Now, suppose the van is dispatched to an event only a mile or so from the station. The news report will go out of the van at relatively low power across a directional antenna aimed at the station. A CR located outside the directional antenna's influence may not detect the transmission. If the

CR decides that the channel is not in use and sends its own signal to a receiver on the far side of the TV station's main transmitter, it can blow the news right off the air. Interference temperature concepts alone cannot effectively protect the licensee in this situation.

8.2.2 How IT works

FCC envisioned that by using this one measurement it can characterize both noise and interference. For a given geographic area, FCC would set up an Interference Temperature limit or threshold T_L. Any unlicensed user utilizing this band must make sure that they do not exceed this limit $T_I < T_L$, where T_I is the measured interference consisting of both noise and other licensed and unlicensed users.

IT expression T_I as shown in (8.15) is a function of frequency and bandwidth (B). It is a measure of power in a given B where $P_I(f_c, B)$ is the average power in Watts centered at f_c over a bandwidth B in Hertz and *k* is the Boltzmann's constant in Joules per Kelvin degree. The expression in (8.15) can also be expressed in terms of power spectral density $S(f)$ of current RF environment as shown in (8.16).

$$T_I(f_c, B) = \frac{P_I(f_c, B)}{kB} \tag{8.15}$$

$$\begin{aligned} T_I(f_c, B) &= \frac{1}{Bk} P_I(f_c, B) \\ &= \frac{1}{Bk}\left(\frac{1}{B}\int_{f_c-B/2}^{f_c+B/2} S(f)df\right) \\ &= \frac{1}{B^2k}\left(\int_{f_c-B/2}^{f_c+B/2} S(f)df\right). \end{aligned} \tag{8.16}$$

To satisfy FCC's IT condition, an unlicensed user has to show that their added transmission power will not exceed T_L . This brings up number of questions such as which transmission

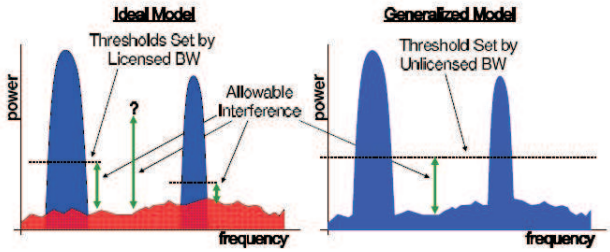

Figure 8.5: Interference Temperature model [13, 14].

are to be considered as interference, unlicensed, licensed or both. To address some of these scenarios, two conceptual models 1) Ideal and 2) Generalized are shown in Fig.8.5.

In an ideal IT model interference is just limited to licensed users. As shown in Fig. 8.5 , unlicensed users might be operating across multiple licensed user bands each with its own T_L. The unlicensed users challenge is to assure the all the licensed user's condition are met and also maximize the spectral efficiency.

$$T_I(f_i, B_i) + \frac{M_i P}{k B_i} \leq T_L(f_i) \quad \forall \quad 1 \leq i \leq n. \tag{8.17}$$

It is assumed that the T_L value is set forth by the licensed transmitter. M is a value between $0, 1$ representing the attenuation between the licensed transmitter and unlicensed receiver.

In the generalized model, no a priori knowledge of the licensed user in a given RF environment is assumed to be available; therefore an unlicensed user cannot distinguish between licensed signals from interference and noise as shown in Fig. 8.5. In this scenario there is just one T_L resulting in one constraint rather than multiple constraint as in (8.17).

$$T_I(f_c, B) + \frac{MP}{kB} \leq T_L(f_c). \tag{8.18}$$

Bibliography

[1] P. Marshall, "XG - Next Generation Communication,www.darpa.mil/darpatech2002/presentations/atopdf/speeches/marshall.pdf," Dec. 2003.

[2] Q. Zhao and B. M. Sadler, "A survey of dynamic spectrum access," *IEEE Signal Processing Magazine*, vol. 24, pp. 79–89, May 2007.

[3] J. Mitola, "Cognitive Radio - An Integrated Agent Architecture for Software Defined Radio, Ph.D. Dissertation," *Teleinformatics, Royal Institute of Technology - Sweden*, 2000.

[4] S. Mangold, A. Jarosch, and C. Monney, "Cogntitive radio: Trends and research challenges," *htpp://www.swisscom-comtec.ch/pdf/comtec032005242.pdf*, March 2005.

[5] A. M. Wyglinski, "Effects of bit allocation on non-contiguous multicarrier-based cognitive radio transceivers," *Proceedings of the 64th IEEE Vehicular Technology Conference*, September 2006.

[6] L. Hanzo, M. Munster, B. Choi, and T. Keller, *OFDM and MC-CDMA for Broadband Multi-User Communications*. Wiley, 2003.

[7] V. Chakravarthy, A. Shaw, M. Temple, and A. Nunez, "Tdcs, ofdm and mc-cdma : A brief tutorial," *IEEE Communications Magazine*, vol. 43, p. S11=S16, September 2005.

[8] V. Chakravarthy, Z. Wu, A. Shaw, M. Temple, R. Kannan, and F. Garber, "A general overlay/underlay analytic expression representing cognitive radio waveform," *in IEEE Int'l Conf. on Waveform Diversity and Design*, June 2007.

[9] T. Rappaport, *Wireless Communications - Principles and Practice*. Prentice Hall Communications Engineering and Emerging Technology Series, 2nd ed., 2002.

[10] M. Roberts, "A General Framework For Analyzing, Characterizing and Implementing Spectrally Modulated, Spectrally Encoded Signals, Ph.D. Dissertation," *Electrical and Computer Engineering, Air Force Institute of Technology*, September 2006.

[11] E. Like, V. Chakravarthy, and Z. Wu, "Reliable modulation classification at low snr using spectral correlation," *IEEE Consumer communications and Networking Conference*, January 2007.

[12] E. Like, V. Chakravarthy, and Z. Wu, "Modulation recognition in multipath fading channels using cyclic spectral analysis," *accepted for publication in IEEE GLOBECOM*, 2008.

[13] T. Clancy, "Dynamic Spectrum Access in Cognitive Radio Networks, Ph.D. Dissertation," *Computer Science, University of Maryland*, April 2006.

[14] T. Clancy and W.Arbaugh, "Measuring interference temperature," *Virginia Tech Wireless Personal Communication Symposium*, June 2006.

[15] J. Neel, "Analysis and Design of Cognitive Radio Network and Distributed Radio Resource Management Algorithms, Ph.D. Dissertation," *Electrical Engineering, Virginia Polytechnic Institute and State University*, September 2006.

[16] Private conversation with Ramesh N. Patel, *Emeritus Professor of Philosophy and Religion Antioch College*. August 2008.

[17] H. Arslan, ed., *Cognitive Radio, Software Defined Radio and Adaptive Wireless Systems*. Dordrecht, Netherlands: Springer, 2007.

[18] "National Telecommunications and Information Adminstration (NTIA), FCC Frequency allocation chart," Dec. 2003.

[19] "FCC - Notice of Proposed Rulemaking and Order, Facilitating Opportunities for flexible, efficient and Reliable spectrum use Employing Cognitive Radio technologies," *FCC Document ET Docket No. 03-108*, December 2003.

[20] "FCC - Adopts Rule Changes for Smart Radios, Facilitating Opportunities for flexible, efficient and Reliable spectrum use Employing Cognitive Radio technologies," *FCC Document ET Docket No. 03-108*, March 2005.

[21] B. Fette, ed., *Cognitive Radio Technology*. Newnes, 2006.

[22] A. N. Mody, S. R. Blatt, D. G. Mills, T. P. McElwain, N. B. Thammakhoune, J. D. Niedzwiecki, M. J. Sherman, and C. S. Myers, "Recent advances in cognitive communications," *IEEE Communication Magazine*, vol. 45, no. 10, pp. 54–59, October, 2007.

[23] S. Srinivasa and S. A. Jafar, "The throughput potential of cognitive radio: A theoretical prespective," *IEEE Communication Magazine*, vol. 45, pp. 73–79, May 2007.

[24] J. Mitola, "Software radio: Survey, critical evaluation and future directions," *Proccedings in National Telesystems Conference*, May 1992.

[25] J. Mitola, "The software radio architecture," *IEEE Communication Magazine*, vol. 33, pp. 26–38, May 1995.

[26] W. Bonser, "Speakeasy military software defined radio," *in Proc. International symposium on advanced radio technology*, 1998.

[27] J. Mitola and G. Q. Magquire, "Cognitive radio: Making software radios more personal," *IEEE Personal Communications*, Aug. 1999.

[28] S. Haykin, "Cognitive radio: Brain-empowered wireless communications," *IEEE Journal in Selected Areas in Communications*, vol. 23, pp. 1–20, 2005.

[29] R. W. Thomas, L. A. DaSilva, and A. B. MacKenzie, "Cognitive networks," *EEE Dynamic Spectrum Access Networks*, Nov. 2005.

[30] R. W. Thomas, "Cognitive Networks, Ph.D. Dissertation," *Computer Engineering, Virginia Polytechnic Institute and State University*, June 2007.

[31] D. Cabric, S. Mubaraq, Mishra, and R. W. Brodersen, "Implementation issues in spectrum sensing for cognitive radios," *Asilimar Conference on Signals, Systems and Computers Conference*, vol. 1, pp. 772–776, Nov. 7-10 2004.

[32] S. Shankar, C. Cordeiro, and K. Challapali, "Spectrum agile radios: Utilization and sensing architectures," *IEEE Dynamic Spectrum Access Networks*, pp. 160–169, Nov. 8-11, 2005.

[33] P. D. Sutton, K. E. Nolan, and L. E. Doyle, "Cyclostationary signatures in practical cognitive radio applications," *IEEE Journal on Selected Areas in Communications*, vol. 26, pp. 13–23, January 2008.

[34] R. Tandra and A. Sahai, "Fundamental limits on detection in low snr under noise uncertainity," *IEEE International Conference on Wireless Networks, Communication and Mobile Computing*, vol. 1, pp. 464–469, June 2005.

[35] S. Geirhofer, B. Sadler, and L. Tong, "A measurement-based model for dynamic spectrum access in wlan channels," *IEEE Military Communication Conference*, October 2006.

[36] S. M. Mishra, R. Tandra, and A. Sahai, "The case for multiband sensing," *Forty Fifth Annual Allerton Conference in Communication, Control and Computing*, September 2007.

[37] B. F. Boroujeny and R. Kempter, "Multicarrier communication techniques for spectrum sensing and communications in cognitive radio," *IEEE Communication Magazine*, vol. 46, pp. 80–85, April 2008.

[38] R. Kolodziejski and J. Betz, "Detection of weak random signals in idd non-gaussian noise," *IEEE Transaction on Communication*, vol. 48, February 2000.

[39] S. M. Mishra, A. Sahai, and R. W. Brodersen, "Cooperative sensing among cognitive radios," *IEEE International Conference in Communication*, vol. 4, pp. 1658–1663, June 2006.

[40] C.-H. Lee and W. Wolf, "Multiple access-inspired cooperative spectrum sensing for cognitive radio," *IEEE Military Communication Conference*, October 2007.

[41] J. Kruys, "Co-existence of disimmilar wireless systems," *http://main.wi-fi.org/opensection*, Dec. 2003.

[42] B. Fette, "The promise and challenge of cognitive radio," *http://www.sdrforum.org/MGTS/seoul0904agenda.html*, September 2004.

[43] B. Sklar, *Digital Communications, Fundamentals and Applications*. Saddle River, New Jersey: Prentice Hall, 2001.

[44] T. R. Marko Hannikainen and J. Routsalainen, "Co-existence of bluetooth and wireless lans," *IEEE ICT*, 2001.

[45] G. Ennis, "Impact of bluetooth on 802.11 directsequence," *IEEE P802.11 Working group contribution, IEEE P802.11-98/319*, September 1998.

[46] X. Jing, S.-C. Mau, D. Raychaudhuri, and R. Matyas, "Reactive cognitive radio algorithms for co-existence between ieee 802.11b and 802.16a networks," *IEEE GLOBECOM*, 2005.

[47] M. Hamalainen, V. Hovinen, A. E. Spezio, R. Test, . H. J. Iinatti, and M. Latvaaho, "On the uwb system coexistence with gsm900, umts/wcdma, and gps," *IEEE Journal on Slected Areas in Communications*, vol. 20, no. 9, pp. 1712–1721, 2002.

[48] T. A. Weiss and F. K. Jondral, "Spectrum pooling: An innovative strategy for the enhancement of spectrum efficieny," *IEEE Communication Magazine*, vol. 42, no. 3, pp. S8–S14, March 2004.

[49] H. Tang, "Some physical layer issues of wide-band cognitive radio systems," *IEEE Dynamic Spectrum Access Networks*, pp. 151–159, Nov. 8-11, 2005.

[50] J. D. Poston and W. D. Horne, "Discontigous ofdm considerations for dynamic spectrum access in idle tv channels," *IEEE Symposium on New Frontiers in Dynamic Spectrum Access Networks*, pp. 607–610, Nov. 8-11, 2005.

[51] J. D. Guffey, A. M. Wyglinski, and G. J. Minden, "Agile radio implementation of ofdm physical layer for dymanic spectrum access research," *Proceedings of the IEEE Global Telecommunication Conference*, pp. 4051–4055, November 2007.

[52] Q. Zhang, A. B. Kokkeler, and G. J. Smit, "An efficient fft for ofdm based cognitive radio on a reconfigurable architecture," *IEEE International Conference on Communication, COGNET Workshop*, 2007.

[53] K. Nishi, S. Yoshizawa, and Y. Miyanaga, "A study of dynamic reconfigurable fft processor for ofdm based cognitive radio," *International Symposium on Communication and Information Technologies (ISCIT)*, 2007.

[54] R. Rajbanshi, A. M. Wyglinski, and G. J. Minden, "An efficient implementation of nc-ofdm transceivers for cognitive radios," *Proceedings of the First International Conference on Cognitive Radio Oriented Wireless Networks and Communications (Mykonos Island, Greece)*, June 2006.

[55] M. B. Pursley and T. C. R. IV, "Low-complexity adaptive transmission for cognitive radio in dynamic spectrum access networks," *IEEE Journal on Selected Areas in Communication*, vol. 26, no. 1, pp. 83–94, January, 2008.

[56] Q. Qu, L. B. Milstein, and D. R. Vaman, "Cognitive radio based multi-user resource allocation in mobile ad hoc networks using multi-carrier cdma modulations," *IEEE Journal on Selected Areas in Communication*, no. 1, pp. 70–82, January, 2008.

[57] S. Hara and R. Prasad, "High-performance mc-cdma via carrier interferometry codes," *IEEE Communications Magazine*, vol. 35, pp. 126–133, December 1997.

[58] B. Natarajan, C. Nassar, S. Shattil, and Z. Wu, "High-performance mc-cdma via carrier interferometry codes," *IEEE Transactions on Vehicular Technology*, vol. 50, pp. 1344–1353, November 2001.

[59] B. Natarajan, Z. Wu, and C. R. Nassar, "Large set of ci spreading codes for high-capacity mc-cdma," *IEEE Transactions on Communications*, vol. 52, pp. 1862–1866, November 2004.

[60] R. Rajbanshi, Q. Chen, A. Wyglinski, G. Milden, and J. Evans, "Quantitative comparision of agile modulation technique for cognitive radio tranceivers," *IEEE Consumer Communications and Networking Conference*, January 2007.

[61] S. Hijazi, M. Michelini, B. Natrajan, Z. Wu, and C. Nassar, "Enabling fcc's proposed spectral policy via carrier interferometry," *IEEE Wireless Communication and Networking Conference*, 2004.

[62] Z. Wu and B. Natrajan, "Interference tolerant agile cognitive radio: Maximize channel capacity of cognitive radio," *IEEE Consumer Communications and Networking Conference*, January 2007.

[63] V. Chakravarthy, A. Shaw, M. Temple, and J. Stephens, "Spectrum re-use employing transform domain communication system," *US Patent pending: 5-029-184*, 2006.

[64] V. Chakravarthy, A. Shaw, M. Temple, and J. Stephens, "Cognitive radio: An adaptive waveform with spectrum sharing capabilities," *IEEE WCNC*, March 2005.

[65] M. Manju, B. Premkumar, and C. T. Lau, "An adaptive waveform generation technique for cognitive radio," *The 67th IEEE Vehicular Technology Confernce*, May 2008.

[66] M. Roberts, M. A. Temple, M. E. Oxley, R. F. Mills, and R. A. Raines, "A general analytic framework for spectrally modulated, spectrally encoded signals," *IEEE Journal of Selected Areas on Signal Processing)*, January 2007.

[67] M. Roberts, M. A. Temple, M. E. Oxley, R. F. Mills, and R. A. Raines, "A general analytic framework for spectrally modulated, spectrally encoded signals," *IEEE Waveform Diversity Conference*, January 2006.

[68] M. Roberts, M. A. Temple, M. E. Oxley, R. F. Mills, and R. A. Raines, "A spectrally modulated, spectrally encoded analytic framework for carrier interferometry signals," *International Wireless Communications and Mobile Computing Conference (IWCMC)*, July 2006.

[69] M. Sherman, A. N. Mody, R. Martinez, C. Rodriguez, and R. Reddy, "Ieee standards supporting cognitive radio and networks, dynamic spectrum access, and coexistence," *IEEE Communication Magazine - Special Issue on IEEE Standards in Communications and Networking*, pp. 72–79, July 2008.

[70] "FCC - Notice of Proposed Rulemaking and order, facilitating analog TV bands for unlicensed wireless applications", Journal = "FCC Document ET Docket No.04-113," May 2004.

[71] N. Yee, J. Linnartz, and G. Fettweis, "Multi-carrier cdma in indoor wireless radio networks," *PIMRC*, 1993.

[72] D. Wiegandt, C. Nassar, and Z. Wu, "Overcoming peak-to-average power ratio issues in ofdm via carrier interferometry codes.," *IEEE Vehicular Technology Conference*, 2001.

[73] Z. Wu and C. R. Nassar, "Narrowband interference rejection in ofdm via carrier interferometry spreading codes.," *IEEE Transactions on Wireless Communications*, vol. 4, pp. 1491–1505, July 2005.

[74] L. Milstein and P. Das, "An analysis of a real-time transform domain filtering digital communication system-part i: Narrow-band interference rejection," *IEEE Transactions on Communications*, vol. 28, pp. 816–824, June 1980.

[75] L. Milstein and P. Das, "An analysis of a real-time transform domain filtering digital communication system-part ii: Wide-band interference rejection," *IEEE Transactions on Communications*, vol. 31, pp. 21–27, January 1983.

[76] C. Andren, "Low probability-of-intercept communication system.," *US Patent: 5-029-184*, 1991.

[77] E. German, "Transform domain signal processing study final report.," *Technical Report, Reistertown, MD, Contract: F30602-86-C-0133*, August 1988.

[78] R. Radcliffe, "Design and simulation of a transform domain communication system," Master's thesis, Air Force Institute of Technology, 1996.

[79] P. J. Swackhammer, M. A. Temple, and R. A. Raines, "Performance simulation of a transform domain communication system for multiple access applications," *Military Communications Conference Proceedings, MILCOM 1999*, vol. 2, pp. 1055–1059, October 1999.

[80] M. Roberts, "Initial acquisition performance of a transform domain communication system: Modeling and simulation results," *MILCOM 2000 Proceedings. 21st Century Military Communications Architectures and Technologies for Information Superiority*, vol. 2, pp. 1119–1123, 2000.

[81] P. J. Lee, "Computation of the bit error rate of coherent m-ary psk with gray code bit mappting," *IEEE Transactions on Communications*, vol. COM-34, pp. 488–491, 1986.

[82] M. Lee, M. Temple, and R. Raines, "Wavelet domain communication system: Bit error sensitivity characterization for geographically separted transceivers," *IEEE MILCOM*, vol. 2, pp. 1378–82, 2002.

[83] A. S. Nunez, "Interference suppression in multiple access communications using m-ary phase shift keying generated via spectral encoding," Master's thesis, Air Force Institute of Technology, 2004.

[84] A. Nunez, M. Temple, R. Mills, and R. Raines, "Interference avoidance in spectrally encoded multiple access communications using mpsk modulation," *IEEE WCNC*, March 2005.

[85] C. Gaona, "Analysis of ultra wideband spectral coexistence with advanced wireless communication systems," Master's thesis, Air Force Institute of Technology, 2006.

[86] S. Weinstein and P. Ebert, "Data transmission by frequency division multiplexing using discrete fourier transform," *IEEE Transactions Communication Technology*, pp. 628–634, 1971.

[87] W. Zou and Y. Wu, "Cofdm: An overview," *IEEE Transactions Broadcast*, vol. Vol.41,no.1, pp. 1–8, March 1995.

[88] A.Chouly, A.Brajal, and S.Jourdan, "Orthogonal multicarrier techniques applied to direct sequence spread spectrum cdma systems," *IEEE Global Telecommunications Conference*, pp. 1723–1728, 29 Nov-02 Dec 1993.

[89] G.Fettweis, A.Bahai, and K.Anvari, "On multi-carrier code division multiple access (mc-cdma) modem design," *IEEE Vehicular Technology Conference*, pp. 1670–1674, 8-10 June 1994.

[90] D. Wiegandt, Z. Wu, and C. Nassar, "High-throughput, high performance ofdm via pseudo-orthogonal carrier interferometry spreading codes," *IEEE Transaction on Communication*, vol. 51(7), pp. 1123–1134, July 2003.

[91] A. Nunez, V. Chakravarthy, and J. Caldwell, "A transform domain communication and jamming waveform," *IEEE Waveform Diversity Conference*, January 2006.

[92] D. P. Bertsekas, *Non Linear Programming*. Athena - Scientific Publisher, 2nd ed., 2004.

[93] R. Kannan, V. Chakravarthy, S. Wei, Z. Wu, and M. Rangaswamy, "Soft-decision cognitive radio power control based on intelligent spectrum sensing," *in IEEE Int'l Conf. on Waveform Diversity and Design*, June 2007.

[94] C. T. Chou, S. Shankar, H. Kim, and K. G. Shin, "What and how much to gain by spectrum agility," *IEEE Journal on Selected Areas in Communications*, vol. 25 NO. 3, pp. 576 – 588, April 2007.

[95] E. Like, V. Chakravarthy, and Z. Wu, "Modulation recognition in fading channels using higher order cyclic cumulants," *IEEE CROWNCOM*, 2007.

[96] A. Goldsmith, *Wireless Communications*. New York, New York: Cambridge University Press, 1st ed., 2005.

[97] B. Natrajan, C. Nassar, and V. Chandrasekar, "Generation of correlated rayleigh fading envelops for spread spectrum applications," *IEEE Communications Letters*, vol. 4, pp. 9–11, January 2000.

[98] W. Gardner, W. Brown, and C. Chen, "Spectral correlation of modulated signals: part ii - digital modulations," *IEEE Transactions on Communications*, vol. 35, pp. 595–601, June 1987.

[99] W. A. Gardner, "Measurement of spectral correlation," *IEEE Transactions on Acoustics, Speech and Signal Processing*, vol. 34, October 1986.

[100] A. Fehske, J. Gaeddert, and J. H. Reed, "A new approach to signal classification using spectral correlation and neural networks," *1st IEEE International Symposium on New Frontiers in Dynamic Spectrum Access Networks*, 2005.

[101] R. S. Roberts, W. A. Brown, and H. H. Loomis, "Computationally efficient algorithms for cyclic spectral analysis," *IEEE Signal Processing Magazine*, April 1991.

[102] B. Krenik, "Clearing interference for cognitive radio," *EE Times.*, August 2004.